The Hilbert Book Test Model

By J.A.J. van Leunen

Abstract

The Hilbert book test model is a purely mathematical test model that starts from a solid foundation from which the whole model can be derived by using trustworthy mathematical methods. What is known about physical reality is used as a guidance, but the model is not claimed to be a proper reflection of physical reality. The mathematical toolkit still contains holes. These holes will be encountered during the development of the model and suggestions are made how those gaps can be filled. Some new insights are obtained and some new mathematical methods are introduced. The selected foundation is interpreted as part of a recipe for modular construction and that recipe is applied throughout the development of the model. This development is an ongoing project. The main law of physics appears to be a commandment: "Thou shalt construct in a modular way". The paper reveals the possible origin of several physical concepts. This paper shows that it is possible to discover a mathematical structure that is suitable as an extensible foundation. However, without adding extra mechanisms that ensure dynamic coherence, the structure does not provide the full functionality of reality. These extra mechanisms apply stochastic processes, which generate the elementary modules that populate the model.

All discrete items in universe are configured from dynamic geometric locations. These items are stored in a repository that covers the past history, the current static status quo and the future. The elementary modules float over the static framework of the repository. Dedicated mechanisms ensure the coherent behavior of these elementary modules. Fields exist that describe these elementary modules. These fields are supported by an encapsulating repository. Both repositories are formed by quaternionic Hilbert spaces.

Contents

3

5

1 Foreword of the author

I am born with a deep curiosity about my living environment. When I became aware of this, I was astonished why this environment appeared to be so complicated and at the same time it behaved in such a coherent way. In my childhood I had no clue. Later some unique experiences offered me some indications. After my retirement I started in 2009 a personal research project in order to discover some of the clues.

The "Hilbert Book Model" is the name of my personal research project. My interest in the structure and phenomena of physical reality started in the third year of my physics study when I was first confronted with how quantum mechanics was configured. I was quite astonished by the fact that its methodology differed fundamentally from the way that classical mechanics was done. So I asked my very wise lecturer on what origin this difference is based. His answer was that this difference was caused by the **superposition principle**. I was not very happy with this answer, because the superposition principle was indeed part of the methodology of quantum mechanics, but in those days I did not comprehend how that could present the main cause of the difference between the two methodologies. I decided to dive into literature and after some search I encountered the booklet of Peter Mittelsteadt, " Philosophische Probleme der Modernen Physik" (1963). This booklet contained a chapter about quantum logic and that appeared to me a more appropriate answer. Garret Birkhoff and John von Neumann published in 1936 a paper that published their discovery of what they called "quantum logic". Quantum logic is since then in mathematical terminology known as an **orthomodular lattice**. The relational structure of this lattice is quite similar to the relational structure of classical logic. That is why the duo gave their discovery the name "quantum logic". This was an unlucky choice, because no good reason exist to consider the orthomodular lattice as a system of logical propositions. In the same paper, the duo indicated that the set of closed subspaces of a **separable Hilbert space** has exactly the relational structure of an orthomodular lattice. That appears to be the reason why quantum physicists prefer Hilbert spaces as a realm in which they do their modeling of quantum physical systems.

Another habit of quantum physicists also intrigued me. My lecturer thought me that all observable quantum physical quantities are eigenvalues of Hermitian operators. Hermitian operators feature real eigenvalues. When I looked around I saw a world that had a structure that was configured from a three dimensional spatial domain and a one dimensional time domain. In the quantum physics of that time, no operator represents the time domain and no operator was used to deliver the spatial domain in a compact fashion. After some research I discovered a four dimensional number system that could provide an appropriate normal operator with an eigenspace that represented the full four dimensional representation of my living environment. At that moment I had not yet heard from quaternions, but an assistant professor quickly told me about the discovery of Rowan Hamilton that happened more than a century earlier.

My university, the TUE, targeted applied physics and there was not much time nor support for diving deep into the fundamentals of quantum physics. After my study I started a career in high-tech industry where I joined the development of image intensifier devices. There followed my confrontation with optics and with the actual behavior of elementary particles. See: http://www.e-physics.eu/#_What_image_intensifiers reveal.

Only after my retirement I got sufficient time to dive deep into the foundations of physical reality. In 2009 after the recovery of a severe disease, I started my personal research project that in 2011 got

its current name "The Hilbert Book Model". The author takes the freedom to upgrade the related papers in a steady rate.

1.1   My papers

I use vixra.org as my personal e-print archive: http://vixra.org/author/j_a_j_van_leunen . Vixra provides full two sided open access and has a flexible revision service, which I use extensively. In this way it is possible to follow how my ideas evolved. I put preliminary papers on my website http://www.e-physics.eu . There my papers are available in .pdf and also in .docx format. I do not request copyright on these documents.

I try to avoid the burden of peer review publishing. The peer review publishing industry has turned into a complete chaos. Since no omniscient reviewers exist and most existing reviewers are biased, peer review publishing cannot realize its promise. Instead I try to keep the quality of my papers at a high standard.

The most recent versions of the author's papers will appear on his website. Most of the older papers are superseded by newer ones that got different names. Older papers started with knowledge that was lectured in universities and or could be found in literature. Newer papers also contain corrections and discoveries that are made by the author

1.2   Text e-book

"The Hilbert Book Test Model" is aimed to be a condensed description of the project, which contains all items that cannot be easily found in literature. Everybody is free to use or criticize its content.

We try to derive everything from the selected foundation, but when necessary we accept guidance from what we know from the results of physical theories. In the first part of the paper the story will be told with a minimum of symbols or formulas.

In the second part the results of the investigation are collected and reformulated by using symbols and formulas. This approach allows to deepen the investigation and offers a more precise formulation.

The appendix contains subjects that are related, but are not easily found in literature.

2 Motivation

Some scientists start a research project that has as target to develop a theory of everything. This is an implausible enterprise because the target is far too complicated in order to be comprehended by a human being. In fact what these scientists pursue is the discovery of a foundation, whose extension automatically leads to a theory that in principle can cover all aspects of physical reality. I never had the intention to develop a theory of everything. Instead I am interested in the structure and the functioning of the lower levels of physical reality.

I started a study in physics because I was interested in what destined my environment to be so complicated and yet controlled that environment such that it appeared to be so well coordinated. The belief in a creator that settles everything seemed to me a far too simple solution. My environment must have a built-in principle that in one way or another installed the necessary coherence. That principle must therefore be incorporated in the foundation of the structure of reality.

If you think about it, then this foundation must be relatively simple. This means that this foundation can easily be comprehended by skilled scientists. The question now is how exactly this foundation will be structured. A great chance exists that this structure is already added as a part to mathematics. Mathematics represents the library of self-consistent trustworthy exact human knowledge. Mathematicians support and maintain that library. Physicists apply that library.

The challenge of the rediscovery of the founding structure is the fact that the extension of this structure to a more complicated structure must automatically restrict to a structure, which shows more features that can be recognized as features of physical reality.

The simplest mathematical structures are sets and relational structures. Relational structures define what kind of relations between elements of a set are allowed. Relational structures exist in many forms. For example, the classical logic that we use in order to characterize a proper way of reasoning is in fact a relational structure. This logic describes what kind of statements are allowed and what relationships between these statements are tolerated.

The difficulty is not comprehending a suitable foundation. The difficulty is located in finding a structure, whose extension is restricted such that it automatically leads to a base model, which has a similar structure and similar behavior as the lower levels of perceivable physical reality has. The most challenging requirement is that the foundation and its extensions must ensure the dynamic coherence of the developed model.

This paper shows that it is possible to discover a mathematical structure that is suitable as an extensible foundation. However, without adding extra mechanisms that ensure dynamic coherence, the structure does not provide the full functionality of reality. These extra mechanisms apply stochastic processes, which generate the elementary modules that populate the model.

The author has long thought that the foundation of physical reality is not observable. However, recently the author came to the conclusion that a signature of the foundation can be observed all over universe. This signature is shown by the fact that all discrete objects in universe are either modules or they represent modular systems. However, translating this signature into a mathematical structure requires deep insight in both modular construction and in mathematical structures.

3 Generating the base model

3.1 Observation

The foundation of physical reality must necessarily be very simple and as a consequence its structure must be easily comprehensible by skilled scientists. So, quite probable the structure was long ago discovered and added as a part to mathematics. As a consequence the best way to investigate the foundation of reality is to use mathematical test models. The rediscovery of this structure as a foundation of reality is a complicated task because extending this foundation must automatically lead to a higher level of the structure of physical reality that shows more features that can be recognized as features of physical reality. In addition, the lower levels of the structure of physical reality must leave some signatures that are visible in many facets of the universe.

Several of such signatures exist. For example the fact that all discrete items in universe are either modules or they are modular systems is probably a signature of the foundation or of the lower levels of the structure of physical reality. Considering this observation as a signature requires the investigation of the peculiarities of modular design and modular construction. That analysis learns that relations between modules and relations that are relevant inside modules or modular systems play a major role. Especially the relations that determine that an object is a module or is part of a module are important. It is quite probable that the foundation of physical reality is a relational structure. A relational structure is a set in which the relations that can exist between the elements are restricted in a well-defined way.

About eighty years ago a relational structure was discovered, which was thought to play a significant role in the description of physical reality by physical theories. The discoverers of the relational structure called it "quantum logic". The mathematicians used a more technical name and called it "orthomodular lattice". In their introductory paper the discoverers showed that the set of closed subspaces of the somewhat earlier discovered Hilbert space has exactly the relational structure of an orthomodular lattice. With other words this Hilbert space is a realization of the orthomodular lattice. The question that arises now is whether this Hilbert space is also a realization of modules and modular systems. This question has a positive answer but the argumentation requires a deep dive into the concept of modularization and into advanced mathematics.

More signatures exist but in this paper we first focus on this one.

3.2 Task

The base model must include a simple foundation from which a dynamic geometric universe can be derived by extending the selected foundation in a coherent and straightforward way. The toughest task is to find a foundation that puts sufficient restrictions to its own extension such that it becomes comprehensible why the resulting model shows the degree of coherence that we know from observing reality. The nice part of this task is that obviously an important part of that foundation was discovered long ago. However, that part alone is not enough in order to ensure sufficient coherence. The foundation must be helped by mechanisms that ensure extra coherence. These mechanisms are not part of conventional physical theories. In this paper we will try to get more information about these mechanisms.

4 Modular construction

Diving deep into the fundamental structure of physical reality requires a deep dive into advanced mathematics. Usually this goes together with formulas or other descriptions that are incomprehensible to most people. The nice thing about this situation is that the deepest foundation of reality must be rather simple and as a consequence it can be described in a simple way and without any formulas. For example, if the observed signature characterizes physical reality, then the

most fundamental and most influential law of physical reality can be formulated in the form of a commandment:

"THOU SHALT CONSTRUCT IN A MODULAR WAY"

This law is the direct or nearly direct consequence of the structure of the deepest foundation. That foundation restricts the types of relations that may play a role in physical reality. That structure does not yet contain numbers. Therefore it does not yet contain notions such as location and time.

This law is intentionally expressed in the form of a commandment. It is not possible to express this law in the form of a formula, such as $K = m\,a$ or $E \;=\; m\,c^2$. At the lowest level numbers that can be used as variables in formulas do not yet exist. The impact of the commandment is far more influential, than the impact of these famous formulas.

Modular construction acts very economic with its resources and the law thus includes an important lesson:

"DO NOT SPOIL RESOURCES!"

4.1 Modular design

Understanding that the above statements indeed concern the deepest foundation of physics requires deep mathematical insight. Alternatively it requests belief from those that cannot (yet) understand this methodology. On the other hand intuition quickly leads to trust and acceptance that the above major law must rule our existence! Modular design has the intention to keep the relational structure of the target system as simple as is possible.

Modular design is a complicated concept. Successful modular construction involves the standardization of module types and it involves the encapsulation of modules such that internal relations are hidden from the outside. Systems become complicated when many relations and many types of relations exist inside that system, which must be reckoned when the system is analyzed, configured, operated or changed. The reduction in relational complexity plays a significant role during system configuration. The ability to configure modular systems relies heavily on the ability to couple modules and on the capability to let these modules operate in concordance.

The modular design method becomes very powerful when modules can be constructed from lower level modules. The standardization of modules enables reuse and may generate type communities. The success of a type community may depend on other type communities.

An important category of modules are the elementary modules. This are modules, which are themselves not constructed from other modules. These modules must be generated by a mechanism that constructs these elementary modules. Each elementary module type owns a private generation mechanism.

Another category are modular systems. Modular systems and modular subsystems are conglomerates of connected modules. The constituting modules are bonded. Often the modules are coupled via interfaces that channel the information paths that are used by the relations. Modular subsystems can act as modules and often they can also act as independent modular systems.
The hiding of internal relations inside a module eases the configuration of modular (sub)systems. In complicated systems, modular system generation can be several orders of magnitude more efficient than the generation of equivalent monoliths. This means that stochastic modular system generation gets a winning chance against monolithic system construction.

The generation of modules and the configuration of modular (sub)systems can be performed in a stochastic or in an intelligent way. Stochastic (sub)system generation takes more resources and requires more trials than intelligent (sub)system generation. An inexperienced modular designer must first learn to discern which relations are relevant and which relations can be neglected. Predesigned interfaces that combine provide relations and require relations can save much resources.

If all discrete objects are either modules or modular systems, then intelligent (sub)system generation must wait for the arrival of intelligent modular systems.
Intelligent species can take care of the success of their own type. This includes the care about the welfare of the types on which its type depends. Thus for intelligent modular systems, modularization also includes the lesson "TAKE CARE OF THE TYPES ON WHICH YOU DEPEND".

In reality the elementary modules appear to be generated by mechanisms that apply stochastic processes. In most cases system configuration occurs in a trial and error fashion. Only when intelligent species are present that can control system configuration will intelligent design occasionally manage the system configuration and binding process. Thus in the first phase, stochastic evolution will represent the modular system configuration drive. Due to restricted speed of information transfer, intelligent design will only occur at isolated locations. On those locations intelligent species must be present.

5   Mathematical model

We will treat some aspects that involve advanced mathematics. We mainly do that in a descriptive way. However, if they really elucidate, then we will apply formulas. In this model we give **_new names_** to items that we want to discuss in detail. This eases the discussion.

In a modular system, relations play a major role. The success of the described modular construction methodology depends on a particular relational structure that characterizes modular systems.

In 1936 the discoverers of the orthomodular lattice published their discovery in a paper in which they called that lattice "quantum logic". Garret Birkhoff was an expert in lattice theory and John von Neumann was a broadly oriented scientist that was especially interested in quantum physics. "quantum logic" is a strange name because in the same paper the duo showed that the set of closed subspaces of a separable Hilbert spaces has exactly the relational structure of this orthomodular lattice. The name "quantum logic" is only comprehensible, because the relational structure of the orthomodular lattice is quite similar to the relational structure of classical logic and the elements of classical logic are logical propositions. It is not likely that the elements of the orthomodular lattice can be represented by logical propositions, but this immediately creates the question what kind of other objects the elements of the orthomodular lattice represent. The answer is that they represent storage locations of dynamic geometric data. Representations of modules are gathered in a subset of the lattice. This will be elucidated later.

5.1   Separable Hilbert space

The orthomodular lattice extends naturally into a separable Hilbert space. Separable Hilbert spaces are mathematical constructs that act as storage media for dynamic geometric data. Quantum physicists use Hilbert spaces as a base model in which they perform their quantum physical modelling. Each separable Hilbert space is a realization of the orthomodular lattice.

Hilbert spaces are linear vector spaces and each pair of Hilbert vectors owns an ***inner product*** that represents a number, which is a member of a division ring. Hilbert spaces can only cope with number systems that are division rings. The inner product of two perpendicular vectors equals zero. Quantum physicists use the Hilbert space as a storage medium for dynamic geometric data. That happens in the form of eigenvalues of operators, which map some of the Hilbert vectors onto themselves.

The Hilbert space appears to be no more and no less than a flexible structured repository for dynamic geometric data. However, the concept of the Hilbert space appears to be ***very flexible and very feature rich***. This is mainly due to its support of division rings and its ability to embed Hilbert spaces inside an encapsulating infinite dimensional Hilbert space.

5.2   Division rings

For a number system, being a division ring means that every non-zero element of that number system owns a unique inverse. Only three suitable continuum division rings exist. These are the real numbers, the complex numbers and the quaternions. Their rational subsets form discrete division rings. The quaternions form the most elaborate division ring and comprise the other division rings. Number systems exist in several versions that differ in the way that they are ordered. For example multidimensional number systems can be ordered by a selected Cartesian coordinate system and subsequently the result can be ordered by a polar coordinate system. The imaginary part of the quaternionic number system represents a three dimensional space that can be ordered in eight independent ways by a Cartesian coordinate system. The ordering affects the arithmetic properties of the quaternions. Left handed multiplying quaternions exist and right handed multiplying quaternions exist. [6] [7] [8]

5.2.1   Representation of quaternions

Quaternions will be represented by a scalar part that represents the real part of the quaternion and a three dimensional vector part that represents the imaginary part of the quaternion. Bold type face is used for the imaginary parts. The real parts get a suffix $_0$. In many applications the real part represents progression, while the imaginary part represents a spatial location. This representation concerns dynamic geometric data. Quaternions can represent other subjects, but in this paper the representation of dynamic geometric data plays a major role.

5.2.2   Quaternionic multiplication

The quaternionic multiplication rule now follows from:

$$h = f\,g = (f_0 + \boldsymbol{f})\,(g_0 + \boldsymbol{g}) \tag{1}$$

$$h_0 = f_0\,g_0 - \langle \boldsymbol{f}, \boldsymbol{g} \rangle \tag{2}$$

$$\boldsymbol{h} = f_0\,\boldsymbol{g} + \boldsymbol{g}\,f_0 \pm \boldsymbol{f} \times \boldsymbol{g} \tag{3}$$

The $\pm$ sign reflects that left handed and right handed quaternions exist.

5.2.3   Construction and dismantling of numbers

Both Cayley and Conway-Smith produced formulas for ***constructing*** members of number systems from lower dimensional number systems [7]. The dimension increases with a factor two. The reverse

13

process is also possible. The reverse procedure **dismantles** the numbers into two numbers that have a lower dimension. The dimension diminishes with a factor two.

These procedures can be applied inside a quaternionic Hilbert space. There the procedure helps in constructing complex number based subspaces from two real number based subspaces or the construction of quaternion based subspaces from complex number based subspaces. The road back is also possible. These procedures appear to support pair creation and pair annihilation processes.

5.3   Symmetry flavors

Symmetry flavors represent a hardly known feature of quaternionic number systems.

5.3.1   Ordering

Quaternionic number systems exist in many versions that differ in the way that these number systems are ordered. For example it is possible to order the real parts of the quaternions up or down. A Cartesian coordinate system can be used to order the imaginary parts of the quaternions. If the orientation of the coordinate axes is kept fixed, then this Cartesian ordering can be done in eight mutually independent ways. It is also possible to apply spherical symmetric ordering by using a polar coordinate system. This can be done by starting with the azimuth and order it up or down and then order the polar angle and order it up or down. It is also possible to start with the polar angle. A spherical coordinate system starts from a selected Cartesian coordinate system.

5.3.2   Defining symmetry flavors

Quaternions can be mapped to Cartesian coordinates along the orthonormal base vectors 1, $\boldsymbol{i}$, $\boldsymbol{j}$ and $\boldsymbol{k}$; with $\boldsymbol{ij} = \boldsymbol{k}$

Due to the four dimensions of quaternions, quaternionic number systems exist in 16 well-ordered versions $\{q^x\}$ that differ only in their discrete Cartesian symmetry set. The quaternionic number systems $\{q^x\}$ correspond to 16 versions $\{q_i^x\}$ of rational quaternions.

Half of these versions are right handed and the other half are left handed. Thus the handedness is influenced by the symmetry flavor.

The superscript ^{x} can be ⓪, ①, ②, ③, ④, ⑤, ⑥, ⑦, ⑧, ⑨, ⑩, ⑪, ⑫, ⑬, ⑭, or ⑮.

Quaternionic number systems can be used in order to define parameter spaces. We use a superscript ^{x} in order to indicate the symmetry flavor of parameter space $\mathcal{R}^x$. For the **reference parameter space** $\mathcal{R}^⓪$ we often will neglect the superscript ⓪. Later, we will use index ⓪ for the **background parameter space**. The imaginary part of the parameter space $\mathcal{R}^x$ gets a special symbol $\mathfrak{S}^x$. We will call such parameter spaces **symmetry centers**.

Elementary modules own a private symmetry center. The reference parameter space $\mathcal{R}$ owns reference center $\mathfrak{S}$. Graphically the symmetry flavor of $\mathcal{R}$ can be represented by:

⬆⬆⬆⬆

The symmetry related charge of a parameter space follows in three steps.

1. Count the difference of the spatial part of the symmetry flavor of symmetry center $\mathfrak{S}^x$ with the spatial part $\mathfrak{S}$ of the symmetry flavor of reference parameter space $\mathcal{R}$.
2. If the handedness changes from **R** to **L**, then switch the sign of the count.
3. Switch the sign of the result for anti-particles.

We use the names of the corresponding particles that appear in the standard model in order to distinguish the different symmetry flavor combinations. Elementary fermions relate to solutions of a corresponding second order partial differential equation that describes the embedding of these particles.

In a suggestive way, we use the names of the elementary fermions that appear in the Standard Model in order to distinguish the possible combinations of symmetry flavors.

Fermion symmetry flavor					
Ordering x y z τ	Super script	Handedness Right/Left	Color charge	Electric charge * 3	Symmetry center type. Names are taken from the standard model
↑↑↑↑	⓪	**R**	N	+0	neutrino
↓↑↑↑	①	**L**	R	−1	down quark
↑↓↑↑	②	**L**	G	−1	down quark
↓↓↑↑	③	**L**	B	−1	down quark
↑↑↓↑	④	**R**	B	+2	up quark
↓↑↓↑	⑤	**R**	G	+2	up quark
↑↓↓↑	⑥	**R**	R	+2	up quark
↓↓↓↑	⑦	**L**	N	−3	electron
↑↑↑↓	⑧	**R**	N	+3	positron
↓↑↑↓	⑨	**L**	R	−2	anti-up quark
↑↓↑↓	⑩	**L**	G	−2	anti-up quark
↓↓↑↓	⑪	**L**	B	−2	anti-up quark
↑↑↓↓	⑫	**R**	B	+1	anti-down quark
↓↑↓↓	⑬	**R**	R	+1	anti-down quark
↑↓↓↓	⑭	**R**	G	+1	anti-down quark
↓↓↓↓	⑮	**L**	N	−0	anti-neutrino

Spherical ordering can be done by first starting with the azimuth and next proceeding by the polar angle. Both can be done up or down.

Fermions and bosons appear to differ in this choice. Quarks are fermions that are anisotropic and therefore they feature a color charge. That color charge becomes noticeable via the Pauli principle when quarks bind into hadrons. Whether bosons also feature color charge cannot be observed because their binding is not restricted by the Pauli principle. A phenomenon that is known as color confinement hides the appearance of free unbounded quarks.

Also continuous functions and continuums feature a symmetry flavor. Continuous quaternionic functions $\psi^x(q^x)$ and corresponding continuums do not switch to other symmetry flavors ^{y}.

The preferred symmetry flavor version $\psi^y(q^y)$ of a continuous function $\psi^x(q^y)$ is the symmetry flavor of the parameter space $\{q^y\}$.

If the continuous quaternionic function describes the density distribution of a set $\{a_i^x\}$ of discrete objects a_i^x, then this set must be attributed with the same symmetry flavor ^{x}. The real part describes the location density distribution and the imaginary part describes the displacement density distribution.

This section shows that ordering of an embedded (parameter) space can represent specific properties of that space that distinguishes this embedded space from differently ordered embedded (parameter) spaces. This also hold for embedding fields. The consequences comes to the front in situations where differences in ordering play an essential role. We will encounter that situation where different parameter spaces are used in the integration procedure as occurs in the extended Stokes theorem. First we take a look at modules and especially the elementary modules will be investigated. Elementary modules appear to possess their own private parameter space.

5.3.3 Color shift

Pairs of quaternions can shift other quaternions, sets of quaternions and complete quaternionic functions to a different symmetry flavor. The operation

$$c = a\, b/a; \ \text{ where } |a_0| = |\boldsymbol{a}| \tag{1}$$

rotates the imaginary part of b that is perpendicular to $\boldsymbol{a}$ over $\pi/2$ radians. The rotation axis is perpendicular to the imaginary parts of a and b. The direction of the rotation depends on the handedness of the involved numbers.

Especially quaternions for which the size of the real part equals the size of the imaginary part can perform this trick. In this way such quaternions can implement the behavior of **gluons** and **quarks**.

This capability also supports the manipulation of **tri-states**. These are states that exist in three mutually independent versions. In fact the color charge of quarks is an example of a tri-state.

Isotropic particles are not affected by rotating and color shifting quaternions. However, the color confinement phenomenon indicates that the generation of anisotropic elementary particles may get disturbed by color shifts. The controlling mechanisms appear to react by conspiring with mechanisms that control the generation of other anisotropic elementary particles and cooperate in the common generation of isotropic conglomerates. These conglomerates are hadrons and the cooperation represents a binding of the concerned elementary particles. Hadrons have neutral color charge.

5.4 Inner product

Paul Dirac introduced a clear and simple notation for the inner product that is based on the existence of bra's and ket's.

$$\langle x|y \rangle = \langle y|x \rangle^* \tag{1}$$

$$\langle x + y|z \rangle = \langle x|z \rangle + \langle y|z \rangle \tag{2}$$

$$\langle \alpha x|y \rangle = \alpha \langle x|y \rangle \tag{3}$$

$$\langle x|\alpha y \rangle = \langle x|y \rangle \, \alpha^* \tag{4}$$

$\langle x|$ is a **bra vector**. $|y \rangle$ is a **ket vector**. α and $\langle x|y \rangle$ are quaternions.

5.5 Operators

Hilbert space **operators** describe how Hilbert spaces map into other Hilbert spaces and can describe how Hilbert spaces map onto themselves. In the latter case, the inner product describes the relation between a Hilbert vector and its map. If the vector is mapped onto itself then the inner product adds an **eigenvalue** to that vector and the vector is called an **eigenvector**. Thus eigenvalues of normal operators must be members of a division ring. If two eigenvalues differ, then their eigenvectors are perpendicular and the inner product of the two eigenvectors equals zero.

Operators map Hilbert vectors onto other Hilbert vectors. For all Hilbert vectors $|y \rangle$ holds

$$\langle Tx|y \rangle = \langle z|y \rangle \Rightarrow \langle Tx| = \langle z| \tag{1}$$

Via the inner product, the operator T may be linked to an adjoint operator $T^\dagger$.

$$\langle Tx|y \rangle \overset{\text{def}}{=} \langle x|T^\dagger y \rangle \tag{2}$$

$$\langle Tx|y \rangle = \langle y|Tx \rangle^* = \langle T^\dagger y|x \rangle^* \tag{3}$$

A linear quaternionic operator T, which owns an adjoint operator $T^\dagger$ is **normal** when

$$T^\dagger T \ = \ T \, T^\dagger \tag{4}$$

If T is a normal operator, then $T_0 = \left(T + T^\dagger \right)/2$ is a **self adjoint operator** and $\boldsymbol{T} = \left(T - T^\dagger \right)/2$ is an imaginary normal operator. Self adjoint operators are also **Hermitian operators**. Imaginary normal operators are also **anti-Hermitian operators**.

Within a set of mutually orthogonal Hilbert vectors exists no notion of closest member. Only the corresponding eigenvalues may provide a notion of neighborhood. The normal operator that represents an elementary module has no means for controlling the nearness of the subsequent eigenvalues. The normal operator only acts as a descriptor. It does not act as a controller of the nearness of the eigenvalues!

Several mutual orthogonal eigenvectors of a normal operator may share the same eigenvalue. These eigenvectors span a subspace and in that subspace all Hilbert vectors are eigenvector of the normal operator.

If eigenvalues differ, then the corresponding eigenvectors are mutually orthogonal.

5.1 Countable infinity

The dimension of a separable Hilbert space can be countable infinite. It means that all its base vectors can be enumerated with a natural number. This holds for the real number based separable Hilbert space, but it also holds for the quaternionic separable Hilbert space. For finite dimensional separable Hilbert spaces the selection of the number system makes a significant difference.

This facts plays a significant role when the real number based Hilbert space is considered to be embedded inside the quaternionic Hilbert space.

Physical reality appears to apply finite subspaces of infinite dimensional separable Hilbert spaces. Only infinite dimensional separable Hilbert spaces own a unique non-separable companion Hilbert space. Non-separable Hilbert spaces feature operators with uncountable eigenspaces.

5.2 The real number based separable Hilbert space

Inside the real number based separable Hilbert space only operators that feature. We can construct such operator by starting from an orthonormal base that spans this Hilbert space. Next we take all rational numbers and use them to enumerate the base vectors. The corresponding Hermitian operator connects the enumerator with the base vector and in this way they become eigenvalue and eigenvector. This real number based separable Hilbert space can be embedded into a complex number based Hilbert space or in a quaternionic number based Hilbert space. In that case the eigenspace of the specified Hermitian operator can be used as a *model wide clock*.

5.3 Reference operators in a quaternionic separable Hilbert space

Number systems that are division rings can be used to define a category of operators that we will call *reference operators*. The rational values of the number system are used to enumerate the members of an orthonormal base of the Hilbert space. The reference operator connects the enumerator with the base vector and in this way they become eigenvalue and eigenvector. Each reference operator implements a *parameter space* that is defined by its eigenspace.

Reference operators are normal operators and normal operators can be split into a Hermitian operator that has an eigenspace, which is formed by all rational real numbers and an anti-Hermitian operator that has an eigenspace, which is formed by the imaginary parts of the eigenvalues of the normal operator. For each real eigenvalue the Hermitian part of the reference operator owns a complete subspace that is spanned by corresponding eigenvectors. The anti-Hermitian part of the reference operators treats the spatial part of the reference operator.

The Hilbert space can harbor multiple reference operators and in that way it can harbor multiple parameter spaces. Those parameter spaces will in general not share their geometric origins.

5.3.1 Families

In a *family* of reference operators the anti-Hermitian parts are ordered such that the Cartesian coordinate axes run in parallel to each other.

A subset of the reference operators can be considered to be part of the *household* of the Hilbert space. These reference operators form a family. The household family members all share the eigenvectors of the Hermitian operator that has been assigned the task to act as a model wide clock. A special member of this family plays the role of the generator of the *background parameter space*. The parameter spaces that are generated by other family members can *float* with respect to the background parameter space and they can float with respect to each other.
The clock relates to the *kinematics* of the *geometric centers* of these floating parameter spaces.

It must be realized that the clock operator for each of its real eigenvalues corresponds with a one-dimensional subspace and that in relation with a member of the family these one-dimensional subspaces define a **hopping path** rather than a full parameter space. This hopping path is defined relative to the parameter space of the considered reference operator.

In the separable quaternionic Hilbert space, each reference operator that is a family member represents a **hopping path** of the geometric center of the eigenspace of the anti-Hermitian operator through the eigenspace of the anti-Hermitian operator that corresponds to the background reference operator. These two hopping paths are related by the clock operator.

5.3.2   Platforms

Platforms are eigenspaces of a **selected family** of reference operators. The **background platform** belongs to this family. Thus platforms are considered to belong to the household of the Hilbert space. Apart from the background platform will platforms represent **floating parameter spaces**. Each platform owns a geometric center. The anti-Hermitian part of the platform operator describes a **symmetry center**. This is the spatial representative of the platform. The **clock operator** relates to a **hopping path** through the symmetry center. The clock operator relates the hopping path of the considered platform operator with the hopping path of the background platform operator.

5.4   The scanning vane

If the family of a certain reference operator, such as the background reference operator, is singled out, then a special subspace of the Hilbert space can be specified that represents **the current static status quo** of the Hilbert space. In the subspace all eigenvalues of the selected reference operator share the same real part. This specification divides the Hilbert space into three subspaces. The first subspace represents the **past history**. The third part represents the **future**. If the selected real value, which represents progression is allowed to increase, then the second subspace represents a **vane** that scans over the Hilbert space. This simple model represents a very powerful **mathematical test model**.

Several processes occur that have a fixed **duration**. This means that for such processes the passage of the vane has this duration. The duration defines the **regeneration cycle** of discrete objects. The fixed duration enables the capability to discern **properties** of certain objects and/or enables the definition of their **types**.

5.5   Defined operators

By starting from a selected reference operator, it is possible to define a category of **defined normal operators** that use a **continuous function** in order to replace the parameter value by the function value and connect this value with the corresponding eigenvector of the reference operator. In fact the reference operators are special versions of the defined operators for which the defining functions use the parameter value as the function value. This procedure is very powerful and merges Hilbert space operator technology with function theory.

5.5.1   The reverse bra-ket method

Reference operators and defined operators can be described with the help of the reverse bra-ket method. The following procedure defines the background reference operator $\mathcal{R}$.

We start with a very simple defining function $\mathcal{R}(q) = q$ and the corresponding operator $\mathcal{R}$.

Let $\{q_i\}$ be the set of **rational** quaternions in a selected quaternionic number system and let $\{|q_i\rangle\}$ be the set of corresponding base vectors. They are the eigenvectors of a normal operator $\mathcal{R}$. Here we enumerate the base vectors with index i.

$$\mathcal{R} \stackrel{\text{def}}{=} |q_i\rangle q_i \langle q_i| = |q_i\rangle \Re(q_i)\langle q_i| \tag{1}$$

$\mathcal{R}$ is the **configuration parameter space operator**. $\mathfrak{R}(q)$ is a quaternionic function, whose target equals its parameter space. The definition (5) also covers the situation where the dimension of the (sub) space is infinite.

This **reverse bra-ket notation** must not be interpreted as a simple outer product between a ket vector $|q_i\rangle$, a quaternion q_i and a bra vector $\langle q_i|$. Actually, it involves a complete set of eigenvalues $\{q_i\}$ and a complete orthomodular set of Hilbert vectors $\{|q_i\rangle\}$. It implies a summation over these constituents, such that for all bra's $\langle x|$ and all ket's $|y\rangle$:

$$\langle x|\mathcal{R}\ y\rangle = \sum_i \langle x|q_i\rangle q_i\langle q_i|y\rangle \tag{2}$$

Thus formula (6) represents the full definition for the shorthand (5). $\mathfrak{R}$ is a special operator. It can be considered as a property of the combination of the separable Hilbert space $\mathfrak{H}$ and one of the existing versions of the quaternionic number system.

$\mathcal{R}_0 = \left(\mathcal{R} + \mathcal{R}^\dagger\right)/2$ is a self-adjoint operator. Its eigenvalues can be used to arrange the order of the eigenvectors by enumerating them with the real eigenvalues. The ordered eigenvalues can be interpreted as **progression values**.

$\boldsymbol{\mathcal{R}} = \left(\mathcal{R} - \mathcal{R}^\dagger\right)/2$ is an imaginary operator. Its eigenvalues can also be used to order the eigenvectors. The eigenvalues can be interpreted as **spatial locations** and can be ordered in several ways. For example eight independent ways exist to order the 3D spatial domain by using Cartesian coordinates. We will use special indices in order to attach operators to versions of number systems.

Let $f(q)$ be a mostly continuous quaternionic function. Now the reverse bra-ket notation defines operator f as:

$$f \overset{\text{def}}{=} |q_i\rangle f(q_i)\langle q_i| \tag{3}$$

f defines a new operator that is based on function $f(q)$. Here we suppose that the target values of f belong to the same version of the quaternionic number system as its parameter space does.

Operator f has a countable set of discrete quaternionic eigenvalues.

For this operator the reverse bra-ket notation (7) is a shorthand for

$$\langle x|f\ y\rangle = \sum_i \langle x|q_i\rangle f(q_i)\langle q_i|y\rangle \tag{4}$$

Alternative formulations for the reverse bra-ket definition are:

$$f \overset{\text{def}}{=} |q_i\rangle f(q_i)\langle q_i| = |q_i\rangle\langle f(q_i)q_i| = |q_i\rangle\langle fq_i| = |f^*(q_i)q_i\rangle\langle q_i| = \left|f^\dagger q_i\rangle q_i\langle q_i\right| \tag{5}$$

Here we used the same symbol for the operator f and the function $f(q_i)$. For this operator the eigenvalues of the Hermitian part $f_0 = \left(f + f^\dagger\right)/2$ are not interpreted as progression values. Often (not always!), these values can be interpreted as dynamic location density descriptors. Similarly, the eigenvalues of the anti-Hermitian part $\boldsymbol{f} = \left(f + f^\dagger\right)/2$ are not interpreted as spatial location values. The eigenspace of normal operator f will represent fields.

The left side of (8) only equals the right side when the domain over which the summation is taken is restricted to the region of the parameter space $\mathcal{R}$ where $f(q)$ is sufficiently continuous.

5.5.2   Symmetry centers

Reference operators are a special kind of defined operators. The anti-Hermitian parts of the reference operators that belong to the family of the background reference operator play a special role and we will use special symbols for them.

We can define a category of anti-Hermitian operators $\{\mathfrak{S}_n^x\}$that have no Hermitian part and that are distinguished by the way that their eigenspace is ordered by applying a ***polar coordinate system***. We call them symmetry centers $\mathfrak{S}_n^x$. A polar ordering always start with a selected Cartesian ordering. The geometric center of the eigenspace of the symmetry center floats on a background parameter space of the normal reference operator $\mathcal{R}$, whose eigenspace defines a full quaternionic parameter space. The eigenspace of the symmetry center $\mathfrak{S}_n^x$ acts as a three dimensional spatial parameter space. The super script ^{x} refers to the symmetry flavor of $\mathfrak{S}_n^x$. The subscript $_n$enumerates the symmetry centers. Sometimes we omit the subscript.

$$\mathfrak{S}^x = |\mathfrak{s}_i^x\rangle \mathfrak{s}_i^x \langle \mathfrak{s}_i^x| \tag{1}$$

$$\mathfrak{S}^{x\dagger} = -\mathfrak{S}^x \tag{2}$$

It must be noticed that the eigenvalues of the symmetry center operator have no real part! However, when mapped to another parameter space, the geometric center location of the symmetry center eigenvalues can be a function of progression.

The symmetry centers can be ordered with the help of a Cartesian coordinate system as well as with the help of a polar coordinate system. ***In the platform family the ordering of the symmetry center is defined relative to the ordering of the background platform.*** This ordering determines the ***symmetry flavor*** of the symmetry center. The difference of the symmetry flavor of a selected symmetry center with the symmetry flavor of the background platform determines the symmetry related charge of the selected symmetry center. This charge can be split in an isotropic part, an anisotropic part and a spin.

The short list of isotropic symmetry related charges covers: $-3, -2, -1, 0, +1, +2, +3$. For historical reasons, these numbers must be divided by 3 in order to get the equivalent electric charges. The anisotropic symmetry related charges correspond to color charges and correspond with the three perpendicular directions and the opposite directions in which ordering anisotropy can manifest itself.

Symmetry center s can be rotated by a pair of quaternions that are each other's inverse. Special quaternions exist of which the size of the real part equals the size of the imaginary part. These special quaternions can shift the anisotropy of a symmetry center to another dimension.

5.6   Non-separable companion Hilbert space

Each infinite dimensional separable Hilbert space owns a unique companion non-separable Hilbert space that features operators, which have continuum eigenspaces. Such eigenspaces can form flat parameter spaces or dynamic fields. This can easily be comprehended when in the non-separable Hilbert space a similar procedure is used for specifying defined operators as we applied in the separable Hilbert space. In that procedure we specified reference operators and we defined normal operators by using continuous functions. This time we not only use the rational members of the number system, but we also apply the irrational members and we use the same continuous functions. The consequence is that the notion of dimension of the subspaces may lose its sense. The

procedure that creates defined operators now links operator technology with function technology, differentiation technology and integration technology.

The separable Hilbert space can be considered to be embedded in its non-separable companion. Platforms that step in the separable Hilbert space will float in the non-separable companion Hilbert space. In a similar way the clock steps in the separable Hilbert space and the clock floats in its non-separable companion.

The scanning vane can be interpreted as a progressive embedding of the separable Hilbert space into its non-separable companion.

In the non-separable Hilbert space the reverse bracket method applies integration rather than summation in order to define operators that have continuum eigenspaces.

For the shorthand of the reverse bra-ket notation of operator $\mathcal{F}$ the integral over q replaces the summation over q_i.

$$\langle x | \mathcal{F} \, y \rangle = \sum_{i=0}^{i=\infty} \langle x | q_i \rangle \mathcal{F}(q_i) \langle q_i | y \rangle \approx \int_q \langle x | q \rangle \mathcal{F}(q) \langle q | y \rangle \; dq \tag{1}$$

The integral only equals the sum sufficiently close when the function $\mathcal{F}(q)$ is sufficiently continuous in the domain over which the integration takes place. Otherwise the left side only equals the right side when domain is restricted to the region of the parameter space $\mathfrak{R}$ where $\mathcal{F}(q)$ is sufficiently continuous.

5.6.1 Platform dynamics

In the separable Hilbert space, platforms can step relative to the background platform. This can occur with a minimal spatial step size. In the non-separable Hilbert space the corresponding platforms float relative to the background platform.

Quaternionic platforms can be converted into two complex number based platforms and two complex number based platforms can be converted into a quaternionic platform. At conversion, the quaternionic platforms mirror at the vane.

5.6.2 Artifacts

Nearness between mutually orthogonal Hilbert vectors is not defined. Only via eigenvalues of eigenvectors the nearness of the eigenvectors makes sense. In an infinite dimensional separable Hilbert space it is always possible to add or subtract base vectors without changing the dimension of the Hilbert space. After enumerating an orthonormal base with an ordered set of equidistant rational numbers it is possible to add base vectors that disrupt the equidistant ordering. These additional base vectors will act as artifacts in the eigenspace of the operator that uses the orthonormal base as its eigenvectors. Artifacts may occur in coherent swarms and the swarm may feature its own internal ordering that differs from the ordering of the original orthonormal base. Adding a new base vector that does not disrupt the equidistant ordering will not produce a noticeable artifact but that addition is impossible inside infinite equidistant sets.

In the non-separable Hilbert space the addition of a single base vector or of a coherent swarm of ordered base vectors will always present artifacts.

5.7   Modules as subspaces

According to the discoverers of the orthomodular lattice, the elements of the lattice can be represented as closed subspaces of a separable Hilbert space. It also has sense to consider a subset of these elements as representatives of modules or modular systems. Thus, not every closed subspace of a separable Hilbert space represents a module or modular system, but every module and every modular system is represented by a closed subspace of the separable Hilbert space. Compared to general closed subspaces of the Hilbert space, will modules and modular systems have extra characteristics.

5.8   Elementary modules

An elementary module cannot be represented by a single Hilbert vector, because that single vector can on the utmost correspond to a static geometric location and from reality we know that modules possess a dynamic geometric location and that fact also holds for the elementary modules. However, elementary modules cannot be split into other modules. Thus the subspaces that represent elementary modules must have multiple dimensions. Still it is possible that at each progression instant each module represents exactly one spatial location. This is a very special condition, but we **postulate** that this special condition is valid for all elementary modules. As a consequence of this postulate the vane contains representatives of elementary modules that are one-dimensional subspaces. They cannot be split into lower level modules.
The postulate forbids that two elementary modules at the same progression instant take the same geometric location.
The vane contains many subspaces that do not contain Hilbert vectors that represent an elementary module. These subspaces are representing **empty space**.

5.9   Germ operators

The elementary modules are represented by a new category of operators that differ from reference operators and that differ from defined operators but that describe the dynamics of elementary modules. This means that they are coupled to the clock operator, but they are not member of an operator family. The dynamic location of elementary modules hops as a function of progression. After a while the hops form a **swarm** and both the **hopping path** and the swarm represent the elementary module. The operators will be called **germ operators**. We will use symbol σ for the germ operators. The germ operators are controlled by mechanisms that apply stochastic processes for the generation of the dynamic locations.
The germ operator uses its own private reference operator. This means that the elementary modules reside on their own platform, which applies its own private parameter space that may float with respect to the selected background parameter space. The eigenvalues of the anti-hermitic part of the germ operator correspond exactly with the eigenvalues of the anti-hermitic part of the corresponding platform operator. **The germ operators are decoupled from the ordering of the family operators**. Spatial ordering will destroy their coupling to the clock operator. The hop landings act as point-like artifacts!

5.10 Hopping paths and swarms

After generation, the dynamic locations of an elementary module will be ordered with respect to the real value of the quaternions that represents the dynamic location. After ordering of the progression values the elementary module appears to walk along a hopping path and the landing positions form a location swarm. An uncontrolled generation would produce an arbitrary hopping path and a chaotic hop landing location swarm. The mechanism is supposed to ensure that a coherent swarm is generated.

This means that elementary modules are represented by closed subspaces of a Hilbert space that may have a huge dimension. However, at a single progression instant, each elementary module is represented by a subspace that is spanned by a single Hilbert vector. Thus modules and modular

systems are represented by a subset of the orthomodular lattice. Within that subset the elementary modules are represented by elements that act as atoms of the subset.

If the swarm contains a large number of hop landing locations, then its geometric center will move in a much less chaotic way. A large number of elements also means an equivalently long regeneration cycle of the swarm. Increasing the number of hop landings will increase the inertness of the swarm.

5.11 Mechanisms

From reality we know that the hopping path is not an arbitrary path and the location swarm is not a chaotic collection. Instead the swarm forms a coherent set of locations that can be characterized by a rather continuous location density distribution. That does not say that the hopping path is not a stochastic path! ***The location swarm integrates over the regeneration cycle***. Its characteristics are statistical characteristics.

From physics we know that elementary particles own a wave function and the squared modulus of that wave function forms a continuous probability density distribution, which can be interpreted as a location density distribution of a point-like object. The location density distribution owns a ***Fourier transform*** and as a consequence the swarm owns a ***displacement generator***. This means that at first approximation the swarm can be considered to ***move as one unit***. Thus the swarm is a coherent, rather smoothly moving object, which represents the violent stochastic hopping of a point-like object. For a large part this is due to the fact that the swarm contains a huge number of locations that is refreshed in a cyclic fashion.

The fact that at every progression instant the swarm owns a Fourier transform means that at every progression instant the swarm can be interpreted as a wave package. Wave packages can represent interference patterns, thus they can simulate wave behavior. The problem is that moving wave packages tend to disperse. The swarm does not suffer that problem because at every progression instant the wave package is regenerated. The result is that the elementary module shows wave behavior and at the same time it shows particle behavior. When it is detected it is caught at the precise location (the exact swarm element) where it was at this progression instant.

The Hilbert space is nothing more and nothing less than a structured storage medium for dynamic geometric data. It does its storage task in a very precise way, thus without any uncertainty! Neither the separable Hilbert space nor its non-separable companion does contain functionality that ensures the coherent dynamic behavior of the location swarms. Dedicated mechanisms, which do not belong to the household of the Hilbert spaces fill the eigenspaces of the stochastic germ operators that control the elementary modules. The hopping path only stops when the elementary module is "detected" and the controlling mechanism changes to a different mode of operation.

5.12 Dynamic model

We did construct a vane that splits the Hilbert space such that all elementary module eigenvalues that have a selected real value have the corresponding eigenvector inside the vane. The vane splits the Hilbert space in an historic part, the vane itself and a future part. The vane then represents a static status quo that corresponds to the current state of the universe.

This represents an interesting possibility. The Hilbert space can be seen as a storage medium that contains a repository of all historic, present and future data. Or it can be interpreted as a scene that is ***observed by modular systems*** that travel with the vane. These observers might know part of the stored history, but have no notion of the future. Depending on their capabilities, the observers reflect only a part of their history. Information that inside the vane is generated at a distance has still to travel through an information carrying field that acts as the living space for the elementary modules in order to reach the observer. The encounter will take place in the future. Information that

reaches the observer arrives from the past. Those kinds of information travel via information carriers. In addition, the observers meet new conditions when the vane passes over them.

The vane forms a subspace of the Hilbert space and for each elementary module that subspace contains a single Hilbert vector that plays as eigenvector for the corresponding geometric location. This location is the landing point of a hop rather than the geometric center of the location swarm.

Quaternionic platforms can be converted into two complex number based platforms and two complex number based platforms can be converted into a quaternionic platform. At conversion, the quaternionic platforms mirror at the vane. The mirrors carry a particle at one side and an anti-particle at the other side. The conversion takes a fixed duration. The processes are supported by number construction procedures or number dismantling procedures.

5.13 Defining fields

Fields are eigenspaces of defined operators that reside in the companion non-separable Hilbert space and that have continuum eigenspaces. This enables the treatment of fields independent of their defining functions and the corresponding parameter spaces. However, if the dynamic behavior of fields must be investigated, then the quaternionic differential calculus must be applied in order to formulate corresponding defining functions and defined operators.

5.14 Living space

The germ operators have no equivalent inside the non-separable Hilbert space. However, their eigenvalues may be sensed by a field that exists as eigenspace of a defined operator, which resides in the non-separable Hilbert space. This can occur when the separable Hilbert space is *embedded* in its non-separable companion Hilbert space. We will call the mentioned field the *living space* of the modules and modular systems.

The hopping path that represents an elementary module, corresponds to a coherent location swarm, which is characterized by a location density distribution. Via the convolution of the *Green's function* of a field and this location density distribution, the swarm corresponds to a deformed part of the field. In this way the field describes the existing elementary modules. The description of a nearby located elementary particles deforms the field in that region. The convolution means that the Green's function blurs the location density distribution. This can be interpreted as if the hopping landing locations influence the field, but the alternative interpretation is that the field is a kind of blurred descriptor of the hopping landing locations. Anyway the landing locations and the discussed field are intimately coupled. The deformed field can be interpreted as the living space of the modules and modular systems.

5.15 Green's function

At every progression instant, the hop landing locations cause the emission of a spherical shape keeping front. That front keeps its shape, but the amplitude of that shape diminishes as $1/r$ with distance r from the emission location. The fronts proceed outwards with a fixed speed. The shape keeping front is a solution of the homogeneous second order partial differential equation that describes the dynamic behavior of the affected field. Later we will identify both the hop and the corresponding solution by using the name *clamp* for these phenomena. If this effect is integrated over the regeneration cycle of the swarm, then the Green's function results. The integration turns the homogeneous second order partial differential equation into an inhomogeneous second order partial differential equation. The extra term that makes the equation inhomogeneous concerns the Green's function. The amplitude of the Green's also diminishes as $1/r$ with distance r from the emission location.

5.16 Stochastic processes

The mechanisms that generate the hopping landing location control the dynamics of the model. These mechanisms use stochastic processes. These processes appear to belong to a category which is mathematically known as inhomogeneous spatial Poisson point processes. In more detail these processes probably are similar to modified Thomas processes.

This fact is supported by a signature that is visible in the visual trajectory of a category of living species that are called vertebrates. It appears that the visual trajectory of all vertebrates is optimized for low dose rate imaging. This visual system contains noise filters that block information for which the signal to noise ratio is too low. This signal to noise ratio is typical for information generated by Poisson processes that are attenuated by subsequent binomial processes that are implemented by spatial point spread functions. The mechanisms appear to apply inhomogeneous spatial Poisson point processes. See: "Low Dose Rate Imaging"; http://vixra.org/abs/1606.0329 . Humans are vertebrates and their visual perception at starlight conditions is governed by the described processes.

Physical theories stop at the **wave function** of particles. This exposure of the mechanisms dives deeper and reaches the **characteristic function** of the stochastic process that controls the generation of the landing locations that form the hopping path.

5.17 Self-coherence

It is difficult to belief in a creator that installs separate mechanisms, which ensure the dynamic coherence of the generated modules. It is easier to accept that the relation between the generated location swarms and the field that describes these swarms is based on a mathematically explainable kind of self-coherence. In case of self-coherence, the interaction between the field and the swarm restricts the possible location density distribution. As is indicated earlier, this restriction may be influenced by the number of elements that are contained in the swarm. This fact may explain the existence of **generations** of elementary modules. A larger number of elements increases the inertness of the swarm. However, also the living space field takes a role in the self-coherence of the swarm.

In the relation between the swarm and the field, the Green's function of the field plays an important role. It plays the role of a potential that implements an attracting force. Another factor is the kind of stochastic process that generates the individual locations. This process belongs to the category of the inhomogeneous spatial Poisson point processes. Each hop tries to displace the geometric center of the swarm. This displacement represents an acceleration of the geometric center of the swarm.

Let the Green's function represent a scalar potential. When the platform on which the elementary object resides moves with a uniform speed with respect to the background parameter space, then the scalar potential will in that coordinate system turn into a vector potential. Differential calculus learns that the dynamic change of the vector field goes together with a new field that counteracts the acceleration. This effect is similar to the phenomenon that is known as inertia. It looks as if the center of geometry of the swarm is attracting the accelerating hopping elementary object. This is an effective kind of self-coherence that is installed via the living space field.

In order to elucidate this obscure description, we will try to explain this by applying formulas.

The Green's function $G(\boldsymbol{q})$ represents a **scalar potential**. $\boldsymbol{c}$ is the landing location of the hop. The Green's function is given by:

$$G(\boldsymbol{q}) = m_1 / |\boldsymbol{q} - \boldsymbol{c}| \tag{1}$$

If the platform travels with **uniform speed v**, then this corresponds with a **vector potential $A(q)$**:

$$A(q) = G(q)\, v \tag{2}$$

Acceleration goes together with a **new vector field $E(q)$**:

$$E(q) \stackrel{\text{def}}{=} \dot{A}(q) = \nabla\, G(q)\, \dot{v} \tag{3}$$

The new vector field ensures that the total change of the base field stays zero.

This goes together with an attracting **force $F(q)$**

$$F(q) = m_2\, E(q) = \frac{m_1 m_2\, \dot{v}}{|q - c|^2} \tag{4}$$

This attractive force acts between the landing location of the hopping object and the geometric center of the swarm. $\dot{v}$ is the **acceleration** of the geometric center of the swarm that is due to the addition of the individual hop. The swarm covers a huge number of landing locations. This is represented by the factor m_2. The added hop landing concerns just a single location. This indicates that with respect to inertia **the mass of the swarm is proportional to the number of contained hopping locations.**

The concept of force raising field is treated in a special section of this paper.

The location density distribution of the swarm is blurred by the Green's function. If the location density distribution has the form of a Gaussian distribution, then the blurred function is the convolution of this location density distribution and the Green's function. The shape of this **example** is given by:

$$\chi_n(r) = -\frac{C_n}{4\pi}\, \frac{ERF\left(r/_{\sigma\sqrt{2}}\right)}{r} \tag{6}$$

In this function every trace of the singularity of the Green's function has disappeared. It is due to the huge number of participating hop locations. This is just an example. Such extra potentials add a local contribution to the field that acts as the living space of modules and modular systems. The shown extra contribution is due to the local elementary module. The living space is constituted by a myriad of such bumps.

5.18 The symmetry related field

The convolution of the location density distribution of the swarm with the Green's function involves an integration and the local contribution to the integral involves two parameter spaces. One of them is the background parameter space. These parameter spaces may differ in their ordering. In order to cope for this difference the platform on which the elementary object resides must be encapsulated. The integration is an application of the **generalized Stokes theorem**. This theorem converts an integral over a volume into an integral over the boundary of that volume. The boundary must only cross regions of the parameter spaces where the field and the extra potential are both continuous and the amplitude of the extra potential must become negligible. In fact the influences of the ordering characterize the parameter spaces rather than the deformed fields. For the parameter spaces the condition is automatically fulfilled and therefore the shape of the boundary does not

matter. For that reason we select a boundary that has the form of a ***cube***, whose axes are aligned along the axes of the Cartesian coordinate systems that is used to order the background parameter space. This procedure enables the correct accounting for the differences in the ordering. This accounting process reveals values that we will call ***charges*** that go together with the difference in ordering. This reveals the short list of electric charges and the color charges that appear in the Standard Model. The charges will be anchored on the geometric centers of the floating platforms. These ***symmetry related charges*** are the source of a new separate basic field that we will call the ***symmetry related field***. This field differs fundamentally from the field that represents the living space of the elementary modules.

The field that is influenced by the clamps and the new symmetry related field are coupled via the geometric centers of the platforms that carry the swarm elements.

5.19 Partial differentiation

In this section we intensively use formulas. These formulas keep the description compact and comprehensive.

We use the quaternionic nabla ∇ in order to provide a compact description of quaternionic partial differentiation.

$$\nabla = \left\{ \frac{\partial}{\partial \tau}, \frac{\partial}{\partial x}, \frac{\partial}{\partial y}, \frac{\partial}{\partial z} \right\} = \frac{\partial}{\partial \tau} + i\frac{\partial}{\partial x} + j\frac{\partial}{\partial y} + k\frac{\partial}{\partial z} = \nabla_0 + \boldsymbol{\nabla} \tag{1}$$

$$\nabla f = \sum_{\mu=0}^{3} \frac{\partial f}{\partial q_\mu} e_\mu \tag{2}$$

This form of the partial differential equation highlights the fact that in first order and second order partial differential equations ***the nabla operator and some of the related differential operators can be applied as a multiplier***. This means that we can apply the quaternionic multiplication rule. As a consequence these partial differential operators can be used to define corresponding fields and their operators.

$$\Phi_0 = \nabla_0 \psi_0 - \langle \boldsymbol{\nabla}, \boldsymbol{\psi} \rangle \tag{3}$$

$$\boldsymbol{\Phi} = \nabla_0 \boldsymbol{\psi} + \boldsymbol{\nabla}\psi_0 \pm \boldsymbol{\nabla} \times \boldsymbol{\psi} \tag{4}$$

These equations invite the definition of derived vector fields:

$$\mathfrak{E} \stackrel{\text{def}}{=} -\nabla_0 \boldsymbol{\psi} - \boldsymbol{\nabla}\psi_0 \tag{5}$$

$$\mathfrak{B} \overset{\text{def}}{=} \boldsymbol{\nabla} \times \boldsymbol{\psi} \tag{6}$$

The $\pm$ sign indicates that the nabla operator is also afflicted by symmetry properties of the applied quaternionic number system. The above equations represent only low order partial differential equations. Thus, these partial differential equations represent approximations rather than precise descriptions of the considered change. In this form the equations can still describe point-like disruptions of the continuity of the field. We can take the conjugate:

$$\Phi^* = (\nabla\psi)^* = \nabla^*\psi^* \mp 2\,\boldsymbol{\nabla} \times \boldsymbol{\psi} \tag{7}$$

$$\nabla^*(\nabla^*\psi^*)^* = \nabla^*\Phi = \nabla^*\nabla\psi \tag{8}$$

Two different non-homogeneous second order partial differential equations exist that offer different views on the embedding process. The equation that is based upon the double quaternionic nabla $\nabla\nabla^*$ cannot show wave behavior. However, the equation that is based on d'Alembert's operator $\mathfrak{D}$ acts as a wave equation, which offers waves as part of its set of solutions. Both second order partial differential operators can be applied as multipliers.

$$\nabla\nabla^* = \nabla_0\nabla_0 + \langle \boldsymbol{\nabla}, \boldsymbol{\nabla} \rangle \tag{9}$$

$$\mathfrak{D} \overset{\text{def}}{=} -\nabla_0\nabla_0 + \langle \boldsymbol{\nabla}, \boldsymbol{\nabla} \rangle \tag{10}$$

In isotropic conditions the homogeneous equations look like:

$$\frac{\partial^2\psi}{\partial x^2} + \frac{\partial^2\psi}{\partial y^2} + \frac{\partial^2\psi}{\partial z^2} \pm \frac{\partial^2\psi}{\partial \tau^2} = \frac{1}{r^2}\frac{\partial}{\partial r}\left(r^2\frac{\partial\psi}{\partial r}\right) \pm \frac{\partial^2\psi}{\partial \tau^2} = 0 \tag{11}$$

These equations have special solutions in odd numbers of participating dimensions in the form of *shape keeping fronts*.

The d'Alembert's equation offers solutions in the form of waves. That does not hold for the double nabla operator that is defined in (9). That equation can be split into two first order partial differential equations:

$$\Phi = \nabla\,\psi \tag{12}$$

$$\rho = \nabla^*\Phi = \nabla^*\nabla\,\psi \tag{13}$$

The similarity to Maxwell equations is not accidental. Equation (3) has no equivalent in Maxwell equations. In physics this lack is compensated by special gauge equations.

5.20 Elementary behavior

Fields act on point-like artifacts in an elementary way. The d'Alembert's operator offers plane and spherical waves and both second order equations offer shape keeping fronts as elementary solutions.

5.20.1 Waves

Waves are solutions of the wave equation that uses d'Alembert's operator $\mathfrak{D}$:

$$\mathfrak{D} f = \left(-\nabla_0 \nabla_0 + \langle \boldsymbol{\nabla}, \boldsymbol{\nabla}\rangle\right) f = 0 \tag{1}$$

$$\nabla_0 \nabla_0 f = \langle \boldsymbol{\nabla}, \boldsymbol{\nabla}\rangle f = -\omega^2 f \tag{2}$$

For Cartesian symmetry conditions this leads to:

$$f(\tau, \boldsymbol{x}) = a \exp\left(\mathbb{i}\, \omega(c\tau - |\boldsymbol{x} - \boldsymbol{x}'|)\right); \ c = \pm 1 \tag{3}$$

In spherical symmetric conditions, equation (2) leads to a category of solutions that are known as solutions of the Helmholtz equation. However, here proper time τ replaces coordinate time.

5.20.2 One dimensional fronts

These solutions proceed in one spatial dimension, but they may act in a three dimensional spatial setting. Thus :

$$\frac{\partial^2 \psi}{\partial z^2} \pm \frac{\partial^2 \psi}{\partial \tau^2} = 0 \tag{1}$$

We try a solution in the form $\varphi = f(\alpha z + \beta \tau)$:

$$\frac{\partial f}{\partial z} = \alpha f'; \frac{\partial^2 f}{\partial z^2} = \alpha \frac{\partial f'}{\partial z} = \alpha^2 f'' \tag{2}$$

$$\frac{\partial f}{\partial \tau} = \beta f'; \frac{\partial^2 f}{\partial \tau^2} = \beta \frac{\partial f'}{\partial \tau} = \beta^2 f'' \tag{3}$$

$$\alpha^2 f'' \pm \beta^2 f'' = 0 \tag{4}$$

This is solved when $\alpha^2 = \mp \beta^2$.

For the first kind of the second order partial differential equation this means: $\beta = \pm \alpha\, \boldsymbol{i}$, where $\boldsymbol{i}$ is a normalized imaginary quaternion. With $g(z) = f(\beta\, z)$ follows:

$$\varphi = g(z\, \boldsymbol{i} \pm \tau) \tag{5}$$

The function g represents a **shape keeping front**. It also **keeps its amplitude**. It is not a wave.

The imaginary $\boldsymbol{i}$ represents the base vector in the x, y plane. Its orientation θ may be a function of z.

For the second kind of the second order partial differential equation this means: $\beta = \pm \alpha$. With $g(z) = f(\beta\, z)$ follows:

$$\varphi = g(z \pm \tau) \tag{6}$$

The corresponding hop landing that represents the continuity disturbing artifact will be called **warp**. *A warp corresponds to the hop of the geometric center of the platform on which the corresponding elementary particle resides*. Thus the location of the hop is defined relative to a geometric location on the carrier field that is defined with respect to the background parameter space. The platform carries its own private parameter space. Subsequent warps occur in "linear" **strings** that follow the deformation of the carrier field. Such strings will be called **messengers**. Warps can also occur as single hops. Warp hops shift the geometric centers of parameter spaces relative to the background parameter space. As solutions of the second order partial differential equation the warp shifts the map of the geometric center of the platform onto the carrying field to a subsequent location on that carrying field.

Combined in strings the warps can only shift empty platforms. Any clamp in the platform would conflict with the warp speed.

5.20.3 Spherical fronts

Next we focus on the three dimensional spherical symmetric condition. In that case the equations can be separated by writing $\psi = r\, \varphi(r, \tau)$

$$\frac{\partial^2 \varphi}{\partial r^2} + \frac{2}{r}\frac{\partial \varphi}{\partial r} \pm \frac{\partial^2 \varphi}{\partial \tau^2} = 0 \Rightarrow \frac{\partial^2 \psi}{\partial r^2} \pm \frac{\partial^2 \psi}{\partial \tau^2} = 0 \tag{1}$$

With other words ψ fulfills the conditions of the one-dimensional case. Thus solutions in the form $\varphi = f(\alpha r + \beta \tau)/r$ will fit.

For the first kind of the second order partial differential equation this means: $\beta = \pm \alpha\, \boldsymbol{i}$, where $\boldsymbol{i}$ is a normalized imaginary quaternion. With $g(x) = f(\beta\, x)$ follows:

$$\varphi = g(r\,\boldsymbol{i} \pm \tau)/r \qquad\qquad (2)$$

$\boldsymbol{i}$ represents a base vector in radial direction.

The corresponding hop landing that represents the continuity disturbing artifact will be called a **clamp**. The clamp corresponds to a hop relative to the geometric center of the platform on which the elementary particle resides. Thus the location of the hop is defined relative to this geometric location. The description uses the parameter space that is private to the platform and the elementary particle. This description is "mapped" onto the field that represents the living space of the elementary modules. The map represents an interaction. Clamps occur in coherent swarms. All swarm elements share the same platform. Thus the swarm moves as a single unit.

For the second kind of the second order partial differential equation this means: $\beta = \pm\alpha$. With $g(x) = f(\beta\,x)$ follows:

$$\varphi = g(x \pm \tau)/r \qquad\qquad (3)$$

These solutions feature a fixed speed and a fixed shape. However, their amplitude diminishes as $1/r$ with distance r from the sources. When integrated over a long enough period of progression the result takes the form of the fields Green's function.

5.20.4 Sets of clamps, sets of warps and regeneration cycles

The homogeneous second order partial differential equation offers two kinds of solutions that represent shape keeping fronts. One kind concerns the spherical shape keeping fronts. The second kind acts in one-dimension and not only keeps its shape, it also keeps its amplitude.

1.1.1.1   Swarms of clamps

Hops that correspond to solutions, which represent spherical shape keeping fronts will be called clamp hops or clamps. The same name is used for this type of solutions of the homogeneous second order differential equations. Clamps occur in swarms and reside on a platform that as long as the elementary module exists is private to that elementary module. During that episode, the symmetry center carries an ordered parameter space. Each elementary module type exists in a set of generations and each of these generations shows a cyclic regeneration period. The swarms have a corresponding number of elements.

Integration of clamp solutions over the regeneration cycle turns them into Green's functions. During that operation the violent varying function that describes the **living space field** changes in a rather coherently varying function that represents a blurred representation of the original field. This blurred field represents the **living space potential**. From now on, if we speak about the living space, then we mean the living space potential.

1.1.1.2   Strings of warps

Hops that correspond to solutions, which represent one-dimensional shape keeping fronts will be called warp hops or warps. The same name is used for this type of solutions of the homogeneous second order differential equations. Warps correspond to hops of platforms on which elementary modules **may** reside. Warps occur in isolation or equidistant in strings. The platforms that correspond to warp strings have lost their symmetry center. As a consequence these platforms do

not own a symmetry related charge. The warps do not deform their carrying field, which is the living space field.

The warp strings feature a *spatial and a temporal frequency*. We postulate that locally and in the same progression period the warp strings will feature a *fixed regeneration cycle* and a *fixed spatial path length* that are *the same* for all warp strings. This makes it possible to distinguish the individual warp strings via their frequency. This frequency determines the *information capacity* of the string. Each string member carries a *unit of information*. The path of the warp string is located inside and with respect to the carrying field. Thus the path follows the deformation of the field. This field represents the living space of the elementary modules.

The homogeneous second order partial differential equation of the carrying field describes the corresponding warp solutions. These solutions feature a fixed speed. The path length determines the *passage duration* of an information messenger. That duration equals the regeneration cycle of the string.

The behavior of the warp strings invites their interpretation as *information messengers*. The path length postulate only holds locally. Taken over huge ranges of the carrying field or over a long period, the path length may vary in a smooth way. This phenomenon is the subject of the equivalent of Hubble's law.

5.21 Messenger redistribution and messenger redirection

Some types of modular (sub)systems, which we will call *atomic modular systems* are capable of *splitting* information messengers into a set of new information messengers. Further they can *absorb* information messengers and *emit* information messengers. During the split action the hops are *redistributed* over the resulting parts, such that each part has again the correct path length. The emission can occur in a direction that is independent of the direction from which the messenger was absorbed. The duration of the absorption processes and the duration of the emission processes must be in concordance with the local passage duration of the information messengers.

If the absorption takes place at a location that is a huge distance away from the emission location, then a *difference between absorption spectra and emission spectra* can occur. In physics this phenomenon is known as *cosmological redshift*.

The absorption and emission processes must obey spectral rules that determine the absorption and emission spectra.

5.22 The symmetric pair production and annihilation process

The pair creation and pair annihilation processes appear to be supported be procedures that construct quaternions from two complex numbers or that dismantle quaternions into complex numbers.

At symmetric pair annihilation a pair of elementary modules that are each other's antiparticle convert into a pair of linear messengers that leave in opposite directions. It is the *simplest pair annihilation process*. In this process each clamp element of the hopping path of the elementary (anti)particle converts into a warp element of a linear hop string of a leaving messenger. The messengers leave in a direction that is perpendicular to the direction into which the elementary modules were approaching each other. The chance that the geometric centers of the elementary modules will meet head-on is very low. The direction of the difference will further determine the direction in which the messengers leave. The process unravels the two clamp swarms into two

corresponding linear warp strings. The size of the displacement of the geometric centers is supposed to determine the polarization of the messenger string.

The model represents messengers as strings of equidistant hops in a complex number based subspace. The complex numbers represent function values. The leaving messengers are strings of warps that transport empty and thus massless platforms. The lengths of the leaving strings reflect the number of clamps in the annihilated elementary modules. The path length of the information messengers determines the *duration* of the annihilation process.

If each warp in the string carries a fixed bit of energy, then this process explains the ***mass-energy equivalence***.

During the process the symmetry centers of the platforms are annihilated and as a consequence the ***symmetry related charges vanish***.

5.23 Pair creation

At pair creation the reverse process takes place. Two strings of warps that have sufficient length that enter from opposite direction combine in order to generate two swarms of clamps that constitute a particle-antiparticle pair. During the creation process the symmetry centers of the platforms are created. As a consequence the symmetry related charges will emerge.

5.24 Interpreting the pair creation/annihilation process

The creation 'event' and the annihilation 'event' occur in the neighborhood of the vane. These processes are not occurring instantaneously. They take a fixed duration. However, each conversion of a clamp into a warp can take a single instant. In reverse, each conversion of a warp into a clamp can also take a single instant. Similarly the emission and absorption processes of atomic modular systems take the same duration. Thus the surround of the vane is reserved for these processes.

Generations of elementary particles involve different numbers of swarm elements, but if no observable difference exist between the duration of the passage of the involved warp strings, then the active region around the vane can be subdivided in multiple step numbers. These subdivisions correspond to elementary module types and elementary module generations.

5.25 Moving elementary modules

On average, clamp swarms will not move with respect to the geometric center of its platform. The mechanism that ensures coherence of the swarm will ensure that the geometric center of the swarm will on average stay on the geometric center of the platform. The regeneration process can at the utmost generate some *jitter* of the geometric center of the swarm.

Isolated warps and strings of warps may cause the hopping of the platform with respect to the background parameter space. As a consequence the platform hops with respect to the field that represents the living space of the elementary modules. Thus a mixture of clamps and warps may cause the movement of the swarm relative to the geometry of this carrying field.

It is not yet clear what causes the extra insertions of warps, however, a uniform movement of a platform already requires the regular insertion of *isolated warps*. This insinuates that isolated wraps can be generated due to the action of something that generates the displacement. These isolated wraps concern the hop of the platform as well as the hop landing location and the corresponding solution of the second order partial differential equation.

6   The test model

We will first recollect and deepen what we have achieved. After that we will further extend the model by using results of what experimental observation of reality has revealed. In the resulting part of the paper we will use symbols for new and existing concepts and when appropriate, we will use these symbols in equations. In addition, we will refer to scientific documents that support the approach that is taken in this paper.

The Hilbert Book Test Model $\mathcal{M}$ is based on a foundation that has the relational structure of an orthomodular lattice [1] [2]. Nearly a century ago, in 1936, the discovery of this lattice was published by the duo Garret Birkhoff and John von Neumann in a paper in which they also explained its relation to the notion of a ***separable Hilbert space*** [3] [4]. The orthonormal lattice does not contain the notion of number systems. Thus, this foundation cannot represent the concepts that define dynamic geometric data, such as time and location. These notions emerge by extending this foundation in the direction of the separable Hilbert space. By selecting this extension of the foundation, the freedom of selection of derived concepts is significantly restricted. The separable Hilbert space provides operators that have countable eigenspaces that are filled with eigenvalues that must be members of division rings [5]. Only three suitable division rings exist. These are the real numbers, the complex numbers and the quaternions. The separable Hilbert space can only cope with the rational versions of these number systems. These restrictions appear very favorable for the pursued model building process. It strongly limits the range of choices. Still the resulting possibilities appear to be flexible enough in order to generate a powerful base model. The combination of the infinite dimensional separable Hilbert space and its non-separable companion Hilbert space appears to represent a very feature rich and flexible model.

The restrictions limit the freedom of model generation, but if the orthomodular lattice indeed represents the foundation of reality, then at the same time these restrictions limit the way that reality can develop. It means that reality must also show the structure and the behavior that the Hilbert space shows.

$\mathcal{M}$ does not interpret the orthomodular lattice as a logical system and it does not interpret the elements of the lattice as separate spatial locations, which feature a progression stamp. Instead $\mathcal{M}$ interprets atomic elements of the orthomodular lattice as storage places for dynamic geometric data. In addition $\mathcal{M}$ interprets the atoms of a subset of the lattice as elementary modules that are represented by hopping paths and corresponding location swarms. These objects are elementary modules of a modular system. These elementary modules are represented by subspaces of a separable Hilbert space, but these subspaces contain a huge number of dimensions. However, at each progression instant, these subspaces reduce to a subspace that is spanned by a single Hilbert vector. As a consequence $\mathcal{M}$ interprets the orthomodular lattice as part of a recipe for modular construction. Modular construction represents a very beneficial strategy that strongly reduces relational complexity of the target system. For very complex systems the modular construction strategy is orders of magnitude more efficient than a monolithic approach. Modular construction uses its resources in an optimally economic fashion. $\mathcal{M}$ applies modular construction as a general strategy. Modular construction requires the encapsulation of modules, such that internal relations are hidden inside the capsule of the module. In some way, $\mathcal{M}$ must implement that encapsulation.

Reality offers huge resources in available time and in numbers of building components. In this way even stochastic design as is applied by nature can reach high levels of complexity. In advance the model will apply a stochastic design as its generation strategy. This will change when the model has achieved a level in which intelligent species appear. From that instant on

the efficiency of the modular construction strategy will on some locations increase significantly. Intelligent design and construction will use far less design and generation time and other required resources. This will clearly affect the evolution of the model. Due to limited speed of information spread, these effects will appear at isolated locations.

$\mathcal{M}$ applies the fact that the set of closed subspaces of a separable Hilbert space has the relational structure of an orthomodular lattice. Not all closed subspaces of a separable Hilbert space represent modules or modular systems, thus the notion of a module must be further restricted.

$\mathcal{M}$ applies the fact that separable Hilbert spaces can only cope with number systems that are division rings. We use the most elaborate category of these division rings. That category is formed by the quaternionic number systems [8]. Quaternionic number systems exist in multiple versions, that differ in the way that they are ordered. This ordering may influence the arithmetic properties of the number system. For example right handed multiplying quaternions and left handed multiplying quaternions exist. Further, as will be shown in this paper, it appears that ordering influences the behavior of quaternionic functions under integration. This fact has astonishing consequences. It enables the distinction of elementary modules into a small series of types.

Another important fact is that every infinite dimensional separable Hilbert system owns a companion Gelfand triple, which is a ***non-separable Hilbert space*** [10]. Where the separable Hilbert space can only handle discrete data is the Gelfand triple capable of handling continuums. $\mathcal{M}$ uses both kinds of Hilbert spaces as structured storage media, in a model in which discrete quaternionic data and quaternionic manifolds can be archived. By applying Hilbert spaces $\mathcal{M}$ accepts that the model uses a storage medium in which all of its activities are precisely archived. This repository covers history, the present status quo AND the future! A vane that represents the current static status quo scans over this repository. Observation only occurs inside this vane. The observers are modules and modular systems that travel with the vane.

$\mathcal{M}$ uses a separable Hilbert space $\mathfrak{H}$ in order to archive countable sets of discrete quaternionic data and $\mathcal{M}$ uses the companion Gelfand triple $\mathcal{H}$ in order to archive continuous quaternionic manifolds. $\mathcal{H}$ also contains an image of the content of $\mathfrak{H}$. $\mathcal{M}$ Uses this fact in order to describe the embedding of the separable Hilbert space into its Gelfand companion. $\mathcal{M}$ considers the embedding as an ongoing process. In taking this view $\mathcal{M}$ selects between two possible views. The view taken classifies the model as a dynamic model. The alternative view accepts that besides the historic data the Hilbert spaces already contains the future data. In this alternative view a boundary splits the Hilbert space into three parts:

- The past history part of the model
- The current static status quo, which is represented by the boundary
- The future part of the model

This second view treats these three parts as sections of a model that is created as one whole system.

$\mathcal{M}$ introduces ***the reverse bra-ket method*** and uses this method in order to relate operators and their eigenspaces to pairs of functions and their parameter spaces [9]. In this way, subspaces act as Hilbert space domains in relation to which manifolds are defined.

In the first view, the base version $\mathcal{M}$ of $\mathcal{M}$ consists of the foundation, a quaternionic separable Hilbert space, its companion Gelfand triple and a set of mechanisms $\{\mathfrak{M}_n^x\}$ that control the dynamic split of this base version $\mathcal{M}$ in a historic part, a part that represents the present static status quo and a part that represents the future.

The first view shifts the equivalent of the mystery of the origin of the dynamics of physical reality to the mysteries of a set of mechanisms that control the coherence of the dynamics of the model.

$\mathcal{M}$ applies an extended version of the generalized Stokes theorem in order to describe the split of the Hilbert space into the mentioned three parts [11] [12]. The split implements the vane that travels through the base model. The vane represents a static status quo of the model. The generalized Stokes theorem enforces the encapsulation of artifacts that disrupt the continuity of the manifolds. This introduces an extra splitting of the base model in which elementary artifacts and domain cavities are set apart from the domains of the continuous parts of the manifolds.

Via the reverse bra-ket method, smoothing operators are introduced that convolute the defining function of a primary operator with a blurring function. With an appropriate selection of the blurring function, the eigenspace of the smoothing operator will represent the "observable" version of the primary manifold. Here "observable" means the way that discrete objects sense the influence of the local disruptions of the continuity of the primary manifold that are caused by other discrete objects.

In this way $\mathcal{M}$ introduces notions such as the wave function, the uncertainty principle and the equivalent of the gravitation potential.

$\mathcal{M}$ allows two interpretations of the living space of modules and modular systems. One interpretation sees the living space as a field that describes the swarms that are formed by the landing locations of the hopping paths in a way that is blurred by the Green's function of the field. That Green's function represents the average over the regeneration cycle of the dynamic response of the field to the hop landings. These responses are described by particular spherical symmetric solutions of the homogeneous second order partial differential equation that describes the dynamic behavior of the field. During the travel away from the hopping location, these solutions keep the shape of the moving front.

The second interpretation sees the hop landings as the actors that influence the field by deforming it. The model is not affected by these different interpretations.

The fact that $\mathcal{M}$ steps with model wide steps in the separable Hilbert space $\mathfrak{H}$ and flows in the companion Gelfand triple $\mathcal{H}$ is the reason to use the name *Hilbert Book Model* for $\mathcal{M}$. In order to warn that $\mathcal{M}$ is not meant to be a physical model, but instead $\mathcal{M}$ is a pure mathematical test model that is used to investigate the mathematical tools and methods that can be use in order to describe a physical model, the name of $\mathcal{M}$ is extended to *Hilbert Book Test Model*. A separate static status quo of the Hilbert Book Model will be called a *Hilbert book page* or *sheet*.

7 Stokes theorem

7.1 Domains and parameter spaces

The quaternionic **domain** Ω is supposed to be defined as part of the **domain** $\mathfrak{R}$ of a **reference operator** $\mathfrak{R}$ that resides in the non-separable quaternionic Hilbert space $\mathcal{H}$. The reverse bra-ket method relates the eigenspace $\{q\}$ of reference operator $\mathfrak{R}$ to a flat quaternionic **function** $\mathfrak{R}(q)$. The target of function $\mathfrak{R}(q)$ is its own **parameter space** $\{q\}$. Here we explicitly use the same symbol $\mathfrak{R}$ for all directly related objects. In $\mathfrak{M}$, $\mathfrak{R}(q)$ is always and everywhere continuous.

$$\mathfrak{R} = |q\rangle\mathfrak{R}(q)\langle q| = |q\rangle q\langle q| \tag{1}$$

The domain $\mathfrak{R}$ is spanned by the eigenvectors $\{|q\rangle\}$ of operator $\mathfrak{R}$.

The reverse bra-ket method also relates the eigenspace $\mathfrak{R}$ to an equivalent eigenspace $\mathcal{R}$ of a reference operator $\mathcal{R}$, which resides in the infinite dimensional separable Hilbert space $\mathfrak{H}$. Both eigenspaces are related to the same version of the quaternionic number system. However, the second eigenspace $\mathcal{R}$ only uses rational quaternions q_i.

$$\mathcal{R} = |q_i\rangle\mathfrak{R}(q_i)\langle q_i| = |q_i\rangle q_i\langle q_i| \tag{2}$$

Quaternionic number systems can be ordered in several ways. Operator $\mathcal{R}$ corresponds with one of these orderings. $\mathcal{R}$ is supposed to be **Cartesian-ordered**. $\mathcal{R}$ is a normal operator and its eigenspace is countable. Cartesian ordering means that the set of eigenvectors of $\mathcal{R}$ can be enumerated by the separate eigenvalues of $\mathcal{R}$. The eigenspace is the Cartesian product of four partially ordered sets in which the set, which represents the real part takes a special role. The eigenspace of the Hermitian part $\mathcal{R}_0 = \frac{1}{2}(\mathcal{R} + \mathcal{R}^\dagger)$ of normal operator $\mathcal{R}$ can be used to enumerate a division of $\mathfrak{H}$ into a countable number of disjunctive subspaces, which are spanned by eigenvectors of $\mathcal{R}$. Cartesian ordering means partial ordering of the eigenvalues of $\mathcal{R}_0$ and additional ordering of the eigenvalues of the anti-Hermitian operator $\boldsymbol{\mathfrak{R}} = \frac{1}{2}(\mathfrak{R} - \mathfrak{R}^\dagger)$ by selecting a **Cartesian coordinate system**. Eight mutually independent Cartesian coordinate systems exist. $\mathcal{R}_0 = (\mathcal{R} + \mathcal{R}^\dagger)/2$ is a self-adjoint operator. The ordered eigenvalues of $\mathcal{R}_0$ can be interpreted as **progression values**. The eigenvalues of $\boldsymbol{\mathcal{R}}$ can be interpreted as **spatial values.** This differs from the physical notions of time and space. Physical spacetime has a Minkowski signature. Here we are talking about a mathematical test model.

In this way, parameter spaces as well as domains correspond to closed subspaces of the Hilbert spaces. The domain subspaces are subspaces of the domains of the corresponding reference operators. The parameter spaces are ordered by a selected coordinate system. The Ω domain is represented by a part of the eigenspace of reference operator $\mathfrak{R}$. The flat quaternionic function $\mathfrak{R}(q)$ defines the parameter space $\mathfrak{R}$. $\mathfrak{R}$ has an Euclidean signature. It installs an ordering by selecting a Cartesian coordinate system for the eigenspace of its anti-Hermitian part $\boldsymbol{\mathfrak{R}} = \frac{1}{2}(\mathfrak{R} - \mathfrak{R}^\dagger)$. Several mutually independent selections are possible. The chosen selection attaches a corresponding symmetry flavor to this parameter space. In the mathematical test model, this symmetry flavor will become the reference symmetry flavor. Thus, the symmetry flavor of parameter space $\mathfrak{R}^{\circledcirc}$ may be distinguished by its superscript $^{\circledcirc}$.

The manifold ω is also defined as the continuum eigenspace of a dedicated normal operator ω which is related to domain Ω and to parameter space $\Re^{\textcircled{0}}$ via function $\mathfrak{F}$. Within this parameter space $\mathfrak{F}$ may have discontinuities, but these must be excluded from the domain over which integration takes place. This exclusion will be treated below.

Symmetry centers are described by anti-Hermitian operators and their geometric center can float on another parameter space as a function of progression. At every progression step only one location of the symmetry center is used. In combination this produces a **well ordered operator** where a single progression value corresponds with a single spatial location. The spatial location is determined by a stochastic mechanism. This mechanism produces **coherent location swarms**. The swarm can be described by a continuous location density distribution. Further, all swarm elements can be enumerated by a progression value and thus form **a hopping path**.

7.2   Stokes theorem without discontinuities

The conventional generalized Stokes theorem is in fact a combination of multiple versions. One is the using the divergence part of the exterior derivative $d\omega$. It is also known as the generalized divergence theorem. Another version uses the curl part of the exterior derivative. In fact all these versions concern separate terms that exist in the first order partial differential. Thus the generalized Stokes theorem divides the integration along the "lines" in which change takes place. The conventional version of the Stokes theorem does not apply all terms of the first order partial differential. For quaternionic manifolds all terms can be combined in one formula. This results in the extended version of the generalized Stokes theorem and that is the version that will be used here. Usually the domains cover a static status quo or we integrate over the regeneration period such that variation with time becomes small or negligible. The static status quo is characterized by three changes, a divergence, a gradient and a curl. The other two changes concern what disappears into history and what comes in from the future. The parts concerns the change of the scalar and vector fields that represent blurred views of weighted location density distributions.

Without discontinuities in the manifold ω the **conventional generalized Stokes theorem** is represented by a simple formula [11][12].

$$\int_{\Omega} d\omega = \int_{\partial\Omega} \omega \left(= \oint_{\partial\Omega} \omega \right) \tag{1}$$

The theorem can be applied when everywhere in Ω the derivative dω exists and when everywhere in $\partial\Omega$ the manifold ω is continuous and integrable. The domain Ω is encapsulated by a boundary $\partial\Omega$.

$$\Omega \subset \partial\Omega \tag{2}$$

In this paper, the manifolds ω and $d\omega$ represent quaternionic fields $\mathfrak{F}$ and $d\mathfrak{F}$, while inside $\partial\Omega$ the manifold ω represents the quaternionic boundary of the quaternionic field $\mathfrak{F}$. These fields and manifolds correspond to defining functions $\mathfrak{F}(q)$ and $d\mathfrak{F}(q)$.

$d\omega$ is the exterior derivative of ω.

This view is focusing onto the spatial part $\mathfrak{R}$ of the quaternionic parameter space $\mathfrak{R}$. It uses only the spatial parts $\langle \nabla, \boldsymbol{f} \rangle, \nabla f_0$ and $\nabla \times \boldsymbol{f}$ of the first order differential equation.

$$\nabla f = \nabla_0 f_0 - \langle \nabla, \boldsymbol{f} \rangle + \nabla_0 \boldsymbol{f} + \nabla f_0 + \nabla \times \boldsymbol{f} \tag{3}$$

If f represents the living space potential, then in this formula the black terms on the right side can be considered to be small and will be neglected.

In the conventional Stokes theorem the gradient ∇f_0 is neglected. In quaternionic space all five terms contribute to the balance and continuity equations. If both the historic and the future parts are taken into the view then a **new extended Stokes theorem** emerges.

In particular formula (1) does not pay any attention to the what exists outside of the splitting boundary. If the parameter space $\mathfrak{R}$ is an eigenspace of a normal reference operator in a quaternionic Hilbert space then the ignored region concerns the other part of the Hilbert space. A proper balance equation must consider all participating parts. **We will extend the Stokes theorem in that direction**.

7.3   Interpreting the exterior derivative

Via quaternionic defining functions, the reverse bra-ket method couples the separable Hilbert space to its non-separable companion.

The defining function $\mathcal{F}(q)$ links the integral over the full quaternionic q numbers to the summation over the rational q_i numbers.

$$\langle x | \mathcal{F} \, y \rangle = \sum_i \langle x | q_i \rangle \mathcal{F}(q_i) \langle q_i | y \rangle \approx \int_q \langle x | q \rangle \mathcal{F}(q) \langle q | y \rangle \, dq \tag{1}$$

This corresponds to:

$$\oint_{\partial\Omega} \mathcal{F} = \int_{\partial\Omega} \mathcal{F} \iff \sum_i \langle x | q_i \rangle \mathcal{F}(q_i) \langle q_i | y \rangle \tag{2}$$

$$\int_\Omega d\mathcal{F} \iff \int_q \langle x | q \rangle \mathcal{F}(q) \langle q | y \rangle \, dq \tag{3}$$

This divides the region over which the equation works into two parts. One in which summation equals integration and a region or a set of regions where integration does not work properly due to the existence of discontinuities of $\mathcal{F}(q)$ in those sub-regions. Exchanging $\mathcal{F}(q)$ against a smoothed version can completely or partly cure this problem.

Another possibility is the split of the parameter space $\mathfrak{R}$ of $\mathcal{F}(q)$ into the parts $\mathfrak{R}_-$ and $\mathfrak{R}_+$. This splits the real part of the parameter space in two parts. The split occurs at a selected progression value. If the two splits are combined, then the split between summation and integration can be interpreted as a leakage of the second split in which discrete objects pass though the sieve that splits $\mathfrak{R}_-$ and $\mathfrak{R}_+$. A similar interpretation can be given to larger regions in which $\mathcal{F}(q)$ is not defined.

Thus, the **quaternionic extension of the Stokes theorem** may involve multiple splits:

- The split between $\mathfrak{R}_-$ and the static status quo.
- The slit between the static status quo and $\mathfrak{R}_+$.
- The split around point-like artifacts.
- The split around other regions where the defining function is not integrable.

Properly smoothed fields pass straight through the boundaries.

The conventional generalized Stokes theorem exists in the form of a divergence based version and in the form of a curl based version [11][12]. However, for quaternionic manifolds the definition of the exterior derivative requests extra attention. In this section we assume that the quaternionic manifold ω is represented by the target of a quaternionic function $\mathfrak{F}(q)$. Function $\mathfrak{F}(q)$ has a flat parameter space $\mathfrak{R}$.

$\mathfrak{R}$ is a flat quaternionic manifold, which is represented by the target of function $\mathfrak{R}(q) \stackrel{\text{def}}{=} q$.

We presume that the exterior derivative $\mathrm{d}\mathfrak{F}$ of $\mathfrak{F}$ can be interpreted by the following equations:

$$\mathrm{d}\mathfrak{F} = \sum_{\mu=0}^{3} e^{\mu} \frac{\partial \mathfrak{F}}{\partial x_{\mu}} dx_{\mu} = \sum_{\mu=0}^{3} e^{\mu} dx_{\mu} \sum_{\nu=0}^{3} e^{\nu} \frac{\partial \mathfrak{F}_{\nu}}{\partial x_{\mu}} = e^{\mu\nu} D_{\mu} \mathfrak{F}_{\nu} \tag{4}$$

$$D_{\mu} \stackrel{\text{def}}{=} dx_{\mu} \frac{\partial}{\partial x_{\mu}} \tag{5}$$

Thus $\mathrm{d}\mathfrak{F}$ is represented by a tensor. This is not a very attractive presentation. It is more convenient to treat the change along the directions in which change takes place according to the first order partial differential equations.

The exterior derivative differs from the partial differentials that appear in partial differential equations.

$$\mathfrak{G} = \sum_{\varsigma=0}^{3} e^{\varsigma} \mathfrak{G}_{\varsigma} = e^{\varsigma} \mathfrak{G}_{\varsigma} \tag{3}$$

$$= \nabla \mathfrak{F} = \sum_{\mu=0}^{3} e^{\mu} \frac{\partial \mathfrak{F}}{\partial x_{\mu}} = \sum_{\mu=0}^{3} e^{\mu} \sum_{\nu=0}^{3} e^{\nu} \frac{\partial \mathfrak{F}_{\nu}}{\partial x_{\mu}} = e^{\mu} e^{\nu} \partial_{\mu} \mathfrak{F}_{\nu} = e^{\mu\nu} \partial_{\mu} \mathfrak{F}_{\nu}$$

In the right parts of the above formulas, the summation rules for subscripts and superscripts are applied.

We use the fact that quaternions can be considered as a combination of a real scalar and an imaginary vector. Further, we apply the fact that first order quaternionic partial differential operators act as multipliers.

$$\mathfrak{F} = \mathfrak{F}_0 + \boldsymbol{\mathfrak{F}} \tag{4}$$

$$\mathfrak{G} = \nabla\mathfrak{F} = \mathfrak{G}_0 + \boldsymbol{\mathfrak{G}} = (\nabla_0 + \boldsymbol{\nabla})(\mathfrak{F}_0 + \boldsymbol{\mathfrak{F}}) \tag{5}$$

$$\mathfrak{G}_0 = \nabla_0\mathfrak{F}_0 - \langle \boldsymbol{\nabla}, \boldsymbol{\mathfrak{F}} \rangle \tag{6}$$

$$\boldsymbol{\mathfrak{G}} = \nabla_0\boldsymbol{\mathfrak{F}} + \boldsymbol{\nabla}\mathfrak{F}_0 \pm \boldsymbol{\nabla} \times \boldsymbol{\mathfrak{F}} \tag{7}$$

For some fields, some parts of $\mathfrak{G}$ may get special symbols. This is applied in Maxwell-like equations.

$$\boldsymbol{\mathfrak{E}} = -\nabla_0\boldsymbol{\mathfrak{F}} - \boldsymbol{\nabla}\mathfrak{F}_0 \tag{8}$$

$$\boldsymbol{\mathfrak{B}} = \boldsymbol{\nabla} \times \boldsymbol{\mathfrak{F}} \tag{9}$$

Similar definitions are applied in Maxwell equations. However, despite these similarities, the derived fields $\boldsymbol{\mathfrak{E}}$ and $\boldsymbol{\mathfrak{B}}$ are not equivalent to the Maxwell fields **E** and **B**. The Maxwell equations are treated in the appendix.

In general, there is no guarantee that $\boldsymbol{\mathfrak{E}}$ and $\boldsymbol{\mathfrak{B}}$ are perpendicular. Thus in general:

$$\langle \boldsymbol{\mathfrak{E}}, \boldsymbol{\mathfrak{B}} \rangle \neq 0 \tag{10}$$

However, a third vector $\boldsymbol{\mathfrak{P}}$ is perpendicular to both $\boldsymbol{\mathfrak{E}}$ and $\boldsymbol{\mathfrak{B}}$.

$$\boldsymbol{\mathfrak{P}} = \boldsymbol{\mathfrak{E}} \times \boldsymbol{\mathfrak{B}} \tag{11}$$

Equation (6) is not part of the Maxwell set of partial differential equations. However, in physical theories the terms $\nabla_0\mathfrak{F}_0$ and $\langle \boldsymbol{\nabla}, \boldsymbol{\mathfrak{F}} \rangle$ are used in gauge equations.

We may conclude that change covers five terms that do not represent four independent directions as is suggested by the conventional Maxwell differential equations.

Please note that

$$\nabla^*\mathfrak{F}^* = (\nabla_0 - \boldsymbol{\nabla})(\mathfrak{F}_0 - \boldsymbol{\mathfrak{F}}) = \mathfrak{G}_0 - \nabla_0\boldsymbol{\mathfrak{F}} - \boldsymbol{\nabla}\mathfrak{F}_0 \pm \boldsymbol{\nabla} \times \boldsymbol{\mathfrak{F}} \tag{12}$$

$$(\nabla\mathfrak{F})^* = \mathfrak{G}^* = \nabla^*\mathfrak{F}^* \mp 2\boldsymbol{\nabla} \times \boldsymbol{\mathfrak{F}} \tag{13}$$

The $\pm$ sign indicates the fact that quaternionic parameter spaces and quaternionic functions exist in versions that differ in the handedness of their external vector product.

In the integrals below some terms of $\nabla\mathfrak{F}$ are combined.

$$\nabla\mathfrak{F} = -\langle\boldsymbol{\nabla},\boldsymbol{\mathfrak{F}}\rangle \pm \boldsymbol{\nabla} \times \boldsymbol{\mathfrak{F}} \tag{14}$$

$$\nabla\mathfrak{F} = \boldsymbol{\nabla}\mathfrak{F}_0 - \langle\boldsymbol{\nabla},\boldsymbol{\mathfrak{F}}\rangle \pm \boldsymbol{\nabla} \times \boldsymbol{\mathfrak{F}} \tag{15}$$

$$\nabla_0\mathfrak{F} = \nabla_0\mathfrak{F}_0 + \nabla_0\boldsymbol{\mathfrak{F}} \tag{16}$$

It must be noticed that

$$\mathrm{d}\mathfrak{F} \neq \sum_{\mu=0}^{3} e^{\mu}\mathfrak{G}_{\mu}dx_{\mu} \tag{17}$$

This is the reason that the conventional generalized Stokes integral uses the wedge product $dx \wedge dy \wedge dz \wedge d\tau$. These wedge products are merely a warning that a tensor is active. In the quaternionic version of the Stokes theorem, it is not a clear exposure of the mechanism.

The Maxwell-like partial quaternionic differential equations differ from the Maxwell equations that are used in current physical theories. Thus, great care must be applied in comparing the two sets of partial differential equations. Especially equations (6) and (10) signal alarming differences.

7.4   A special domain split

In the special splitting case that is investigated here, the extended generalized Stokes theorem constructs a vane $\mathfrak{F}(\boldsymbol{x}, \tau)$ between the past history of the field $[\mathfrak{F}(\boldsymbol{x}, t)]_{t<\tau}$ and the future $[\mathfrak{F}(\boldsymbol{x}, t)]_{t>\tau}$ of that field. It means that the boundary $\mathfrak{F}(\boldsymbol{x}, \tau)$ of field $[\mathfrak{F}(\boldsymbol{x}, t)]_{t<\tau}$ represents a universe wide static status quo of that field.

More specifically, the form of the generalized Stokes theorem for the sketched situation runs as:

$$\int_{t=0}^{\tau} \iiint_V \mathrm{d}\mathfrak{F}\,(x) = \int_{t=0}^{\tau}\left(\iiint_V \nabla\mathfrak{F}(x)\,dx \wedge dy \wedge dz\right) \wedge d\tau = \left[\iiint_V \mathfrak{F}\,(x)dx\right]_{t=\tau} \tag{1}$$

$$x = \pmb{x} + \tau \tag{2}$$

Here $[\mathfrak{F}(\pmb{x},t)]_{t=\tau}$ represents the static status quo of a quaternionic field at instance τ. V represents the spatial part of the quaternionic domain of $\mathfrak{F}$, but it may represent only a restricted part of that parameter space. This last situation corresponds to the usual form of the divergence theorem.

As mentioned above great care must be taken by interpreting the wedge product in

$$\mathrm{d}\mathfrak{F}(x) = \nabla\mathfrak{F}(x)\,dx \wedge dy \wedge dz \wedge d\tau. \tag{3}$$

Due to the danger of misinterpretation, we will avoid the wedge products that appear in the middle part of equation (1). In the right part of the equation only the divergence, the curl and a gradient play a role. The split that has been selected, sets a category of operators apart that are all Cartesian-ordered in the same way as operator $\mathcal{R}$ is. It enables a space-progression model in which progression steps in the separable Hilbert space $\mathfrak{H}$ and flows in its non-separable companion $\mathcal{H}$. Via the reverse bra-ket method the Cartesian-ordering of $\mathcal{R}$ can be transferred to $\mathfrak{R}$.

7.4.1 Interpretation of the selected encapsulation

The boundary $\partial\Omega$ is selected between the real part and the imaginary part of domain $\mathfrak{R}$. But it also excludes part of the real part. That part is the range of the real part from τ to infinity. τ is interpreted as the current progression value.

The boundary $\partial\Omega$ has one dimension less than the domain Ω. The failing dimension is taken by the form of the partition. In the special case the boundary is formed by most of the three dimensional spatial part of the parameter space. The theorem does not specify the form of the partition, but requires that the **partition form** does not traverse discontinuities or regions in which the defining function is not defined. Thus, if the partition wipes through the parameter space and encounters discontinuities or regions in which the defining function is not defined, then the partition must encapsulate these objects while it passes them. These encapsulating partitions become part of the boundary. In this way these objects stay outside of the boundary $\partial\Omega$. Symmetry centers and space cavities become objects that float as encapsulated modules over the domain Ω. If they enter the partition, then they can be considered to be created. If they keep floating with the partition, then these objects are alive. If they have completely passed the partition, then they can be considered to have been annihilated. A long lifetime will correspond to a tube-like history and a corresponding tube-like future.

The future $\mathfrak{R} - \Omega$ is kept on the outside of the boundary $\partial\Omega$. As a consequence, the mechanisms that generate new data, operate on the rim $\partial\Omega$ between past Ω and future $\mathfrak{R} - \Omega$. Two interpretations are possible. Either, the mechanisms generate data that was not yet present in the Hilbert spaces, or the mechanisms represent the data that are encountered during the passage of the partition. The observers cannot decide which of the two interpretations is correct. It is merely a question of what

you want to belief. For 𝔐 this interpretation does not matter. This paper describes the model in accordance to the first interpretation. This avoids confusion about why and how the creator of the model generated the data that are archived in 𝔐's Hilbert spaces. In 𝔐 the relevant observers live inside the wiping boundary. In the selected interpretation the creator of the model is throwing dices! In this action the creator is represented by a set of dedicated mechanisms. These mechanisms apply stochastic processes.

The described split of quaternionic space results in a space-progression model that is to a significant extent similar to the way that physical theories describe their space time models. However, the physical theories apply a spacetime model that has a Minkowski signature. The quaternionic model, which is represented here, is strictly Euclidean.

The paper does not claim that this quaternionic space-progression model reflects the structure and the habits of physical reality. The quaternionic space-progression model is merely promoted as a mathematical test model.

What according to the selected interpretation happens in the mathematical test model can be seen as an ongoing process that embeds the subsequent static status quo's of the separable Hilbert space into the Gelfand triple.

Controlling mechanisms act as a function of progression τ in a stochastic and step-wise fashion in the realm of the separable Hilbert space. The results of their actions are stored in eigenspaces of corresponding stochastic operators that reside in the separable Hilbert space. These stochastic operators differ from the kind of operators that are handled by the reverse bra-ket method. However, if the stochastic operators produce coherent swarms that feature a continuous density distribution, then that distribution corresponds with an operator that is defined by this distribution via the reverse bra-ket method.

The controlling mechanisms have no notion of the fields. They only work with discrete objects that appear in swarms.

At the same progression instant, this part of the separable Hilbert space is embedded into its companion Gelfand triple. The controlling mechanisms will provide all generated data with a **progression stamp** τ. This progression stamp reflects the state of a model wide clock tick. The whole model, including its "physical" fields will proceed with these progression steps. However, in the Gelfand triple this progression can be considered to flow.

We have selected one of two possible interpretations. The model does not change by selecting an interpretation. The interpretation that is selected, has significant consequences for the description of the model. At the defined vane, any forecasting will be considered as mathematical cheating. Thus, at the vane, the uncertainty principle does not work for the progression part of the parameter spaces. Differential equations that offer advanced as well as retarded solutions must reinterpret the advanced solutions and turn them into retarded solutions, which in that case represent another kind of object. If the original object represents a particle, then the reversed particle is the anti-particle. Thus the tubes that represent elementary modules will appear to reflect on the boundary in one interpretation and will just pass the boundary in the other interpretation. In the panning view the tube just passes undisturbed through the boundary.

As a consequence of the construct, the history, which is stored-free from any uncertainty-in the already processed part of the eigenspaces of the physical operators, is no longer touched. Future is unknown or at least it is inaccessible for observation.

7.4.2 Integrals over regular spatial domains

If in a spatial domain, function $\mathfrak{F}$ obeys the homogeneous equation

$$\boldsymbol{\nabla}\boldsymbol{\nabla}\mathfrak{F} = 0 \tag{1}$$

then the function $\mathfrak{F}$ and the corresponding field $\mathfrak{F}$ is considered to be regular in that domain. For functions $\mathfrak{F}$ that are this kind of regular in spatial domain V hold:

$$\iiint_V \boldsymbol{\nabla}\mathfrak{F} = \oiint_S \boldsymbol{n}\mathfrak{F} \tag{2}$$

$$\iiint_V \boldsymbol{\nabla}\mathfrak{F}_0 = \oiint_S \boldsymbol{n}\mathfrak{F}_0 \tag{3}$$

$$\iiint_V \langle \boldsymbol{\nabla}, \mathfrak{F} \rangle = \oiint_S \langle \boldsymbol{n}, \mathfrak{F} \rangle \tag{4}$$

$$\iiint_V \boldsymbol{\nabla} \times \mathfrak{F} = \oiint_S \boldsymbol{n} \times \mathfrak{F} \tag{5}$$

7.4.3 Integrating irregular functions

We can use the gradient of the inverse of the spatial distance $|\boldsymbol{q} - \boldsymbol{c}|$.

$$\boldsymbol{\nabla}\frac{1}{|\boldsymbol{q} - \boldsymbol{c}|} = -\frac{\boldsymbol{q} - \boldsymbol{c}}{|\boldsymbol{q} - \boldsymbol{c}|^3} \tag{1}$$

The divergence of this gradient is a Dirac delta function.

$$\delta(\boldsymbol{q} - \boldsymbol{c}) = -\frac{1}{4\pi}\langle \boldsymbol{\nabla}, \boldsymbol{\nabla}\frac{1}{|\boldsymbol{q} - \boldsymbol{c}|}\rangle = -\frac{1}{4\pi}\langle \boldsymbol{\nabla}, \boldsymbol{\nabla}\rangle\frac{1}{|\boldsymbol{q} - \boldsymbol{c}|} \tag{2}$$

This means that:

$$\phi(\boldsymbol{c}) = \iiint_V \phi(\boldsymbol{q})\delta(\boldsymbol{q} - \boldsymbol{c}) = -\frac{1}{4\pi}\iiint_V \phi(\boldsymbol{q})\langle \boldsymbol{\nabla}, \boldsymbol{\nabla}\rangle\frac{1}{|\boldsymbol{q} - \boldsymbol{c}|} \tag{3}$$

As alternative, we can also use the Green's function $G(\boldsymbol{q})$ of the partial differential equation.

$$\phi(\boldsymbol{c}) = \iiint_V \phi(\boldsymbol{q}) G(\boldsymbol{q} - \boldsymbol{c}) \tag{4}$$

For the Laplacian $\langle \boldsymbol{\nabla}, \boldsymbol{\nabla} \rangle$ this obviously means:

$$\langle \boldsymbol{\nabla}, \boldsymbol{\nabla} \rangle \mathfrak{F} = \phi(\boldsymbol{q}) \tag{5}$$

$$G(\boldsymbol{q} - \boldsymbol{c}) = \frac{1}{|\boldsymbol{q} - \boldsymbol{c}|} \tag{6}$$

However, when added to the Green's function, every solution f of the homogeneous equation

$$\langle \boldsymbol{\nabla}, \boldsymbol{\nabla} \rangle f = 0 \tag{7}$$

is also a solution of the Laplace equation.

$$\phi(\boldsymbol{c}) = \iiint_V \frac{\phi(\boldsymbol{q})}{|\boldsymbol{q} - \boldsymbol{c}|} \tag{8}$$

Function $\phi(\boldsymbol{c})$ can be interpreted as the potential that is raised by charge distribution $\phi(\boldsymbol{q})$.

In pure spherical conditions the Laplacian reduces to:

$$\langle \boldsymbol{\nabla}, \boldsymbol{\nabla} \rangle \mathfrak{F}(r) = \frac{1}{r^2} \frac{\partial}{\partial r} \left(r^2 \frac{\partial \mathfrak{F}(r)}{\partial r} \right) \tag{9}$$

For the following **test function** $\mathfrak{T}(r)$ this means [13]:

$$\mathfrak{T}(r) = \frac{Q}{4\pi} \frac{ERF\left(r/_{\sigma\sqrt{2}} \right)}{r} \tag{10}$$

$$\rho(r) = \langle \boldsymbol{\nabla}, \boldsymbol{\nabla} \rangle \mathfrak{F}(r) = \frac{Q}{\left(\sigma\sqrt{2\pi}\right)^3} \exp\left(-\frac{r^2}{2\sigma^2}\right) \tag{11}$$

Thus, for a **Gaussian location distribution** $\rho(r)$ of point-like artifacts the corresponding contribution to field $\mathfrak{F}(r)$ equals an error function divided by its argument. At first sight this may look in contradiction with equations $(4) - (8)$, but here the distribution of artifacts extends over the boundary of domain V.

$$\frac{1}{r^2}\frac{\partial}{\partial r}\left(r^2 \frac{\partial}{\partial r}\frac{ERF(r)}{r}\right) = \frac{1}{r^2}\frac{\partial}{\partial r}\left(-ERF(r) + r\frac{2}{\sqrt{\pi}}\exp(-r^2)\right)$$

$$= \frac{1}{r^2}\left(-\frac{2}{\sqrt{\pi}}\exp(-r^2) + \frac{2}{\sqrt{\pi}}\exp(-r^2) - 2r\frac{2}{\sqrt{\pi}}\exp(-r^2)\right) = \frac{4}{\sqrt{\pi}}\exp(-r^2)$$
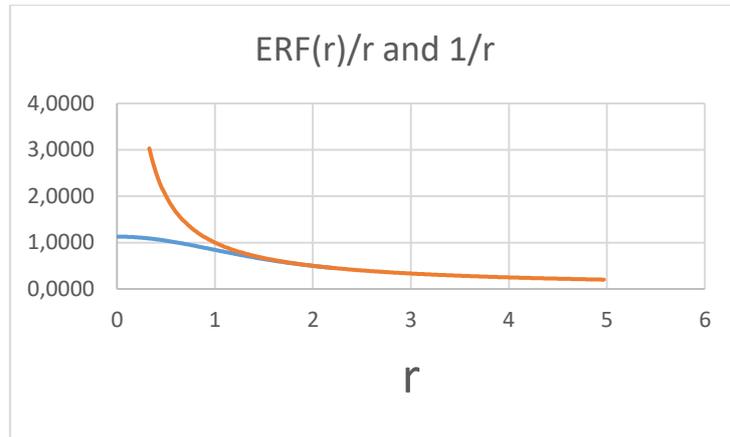
Figure 1. Close to the geometric center the singularities are converted in a smooth function. Further from the center the form of the Green's function (1/r) is retained.

The test function does not represent the action of a mechanism that ensures the dynamic coherence of a real object. It is a pure mathematical example.

7.5 The detailed generalized Stokes theorem

We separate all point-like discontinuities from the domain Ω by encapsulating them in an extra boundary. Symmetry centers represent spherically ordered parameter spaces in regions H_n^x that float on a background parameter space $\mathfrak{R}$. The boundaries ∂H_n^x separate the regions H_n^x from the domain Ω. The regions H_n^x are platforms for local discontinuities in basic fields [x]. These fields are continuous in domain $\Omega - H$.

$$H = \bigcup_n H_n^x \tag{1}$$

The symmetry centers $\mathfrak{S}_n^x$ are encapsulated in regions H_n^x and the encapsulating boundary ∂H_n^x is not part of the disconnected boundary which encapsulates all continuous parts of the quaternionic manifold ω that exist in the quaternionic model.

$$\int_{\Omega-H} d\omega = \int_{\partial\Omega\cup\partial H} \omega = \int_{\partial\Omega} \omega - \sum_n \int_{\partial H_n^x} \omega \tag{2}$$

If we take the unit normal to point outward on all of the boundary, this reverses the direction of the normal on ∂H_n^x, which negates the integral. ***Thus, in this formula, the contributions of boundaries*** $\{\partial H_n^x\}$ *are subtracted from the contributions of boundary* $\partial\Omega$. This means that $\partial\Omega$ also surrounds the regions $\{H_n^x\}$. ***This fact renders the integration sensitive to the ordering of the participating domains***.

Domain Ω corresponds to part of the reference parameter space $\mathfrak{R}^{\textcircled{0}}$. As mentioned before the symmetry centers $\{\mathfrak{S}_n^x\}$ represent encapsulated regions $\{H_n^x\}$ that float on parameter space $\mathfrak{R}^{\textcircled{0}}$.

The geometric center of symmetry center $\mathfrak{S}_n^x$ is represented by a floating location on parameter space $\mathfrak{R}^{\textcircled{0}}$.

The relation between the **subspace** S_Ω that corresponds to the domain Ω and the **subspace** $S_\mathfrak{R}$ that corresponds to the parameter space $\mathfrak{R}^{\textcircled{0}}$ is given by:

$$\underbrace{\Omega}_{S_\Omega} \subset \underbrace{\mathfrak{R}^{\textcircled{0}}}_{S_\mathfrak{R}} \tag{3}$$

Similarly:

$$\underbrace{H_n^x}_{S_{H_n^x}} \subset \underbrace{\mathfrak{S}_n^x}_{S_{\mathfrak{S}_n^x}} \tag{4}$$

7.6   Symmetry flavor and the origin of the symmetry related charge

The symmetry center $\mathfrak{S}_n^x$ is characterized by a private symmetry flavor. That symmetry flavor relates to the Cartesian ordering of this parameter space. When the orientation of the coordinate axes is fixed, then eight independent Cartesian orderings are possible. We use the Cartesian ordering of $\mathfrak{R}^{\text{\textcircled{0}}}$ as the reference for the orientation of the axes. $\mathfrak{R}^{\text{\textcircled{0}}}$ has the same Cartesian ordering as $\mathcal{R}^{\text{\textcircled{0}}}$ has.

$$\int_{\Omega - \mathrm{H}} d\omega = \int_{\partial \Omega} \omega - \sum_n \int_{\partial \mathrm{H}_n^x} \omega \tag{1}$$

In this formula the boundaries $\partial \Omega$ and ∂H_n^x are subtracted from each other. This subtraction is controlled by the difference in ordering of the domains Ω and H_n^x.

Due to the smoothness of the embedding field, we have some freedom with the spatial placement of the encapsulating boundaries. We exploit that freedom by selecting a cubic, rather than a spherical encapsulation of the point-like discontinuities. The cube is aligned along the coordinate axes. This enables us to correctly determine the influence of the differences in ordering along the coordinate axes.

The consequence of the differences of the symmetry flavor on the subtraction can best be comprehended when the encapsulation $\partial \mathrm{H}_n^x$ is performed by a ***cubic space form*** that is aligned along the Cartesian axes. Now the six sides of the cube contribute different to the effects of the encapsulation when the ordering differs from the Cartesian ordering of the reference parameter space $\mathfrak{R}^{\text{\textcircled{0}}}$. Each discrepant axis ordering corresponds to one third of the surface of the cube. This effect is represented by the ***symmetry related charge*** and the ***color charge*** of the symmetry center. It is easily related to the algorithm which is introduced for the computation of the symmetry related charge. Also the relation to the color charge will be clear. ***Thus, this effect couples the ordering of the local parameter spaces to the symmetry related charge of the encapsulated elementary module.*** The differences with the ordering of the surrounding space determines the value of the symmetry related charge of the object that resides inside the encapsulation!

The symmetry related charge and the color charge of symmetry center $\mathfrak{S}_n^x$ are supposed to be located at the geometric center of the symmetry center. A Green's function together with these charges can represent the local defining function $\varphi^x(q)$ of the contribution φ^x to the ***symmetry related field*** $\mathfrak{U}^x$ within and beyond the realm of the floating region H_n^x.

Nothing else than the discrepancy of the ordering of symmetry center $\mathfrak{S}_n^x$ with respect to the ordering of the parameter spaces $\mathcal{R}^{\text{\textcircled{0}}}$ and $\mathfrak{R}^{\text{\textcircled{0}}}$ causes the existence of the symmetry related charge, which is related to the symmetry center. Anything that resides on this symmetry center will ***inherit*** that symmetry related charge.

7.7   Single symmetry center

H_n^x is a spatial domain. The regions H_n^x that are combined in H are excluded from domain Ω. The Stokes theorem does not hold for the separate regions H_n^x. Instead, the difference between the integrals defines a potential. In case of isotropic symmetry flavor of the symmetry center $\mathfrak{S}_n^x$ holds:

$$Q_n^x = |\boldsymbol{q} - \boldsymbol{c}_n^x| \left\{ \int_{\mathrm{H}_n^x} d\omega - \int_{\partial \mathrm{H}_n^x} \omega \right\} \tag{1}$$

c_n^x is the geometric center of symmetry center $\mathfrak{S}_n^x$. Q_n^x is the symmetry related charge. This corresponds to the symmetry related potential $\varphi_n^x(q)$ that exists at the outskirts of the encapsulation.

$$\varphi_n^x(\boldsymbol{q}) = \frac{Q_n^x}{|\boldsymbol{q} - \boldsymbol{c}_n^x|} = \int_{\mathrm{H}_n^x} d\omega - \int_{\partial \mathrm{H}_n^x} \omega \tag{2}$$

The potential $\varphi_n^x(\boldsymbol{q} - \mathbf{c}_n^x)$ contributes to the symmetry related field $\mathfrak{A}^x$.

7.8 Bounded center

A locally a spatially connected union $H_\uplus$ of encapsulations H_n^x is defined by:

$$H_\uplus = \bigcup_{n=1}^{N^x} \mathrm{H}_n^x \tag{1}$$

$H_\uplus$ encapsulates multiple symmetry centers. In case that $H_\uplus$ exists, we consider the objects that reside within that encapsulation $\partial H_\uplus$ as bounded by the symmetry related charges.

$$\phi^x(\boldsymbol{q}) = \sum_{n=1}^{N^x} \frac{Q_n^x}{|\boldsymbol{q} - \boldsymbol{c}_n^x|} \tag{2}$$

At large enough distance from this bounded center, all charges can be considered to be merged in a single charge with symmetry related potential function $\phi(q)$:

$$\phi(\boldsymbol{q}) = \frac{\sum_{n=1}^N Q_n^x}{|\boldsymbol{q} - \boldsymbol{r}|} \tag{3}$$

$$\boldsymbol{r} = \frac{1}{N} \sum_{n=1}^N \boldsymbol{c}_n \tag{4}$$

7.9 Discrepant regions

The symmetry centers correspond to point-like discontinuities. However, also large connected regions of $\mathfrak{R}^\circledcirc$ may exist that disrupt the continuity of the manifold. For example a region that is surrounded by a boundary where the deformation is so strong that information contained in ω cannot pass the boundary of this region. These regions must also be separated from domain Ω. In this way these regions will correspond to *cavities* in the domain Ω. ***The information contained in the***

manifold cannot pass the surface of the cavity. The cavities act as information holes. Within the cavity the manifold can be considered to be non-existent. Within that region it has no defining function.

Current mathematical integration technology appears to lack proper solutions for this situation.

Discrepant regions cannot be hidden by applying a smoothing operator to the underlying field.

The discrepant regions are the "black holes" of the model.

8　Elementary modules

Each elementary module resides on a private platform, whose spatial part corresponds to a private symmetry center. That symmetry center is characterized by a symmetry flavor. The symmetry center will be represented by symbol $\mathfrak{S}_n^x$. The superscript refers to the type of the elementary module and the subscript refers to the identity of the elementary module inside its type group. A germ operator $\mathscr{o}_n^x$ generates the hopping path and the location swarm that correspond to the identity of the elementary module. The mechanism that ensures the dynamic coherence of the location swarm picks the eigenvalues of the germ operator $\mathscr{o}_n^x$ from the platform that corresponds to symmetry center $\mathfrak{S}_n^x$.

For the operator $\mathscr{o}_n^x$ that describes via its eigenvalues the 'life' of the elementary module, each subsequent real progression value is accompanied by an imaginary part and together these parts form the eigenvalue that belongs to the Hilbert vector, which at this progression instant represents the elementary module. This single value has not much to say about the owner of this eigenvalue. Only a series of subsequent eigenvalues can do that job. A large series of these numbers can tell the types of elementary modules apart. These subsequent quaternionic numbers form a **dynamic location swarm**. At the same time these numbers form a **hopping path**. The spatial parts of these numbers are taken from symmetry center $\mathfrak{S}_n^x$. that due to this role determines part of the properties of the elementary module. Thus the hopping path and the location swarm reside on the platform that corresponds to the symmetry center. Thus, all elementary modules reside on a their own individual symmetry center. The symmetry center covers a closed subspace and the module covers a subspace of that subspace. The private symmetry center floats over a background space and its center location is a function of progression.

The location of the geometric center of the floating symmetry center is not part of the eigenspace of the anti-Hermitian operator $\mathfrak{S}_n^x$, but it is a property of the symmetry center. This floating location is a property of the elementary module and is formulated in terms of a value of the background parameter space $\mathfrak{R}$. This reference operator is a normal operator and provides full quaternionic eigenvalues that can represent progression values as well as spatial locations.

The observer maps the swarm to the field that represents its living space. This action involves a convolution with the Green's function of the field that represents this living space. The swarm is in fact an integration over the regeneration cycle of the hopping path and the Green's function is in fact an integration over the dynamic response of the field during this regeneration cycle. Similarly the Green's function is in fact an integration over the regeneration cycle of the dynamic response of the living space field in reaction on the corresponding hop landing. Each landing location in the hopping path corresponds with a sudden point-like trigger that affects the field. That response is described by a particular solution of the homogeneous second order partial differential equation, which describes the behavior of the field when it is triggered by such artifacts. The response of the field deforms this field and the convolution accounts for the deformation due to all triggers that are members of the location swarm. The convolution involves an integral. This reasoning implies that the generation of the swarm is an ongoing process.

If the generation stops, then the swarm collapses this includes the corresponding location density distribution. The reason can be that the mechanism, which is responsible for the generation of the swarm decides to switch to a another operation mode.

Two fields are involved. One field represents the living space. The result of the convolution is the living space potential. The other field is the symmetry related field. The integral that concerns the symmetry related field must take the differences in the ordering of the involved platforms in

account. This is best explained by the generalized Stokes theorem. That theorem converts an integral over a volume into an integral over the boundary that encapsulates this volume. As a consequence of the ordering the contribution is added or subtracted. If the encapsulation is located such that at these locations the added function values are negligible, then only the contributions of the difference in parameter space ordering result. In that case these differences will reveal the symmetry related charges. The symmetry related charges are supposed to be located at the geometric center of the platform on which the elementary module resides. Thus, for the symmetry related field, the volume integral involves a single Green's function.

8.1 Module content

In free translation, the spectral theorem for normal operators that reside in a separable Hilbert space states: "If a normal operator maps a closed subspace onto itself, then the subspace is spanned by an orthonormal base consisting of eigenvectors of the operator." The corresponding eigenvalues characterize this closed subspace.

Germ operator $\mathcal{O}_n^x$ only acts as a descriptor. It describes a hopping path. The operator does not generate its own eigenvalues. It has eigenvalues that are generated by a mechanism $\mathfrak{M}_n^x$, which is not part of the Hilbert space.

8.1.1 Progression window

Operator $\mathcal{O}_n^x$ is a stochastic operator. It is a normal operator. Its eigenvalues are not ordered in the way that the eigenvalues of reference operators are ordered. Still the real parts of operator $\mathcal{O}_n^x$ are in sync with the eigenvalues of the clock operator. Due to the integration over the regeneration cycle, the stochastic ordering of the spatial part of the eigenvalues will become hidden. In fact the location density distribution implements a spatial reordering of the hopping locations. The determination of the location density distribution integrates over the regeneration cycle and turns the hopping path into a location swarm. The integration transfers the hopping path into a location swarm.

Thus, it is possible to define a quaternionic normal operator $\mathcal{S}_n^x$ for which a subset of the eigenvectors span the same closed subspace as is spanned by the eigenvectors of $\mathcal{O}_n^x$ and the corresponding eigenvalues of this new operator describe the reordered dynamic geometric data of this elementary module such that they fit in the ordering of the eigenvalues of symmetry center $\mathfrak{S}_n^x$. After that ordering process, they form a subset of the eigenvalues of $\mathfrak{S}_n^x$. The integration over the regeneration cycle can be installed as a smoothing effect, which dampens the kinematic actions of the eigenvalues of $\mathcal{S}_n^x$. In this way, the geometric data become new functions of what we already have called **progression**. The new operator $\mathcal{S}_n^x$ describes the module content in a reordered fashion that can be interpreted as a location swarm.

A companion normal **reference operator** $\mathfrak{T}_n^x$ provides normal **capsule** for the anti-Hermitian symmetry center $\mathfrak{S}_n^x$. On the other hand it also covers the **progression window** of operator $\mathcal{O}_n^x$ It can be considered as the **capsule** or as the encapsulating operator for the elementary module. Its eigenspace can be viewed as a **tube** in which the elementary module travels. The operator $\mathcal{O}_n^x$ can be considered as an **inner tube**. The progression window covers a harmonica of sheets in which the model steps from sheet to sheet. Outside of the harmonica the model is considered to flow.

The operator $\mathfrak{S}_n^x$ that describes the symmetry center is only a descriptor. This also holds for the operators $\mathcal{O}_n^x$, $\mathcal{S}_n^x$, and $\mathfrak{T}_n^x$ that describe the content and the direct environment of the corresponding elementary module. The real actor is the controlling mechanism $\mathfrak{M}_n^x$, which is responsible for establishing the characteristics that are typical for the elementary module. These characteristics are the statistical characteristics and the symmetry of the swarm and the dynamic characteristics of the

corresponding hopping path. The mechanism $\mathfrak{M}_n^x$ takes care of the fact that the swarm is a ***coherent swarm*** and stays that way.

Stochastic processes that are controlled by dedicated mechanisms provide the elementary modules with dynamic geometric data. Here we only consider elementary modules for which the content is ***well-ordered***. This means that in the eigenspace of the selected operator every progression value is ***only used once***.

For the most primitive modules the closed subspace may be reduced until it covers a ***generation cycle*** in which the statistically averaged characteristics of the module mature to fixed values. The resulting closed subspace acts as a ***sliding progression window***. This sliding window corresponds to a regeneration cycle. The sliding window covers a (large) series of sheets that act as static status quos. It is described by a cycle of operator $\mathfrak{T}_n^x$.

What happens can be integrated over the progression window. This turns the germ operator. which describes the hopping path into a swarm operator $s_n^x = |a_j^x\rangle\, a_j^x \langle a_j^x|$.

The sliding window separates a deterministic history from a partly uncertain future. Inside the sliding window ***a dedicated mechanism*** $\mathfrak{M}_n^x$ ***fills the eigenspace*** of operator s_n^x. The mechanism is a function of progression. If it is a cyclic function of progression, then the module is recurrently regenerated by its private mechanism.

The phrase "recurrently regenerated" is related to the interpretation of the model where mechanisms generate new eigenvalues in contrast to the alternative interpretation where the boundary is passing over data that already exist as eigenvalues in the Hilbert space. The model itself is not influenced by these interpretations. For describing the model, the paper follows the first interpretation. However, it is also good to keep the second interpretation in mind. It throws a slightly different light upon the model.

8.2   Interaction with a continuum

By imaging the discrete eigenvalues into a reference space, the discrete eigenvalues form a ***swarm*** $\{a_j^x\}$, which is a subset of the rational quaternions $\{s_i^x\}$ that are eigenvalues of the symmetry center on which the module resides. At the same time the discrete eigenvalues form a ***hopping path***. They form a subset of the eigenvalues of tube operator $\mathfrak{T}_n^x$. With other words the swarm forms a spatial map of the dynamic hopping of the point-like object. The swarm and the hopping path conform to a stochastic operator o_n^x that is well ordered with respect to its progression values, but is not ordered in spatial sense like reference operators $\mathcal{R}$ or $\mathfrak{S}_n^x$. The swarm is spatially reordered in order to construct the location density distribution.

$$s_n^x = |a_j^x\rangle\, a_j^x \langle a_j^x|$$

Our plan is to construct a map of the elements $\{a_j^x\}$ of the swarm onto the deformable continuum $\mathfrak{C}$. In order to prepare this map the collection $\{a_j^x\}$ must be reordered again such that it conforms to the ordering of the background parameter space. This results in collection $\{b_j\}$. Here the superscript is removed. This collection is eigenspace of operator s_n.

$$s_n = |b_j\rangle\, b_j \langle b_j|$$

In approximation, operator s_n can be considered as a defined operator that uses the location density distribution s_n as its defining function.

Each image b_j of hop landing location a_j^x represents a point-like artifact that leads to a dynamic response of the living space field in the form of a spherical shape keeping front that after integration

over the regeneration cycle corresponds to the Green's function of the living space field and through the convolution with location density distribution $\mathscr{s}_n$ leads to a local contribution to the living space field $\mathfrak{C}$. All contributions of the elementary modules form then the living space potential $\mathfrak{U}$.

The living space potential blurs the living space field with the spread of the test function. The test function represents an artificial elementary module.

The deformed field $\mathfrak{C}$ represents a conglomerate of descriptors of the location density of location swarms. Where the location density becomes negligible the field $\mathfrak{C}$ describes the background parameter space. The convolution process must convert the symmetry flavors of the location swarms to the symmetry flavor of the background parameter space.

In the previous paragraphs the field is viewed as being deformed by the discrete objects that disturb its continuity. It is also possible to view the field as a descriptor that describes the location density distribution of the discrete objects. These views correspond to different interpretations of the same model. The interpretations do not influence the model. However, the selected interpretation does affect the description of the model. This duality indicates that there is nothing mysterious about the fact that the field and the discrete objects appear to interact. However, the situation will look mysterious if information transfer will use the deformed field as it carrier. That is what happens in reality.

The generalized Stokes theorem shows that in the integration process the discrepant regions must be separately handled and for that reason it is necessary to encapsulate the discrepant locations. The corresponding contributions must account the difference in symmetry flavor.

None of the eigenspaces of the parameter space operators are influenced by the interaction process. Only this last step causes space curvature in the deformable target field. The embedding of each of the elements last only a short instant and is immediately released. What results is the impact on the smoothed field $\mathfrak{C}$. Field $\mathfrak{C}$ is not only blurred in spatial sense. It is also averaged over the progression window.

8.3   Coherent elementary modules

Elementary modules that behave in a coherent dynamic way are characterized by a coherent location swarm. The coherent elementary modules are directly related to an individual symmetry center. The elements of the coherent location swarm that characterizes the coherent elementary module are taken from this symmetry center. These elements are ordered with respect to progression, but spatially they are selected in a stochastic fashion. This selection is described by germ operator σ^x. In the map onto the reference continuum, coherent elementary modules feature a hopping path. Inside the symmetry center the hopping path is on average closed. It means that on average it has a static geometric center. That center will correspond to the geometric center of the symmetry center. Further, for coherent elementary modules, the map of the location swarm into the reference continuum corresponds to a density operator ρ that is defined by a **continuous function**. ρ is an approximation of $\mathscr{s}_n$. That continuous function is a **normalized location density distribution** and it has a **Fourier transform**. As a consequence the swarm owns a **displacement generator** and as a further consequence in first approximation the swarm will **move as one unit**.

The new operator ρ has $\mathcal{R}$ and thus $\mathfrak{R}$ as the parameter space of the defining function ρ. It tends to describe the swarm as a whole unit. It no longer describes the hopping path. The operator ρ is no more than a special descriptor. It does not affect the distribution of the density of the locations that is described by this operator and its defining function.

The coherence is ensured by the private mechanism $\mathfrak{M}_n$ that selects the eigenvalues such that a coherent swarm is generated.

This paper gives no full explanation for this special habit of the mechanism. However, this habit is essential for the coherence of the whole model. Some guesses about the way that mechanism $\mathfrak{M}_n$ works are possible. Due to his experience

with low dose intensified imaging, the author assumes that the mechanisms apply something that looks like a combination of a Poisson process and a binomial process. Together they form an ***inhomogeneous spatial Poisson point process***. The test function shows that such a combination results in a coherent swarm. A combination of a Poisson process and a binomial process that is implemented by a spatial spread function can establish a location density distribution, which approaches the Gaussian distribution, which underlies the described test function. This might provide a partial indication of how the mechanism works. A Poisson process that is combined with an attenuating binomial process can again be considered as a Poisson process that has a lower local efficiency than the homogeneous spatial Poisson point process. Thus, in this interpretation, the spread function defines the spatial spread of the efficiency of the local Poisson processes. See the section on low dose rate imaging.

Coherent elementary modules are also characterized by the symmetry flavor of their symmetry center $\mathfrak{S}_n^x$. When mapped into a reference continuum that is eigenspace of reference operator $\mathfrak{R}^{\circledcirc} = |q^{\circledcirc}\rangle q^{\circledcirc} \langle q^{\circledcirc}|$ the module is characterized by a ***symmetry related charge***, which is *located at the center of symmetry*. The symmetry related charge is a property of the local ***symmetry center*** $\mathfrak{S}_n^x$. The symmetry related charge corresponds to an isolated point-like artifact of the ***symmetry related field*** $\mathfrak{U}$ that corresponds to the symmetry related charge.

The size and the sign of the symmetry related charge depends on the difference of the symmetry flavor of the local symmetry center with respect to the symmetry flavor of the surrounding reference continuum $\mathcal{R}^{\circledcirc}$. The coherent swarm $\{a_j^x\}$ inherits the symmetry flavor of the local symmetry center $\mathfrak{S}_n^x$. However, the controlling mechanism $\mathfrak{M}_n^x$ picks the elements of this set in a spatially stochastic way instead of in a spatially ordered fashion. Thus the stochastic operator σ_n^x that reflects the stochastic selection by $\mathfrak{M}_n^x$, corresponds with another operator, this time a density operator $\mathfrak{s}_n^x$ that reflects the spatial ordering and characterizes the coherent stochastic mechanism $\mathfrak{M}_n^x$ with respect to its achievement to establish spatial coherence.

Symmetry related charges are the reason of existence of a symmetry related field $\mathfrak{U}$. This field will be treated later.

8.4   The function of coherence

Embedding of sets of point-like objects into the affected embedding continuum spreads the reach of the separate embedding locations and offers the possibility to bind modules. The spread of a single embedded point-like object is defined by the Green's function. The Green's function represents the integral over the regeneration cycle of the dynamic response of the field on a short trigger. The trigger corresponds with a hop landing and is immediately released. The dynamic response of the field is described by the homogeneous second order partial differential equation. The integration turns the homogeneous equation into an inhomogeneous equation in which the extra term represents the Green's function.

Spurious embedding locations have not enough strength and not enough reach to implement an efficient binding effect. In contrast, coherent location swarms offers enough locality, enough spread and enough embedding strength in order to bind coherent swarms that are sufficiently close.

For example, a Gaussian distribution of the location swarm would turn the very peaky Green's functions into a rather broad spherical painting brush that can be described by the potential:

$$\varphi(r) = \frac{ERF(r)}{r} \tag{1}$$

This is a smooth function without a trace of a singularity. Thus the coherent swarm bends the embedding field in a smooth fashion!. We will give this particular function a name and call it **test function**. At the center location, the amplitude of the test function equals about 1,128379. The test function has a standard spread. The standard deviation is about 0,598758. A graph of function $\varphi(r)$ was shown in figure 1.

The actual location density distribution may differ from the Gaussian distribution. The amplitude of the resulting function will depend on the form of the density distribution will depend on the number of participating point-like obstructions. For large numbers of participating point-like obstructions, the coherence of the swarm ensures that the smoothed embedding field stays integrable, while each of the elements of the swarm would separately cause a singularity. The actual smoothness of the affected field will depend on the number of participating obstructions. This plays a greater role in the outskirts of the distribution. In that region the signal to noise ratio is much lower than in the center. This results in a larger local relative variance in the outskirts.

We assumed that all obstructions have similar impact on the affected field. However, the process that governs the generation of the obstructions has a stochastic nature. The characteristics of this process depends on the properties of the controlling mechanism. The number of elements in the coherent swarms that corresponds to actual elementary modules depends on the type of the module. For most types of elementary modules this number is huge. If the generator of the obstructions is a Poisson process in combination with a binomial process that is implemented by a spatial spread function, then the local signal to noise ratio can be calculated at any location where the number of participating obstructions is still large enough. This is due to the fact that a Poisson process in combination with a binomial process is again a Poisson process with an attenuated efficiency. An object that will approach these outskirts will sense the local relative variance of the field and may act accordingly. As a consequence its behavior in response to the local field value may appear to show some turbulence. Closer to the center of the swarm the signal to noise is much larger and the behavior of the respondent will become more consistent.

If for some reason the generation process is halted, then the controlling mechanism changes to another control mode and because of that the discrete nature of the swarm will becomes noticeable. In this case the last location in the location swarm indicates the exact location where the generation process was disrupted. After this instant the location density distribution has lost its validity and **collapses**. In physics the group of physicists that support the Copenhagen interpretation named this phenomenon "the collapse of the wave function".

Imaging of the location swarm onto the reference continuum is only used to define coherence and it is used to indicate the influence of the symmetry related charges. The embedding onto the affected continuum $\mathfrak{C}$ is used to exploit the corresponding potential binding effect of the swarm. The stochastic process that implements the stochastic location distribution under control of mechanism $\mathfrak{M}_n^x$ is the de facto actuator in establishing the coherent swarm. The embedding field $\mathfrak{C}$ is not affected by symmetry differences. In contrast the symmetry related field $\mathfrak{A}$ is caused by these differences. Thus $\mathfrak{C}$ and $\mathfrak{A}$ differ fundamentally! For the elementary module the symmetry center couples the two fields.

8.5 The effect of the blur

The coherent swarm represents an effective blur of every observation of the spatial location of the corresponding object. **All information about the swarm will be transmitted via the fields** that are influenced by the presence of the swarms. **The model does not support other information carriers**.

In this aspect the model differs from theories that postulate the existence of **force carriers**. This model does not support force carriers. Nor does it support the corresponding force fields. However, the basic fields can cause acceleration of the discrete objects that reside on symmetry centers. The notion of force carriers imposes a dilemma: What supports the force carrier? On the other hand, the variation of a vector field as a function of progression goes together with a new field that is represented in the first order partial differential equation. This new field acts with a force onto artifacts that are embedded in that new field. For the living space this effect is known as **inertia**. For the symmetry related field, the effect is known as **symmetry related force**. In physics it is called electric force.

The blur means that every object that is informed about the properties of the observed object will perceive this observed object with a blur that is defined by the field contribution that represents the

actual location density distribution. This is not the smooth density distribution ρ. It is the convolution of the density distribution with the Green's function of the field.

Due to the blur, no observer will directly perceive the difference between an object that is constructed as a swarm of discrete elements and an object that has a more compact structure such as a sphere. This fact is increased if the observer itself has a similar structure. The location swarms contain a huge number of elements. Only in this way the signal to noise ratio of the transferred information is large enough in order to tolerate reliable reactions of the observer on the signal that it receives via the surrounding fields.

Thus, every interaction is afflicted with a certain signal to noise ratio.

8.6   Modules and subspaces

Only a small fraction of the rational quaternions will represent a dynamic location of an elementary module. Thus, a comparable number of Hilbert vectors will represent the state of an elementary module. Each of these Hilbert vectors spans a closed subspace. With other words, ***the orthomodular lattice that describes the relations between all modules will only sparsely cover the set of closed subspace of the Hilbert space***.

At the next progression instant a new category of Hilbert vectors will represent the elementary modules. In this way the model steps with model wide progression steps. The current state of the model wipes through the model and divides the model in three parts: a historic part, a current part and a future part. The separable Hilbert space exactly registers all of these states. Thus, the Hilbert space is not confronted with any uncertainty. However, everything that travels with the separating blade will be cut off from any information that is stored in the future part. What occurs at a distance will reach the observer in the future. That information is transferred via fields. For all participants uncertainty exists about what the future will bring. The fact that the controlling mechanisms install coherence will reduce the size of the uncertainty.

The elementary modules will follow hopping paths and controlling mechanisms take care that these hopping paths stay within a tube. A map of the hopping path onto the cross section of the tube results in a spatial location swarm. This swarm and the hopping path characterize the properties and therefore the type of the elementary module.

This paper follows the view that is obtained by objects that travel with the scanning vane. Observers are modules that run with the vane. However, it is also possible to take a view in which all eigenvalues that are stored in the Hilbert space are known by the investigator. In that case the uncertainty of the vane traveler is changed into the uncertainty of the process that filled the eigen values at the instance that the whole Hilbert space was established. These uncertainties are the same. The creator generated its own uncertainty!

9   Fields

9.1   Fields in contrast to sets of discrete objects

Coherent sets of discrete quaternions have much in common with the continuums that describe the location density of these swarms. The set of rational quaternions is densely embedded in the continuum of the corresponding quaternionic number system. A continuous function can relate the coherent set that corresponds to the target of the rational quaternionic function and the corresponding smooth continuum. If you want to estimate the impact of point-like disruptions of the continuity, it makes more sense to investigate the set of rational target values of the relating function, than to try investigate the disrupted continuum. Putting the point-like disruptions in

capsules will partly solve integration and differentiation problems. In this way smoothed versions of the fields can be derived that circumvent the problems that integration has with the existence of point-like disruptions.

9.2   Differentiable and integrable basic fields

By applying the reverse bra-ket method, a category of operators can represent quaternionic functions. They do this in combination with reference operators. This is applicable both in the separable Hilbert space and in the Gelfand triple.

In this paper, fields are continuums that are target spaces of quaternionic functions that define eigenspaces of operators, which reside in the Gelfand triple.

Quaternionic functions and their differentials can be split in real scalar functions and imaginary vector functions. Here we will only consider the not too violent disruptions of the continuity of the fields. We also restrict the validity range of the equations. With these restrictions the **quaternionic nabla** can be applied and the discontinuities restrict to point-like artifacts. The quaternionic nabla has the advantage that it works as a multiplying operator. It obeys quaternionic multiplication rules.

Quaternionic functions can represent fields and continuums, but they can also represent density distributions of discrete dynamic locations. A point-like disruption then corresponds to a single exception in a large assembly of smoothly varying values. The vector field that goes together with the scalar field may then represents the displacements of the discrete objects. Quaternionic differentiation of such fields is treated in the next chapter.

Double differentiation of a basic field leads to a non-homogeneous second order partial differential equation that relates the basic field to the corresponding density distributions of discrete dynamic locations of the artifacts that cause the local discontinuities of the basic field. For quaternionic functions two different second order partial differential equations exist. They describe different dynamic behavior of the same basic field and the two second order partial differential equations can offer views on different behavior of the investigated field.

The symmetry related field $\mathfrak{A}$ and the embedding continuum $\mathfrak{C}$ are basic fields. This paper mainly investigates these two basic fields. A third basic field describes the activity of rotator quaternions. In this paper, all other fields are derived from these basic fields.

The symmetry related field $\mathfrak{A}$ is based on the existence of symmetry centers. These symmetry centers float over a reference parameter space that acts as a background in the whole model.

The embedding continuum $\mathfrak{C}$ is based on the existence of a dynamic deformable function $\mathfrak{C}$ that describes the embedding of discrete artifacts, which reside on symmetry centers and interact with $\mathfrak{C}$. The artifacts are selected by mechanisms $\mathfrak{M}_n^x$ that are dedicated to the symmetry center $\mathfrak{S}_n^x$. The results of the activity of these mechanisms can be described by a corresponding stochastic operators $\mathscr{O}_n^x$. All stochastic operators of type $\mathscr{O}$ have countable eigenspaces and can be considered to reside in the separable Hilbert space.

9.3   Subspace maps

The orthomodular base model consist of two related Hilbert spaces.

- An infinite dimensional separable Hilbert space $\mathfrak{H}$ that acts as a descriptor of the properties of all discrete objects.
- A non-separable Hilbert space $\mathcal{H}$ that acts as a descriptor of the properties of all continuums.

The orthomodular base model does not apply Fock spaces because the tensor product of quaternionic Hilbert spaces is no longer a quaternionic Hilbert space. Instead it is a real Hilbert space. It reduces the model to the representation of the model's clock.

In the selected view, an ongoing process which is governed by dedicated mechanisms embeds a part of the separable Hilbert space $\mathfrak{H}$ into its non-separable companion Hilbert space $\mathcal{H}$. The treated part is the vane and a section that covers the regeneration cycle. This ongoing process corresponds to a partition in the form of a vane that moves through the reference parameter spaces $\mathcal{R}^{\circledo}$ and $\mathfrak{R}^{\circledo}$ and splits them into three parts: history, present static status quo and future. We introduce an harmonica that splits the vicinity of this boundary in a series of sheets. The middle sheet is the actual vane. Thus, in the neighborhood of the boundary we treat progression as a discrete parameter. Further away, progression may be considered to flow. The sheets cover a sliding progression window that covers the current regeneration cycles of the swarms. The mechanism $\mathfrak{M}_n^x$ that governs the embedding of an elementary module is active in the splitting boundary, but its control is influenced by historic and future sheets that belong to the harmonica, which covers the regeneration cycle that produces the coherent location swarm, which is characteristic for the elementary module. The behavior of the mechanism is stochastic and only determined by statistical and symmetry related characteristics. Nothing, not even the creator of the model, has deterministic insight in the decisions of the mechanism.

This view corresponds to the interpretation of the model in which mechanisms generate new spatial data as a function of the progression value. An alternative interpretation suspects that the future data are already present in the Hilbert space and are encountered by the moving boundary. In that case the mechanisms must have been active as generators at the instance of the formation of the whole Hilbert space. Also in that case the activity of the mechanisms is stochastic and is not governed and deterministically determined by the creator of the model. The model itself is not affected by these different interpretations.

The two Hilbert spaces are coupled by the Cartesian-ordered reference operator $\mathcal{R}^{\circledo}$ and the corresponding reference operator $\mathfrak{R}^{\circledo}$. Both are defined by the quaternionic function $\mathfrak{R}(q) \overset{\text{def}}{=} q$.

On the rim between history and future will controlling mechanisms $\{\mathfrak{M}_n^x\}$ fill the module related subspaces of separable Hilbert space $\mathfrak{H}$ with data and the new contents of these subspaces are subsequently embedded into the non-separable Hilbert space $\mathcal{H}$. The history stays untouched. The fill of subspaces with data is described by dedicated stochastic operators. The mechanisms $\{\mathfrak{M}_n^x\}$ use stochastic processes in order to generate these data. The author suspects that the stochastic operators represent inhomogeneous spatial Poisson point processes. In more detail these processes are probably modified Thomas processes.

A closed subspace in $\mathfrak{H}$ maps into a subspace of $\mathcal{H}$. Only the countable subspaces of $\mathcal{H}$ have a sensible dimension. By applying the reverse bra-ket method, defining functions can map countable eigenspaces of operators that reside in the separable Hilbert space into continuum eigenspaces in the Gelfand triple. Mapping does not influence the flat reference fields that are in use as parameter spaces. However, the embedding process affects the deformable field $\mathfrak{C}$. In this case the map must be interpreted as interaction. The $\mathfrak{C}$ field describes the generated location swarms that result from the corresponding hopping paths. Indirectly, the embedding process affects the symmetry related field $\mathfrak{A}$. In fact both fields interact by affecting the location of the geometric center of the symmetry centers that correspond to elementary modules.

9.4   Embedding field

The elements of the eigenspace of the stochastic operator σ_n^x, which is used by a controlling mechanism $\mathfrak{M}_n^x$ will be embedded in the eigenspace of operator $\mathfrak{C}$. A more smoothed version $\mathfrak{U}$ of this operator exists that mimics the view that observers get from the field $\mathfrak{C}$. For example $\mathfrak{C}$ is

smoothed by its Green's function and $\mathfrak{U}$ is smoothed by a blur that approaches the blur of the test function. Observers are the receivers of information that is transported by messengers or by other vibrations or deformations of the embedding field. The messengers are objects that use the embedding field as their transport medium. Smoothing blurs the perception of the observer. The smoothing implemented by $\mathfrak{U}$ represents the minimal observation blur for elementary modules.

With this interpretation the embedding process can be seen as the pursuit by the embedding field to follow the density distribution of a set of rational and thus discrete quaternionic target values as close as is tolerated by a selected blurring function. This process involves a convolution and this convolution involves an integration. The target values are the targets of the defining function for a selected set of parameter values. $\mathfrak{C}$ uses a narrower blurring function than $\mathfrak{U}$ does. $\mathfrak{C}$ *is interpreted as a field, while* $\mathfrak{U}$ *is interpreted as a potential*. The difference between $\mathfrak{C}$ and $\mathfrak{U}$ is that $\mathfrak{U}$ blurs all spurious point-like artifacts such that they become "unobservable". Only in huge numbers these spurious point-like artifacts will become noticeable as *large range effects*.

Operator $\mathfrak{C}$ can be described by a quaternionic function $\mathfrak{C}(q^{\circledcirc})$ that has a parameter space $\mathfrak{R}^{\circledcirc}$, which is generated by the eigenspace of reference operator $\mathfrak{R}^{\circledcirc}$. When applicable, we use the same symbol for the parameter space, the defining function and the operator. With the installed restrictions, the dynamics of the embedding process can be described by quaternionic differential calculus.

If the discontinuities that are generated by local discontinuities are not too violent , then the non-homogeneous second order partial differential equation will elucidate the embedding process. This will be treated in detail in the next chapter.

In $\mathcal{H}$ the operator $\mathfrak{C} \overset{\text{def}}{=} |q^{\circledcirc}\rangle \mathfrak{C}(q^{\circledcirc})\langle q^{\circledcirc}|$ is defined by function $\mathfrak{C}(q^{\circledcirc})$ and represents an embedding continuum $\mathfrak{C}$. This continuum gets affected by the embedding process and thus deforms dynamically.

We will show that two different non-homogeneous second order partial differential equations exist that offer different descriptions of the embedding process. The equation that is based upon the double quaternionic nabla $\nabla \nabla^{*}$ cannot show wave behavior. However, the equation that is based on d'Alembert's operator $\mathfrak{D}$ acts as a wave equation, which offers waves as part of its set of solutions.

$$\nabla \nabla^{*} = \nabla_0 \nabla_0 + \langle \boldsymbol{\nabla}, \boldsymbol{\nabla} \rangle \tag{1}$$

$$\mathfrak{D} \overset{\text{def}}{=} -\nabla_0 \nabla_0 + \langle \boldsymbol{\nabla}, \boldsymbol{\nabla} \rangle \tag{2}$$

The embedding continuum $\mathfrak{C}$ *is always and (nearly) everywhere present.*

Space cavities form an exception to this rule. $\mathfrak{C}$ is deformed and vibrated by discrete artifacts that are embedded in this field. In the considered domain, $\mathfrak{C}$ may contain point-like artifacts and connected regions where $\mathfrak{C}(q)$ is not defined.

In $\mathcal{H}$, the representations of symmetry centers float over the natural parameter space $\mathfrak{R}^{\circledcirc}$ of the embedding continuum. The symmetry related charges of the symmetry centers generate local contributions φ to the symmetry related field $\mathfrak{A}$. The location of the center of the symmetry center $\mathfrak{S}_n^x$ within parameter space $\mathfrak{R}^{\circledcirc}$ is affected by the symmetry related field $\mathfrak{A}$. The

symmetry related field $\mathfrak{U} \stackrel{\text{def}}{=} |q^{\textcircled{0}}\rangle \mathfrak{U}(q^{\textcircled{0}})\langle q^{\textcircled{0}}|$ uses the same natural parameter space $\mathfrak{R}^{\textcircled{0}}$ as the embedding field $\mathfrak{C}$ does. This indicates that the fields $\mathfrak{U}$ and $\mathfrak{C}$ influence each other in an indirect way via the symmetry centers. This influence is effectuated by *forces*. For the $\mathfrak{U}$ field these forces relate to the electric charge. For the $\mathfrak{C}$ field the force relates to the mass, which on its turn relates to the number of involved hop landings.

The mechanism $\mathfrak{M}_n^x$ that controls stochastic operator σ_n^x picks members of a symmetry center $\mathfrak{S}_n^x$ and stores them in the eigenvalues of that operator. These eigenvalues are mapped to parameter space $\mathcal{R}^{\textcircled{0}}$ and in that way they become eigenvalues of a new operator $\mathcal{b}_n^x$. This map involves relocation and re-ordering. This fact couples the location of the symmetry related charge of this symmetry center with the locations that get embedded in the eigenspace of operator $\mathfrak{C}$. However, the parameter location of the symmetry related charge does not coincide with the parameter location of the eigenvalue of operator $\mathcal{b}_n^x$, that will be embedded in the eigenspace of operator $\mathfrak{C}$. This embedding involves a map that is described in a blurred way by function $\mathfrak{C}(q)$. The eigenvalues of operator $\mathcal{b}_n^x$ will form a mapped swarm whose center will coincide with the mapped parameter location of the symmetry related charge. That location also coincides with the location of the mapped geometric center of the symmetry center. The images of eigenvalues of $\mathcal{b}_n^x$ onto $\mathfrak{C}$ correspond to *blurred point-like artifacts*. The images of these eigenvalues on the smoothed version $\mathfrak{U}$ of $\mathfrak{C}$ correspond with even more *blurred locations* in $\mathfrak{U}$. The blurs are caused by convolutions.

$\mathfrak{C}$ and $\mathfrak{U}$ lay like thin and thick (3D) snow blankets over the set of discrete rational quaternions. $\mathfrak{U}$ represents a thicker and thus smoother snow blanket than $\mathfrak{C}$.

9.5 Symmetry related fields

Due to their four dimensions, quaternionic number systems exist in sixteen versions that only differ in their symmetry flavor. The elements of coherent sets of quaternions belong to the same symmetry flavor. This is the symmetry flavor of the symmetry center $\mathfrak{S}_n^x$ that supports the original location swarm. Differences between symmetry flavors of a symmetry center $\mathfrak{S}_n^x$ and the symmetry flavor of the eigenspace of the surrounding reference operator $\mathcal{R}^{\textcircled{0}}$ cause the presence of a symmetry related charge at the center location of that symmetry center. The countable reference parameter space $\mathcal{R}^{\textcircled{0}}$ in the separable Hilbert space $\mathfrak{H}$ maps onto the continuum parameter space $\mathfrak{R}^{\textcircled{0}}$, which resides in the Gelfand triple $\mathcal{H}$.

Symmetry related charges are point-like objects. These charges *generate a field* $\mathfrak{U}$ that fundamentally differs from the embedding continuum. This symmetry related field also plays a role in the binding of modules, but that role differs significantly from the role of the embedding continuum $\mathfrak{C}$. The defining function $\mathfrak{U}(q)$ of field $\mathfrak{U}$ and the defining function $\mathfrak{C}(q)$ of field $\mathfrak{C}$ use the same parameter space $\mathfrak{R}^{\textcircled{0}}$.

Symmetry related charges are located at the geometric centers of local symmetry centers. The size and the sign of the symmetry related charge depends on the difference of the symmetry flavor of the symmetry center with respect to the symmetry flavor of the embedding continuum. Symmetry centers that belong to different symmetry related charges appear to react on the symmetry differences. Equally signed charges repel and differently signed charges attract. The attached coherent location sets that are attached to the symmetry centers will be affected by these effects.

The symmetry related charges do not directly affect the embedding continuum $\mathfrak{C}$. Their effects are confined to the map of the symmetry center $\mathfrak{S}_n^x$ to the parameter space $\mathfrak{R}^{\textcircled{0}}$. However, with their

action the symmetry related charges ***relocate*** the centers of the corresponding coherent swarms. The elements of the swarms deform the embedding continuum.

The symmetry related charges are rather isolated point charges. As a consequence the range of the field that is generated by a single charge is rather limited. The corresponding Green's function diminishes as 1/r with distance r from the charge.

Fields of point charges superpose. A wide spread uniform distribution of symmetry related point charges can generate a corresponding wide spread symmetry related field $\mathfrak{A}$. This works well if a majority of the charges have the same sign. Still, relevant values of the symmetry related field $\mathfrak{A}$ depend on the nearby existence of symmetry related charges.

Coherent swarms are recurrently regenerated on their symmetry centers. The symmetry centers are not recurrently generated, but instead their geometric center can get relocated. Together with these symmetry centers, the corresponding symmetry related charges and the residing swarms get relocated.

The relative short range of relevant field values makes the symmetry related field a bad candidate for the medium on which long range messengers can travel. For that purpose the embedding field $\mathfrak{C}$ is a much better candidate.

9.6   Gluon related field

Quaternions exist that can rotate another quaternion or even an entire swarm of quaternions over $\pi/2$ radians. The size of the real part of these special quaternionic rotators equals the size of their imaginary part. These quaternions act in pairs. These special quaternions can switch an anisotropy to another dimension. In other words, they may switch the symmetry related charge of an anisotropic elementary module to a different value (color). Isotropic objects stay unaffected.

The presence of these quaternions during the generation of the swarm of an anisotropic elementary module can interfere with this building process. Thus, the presence of the color shifting quaternions affects the persistence of the anisotropic elementary module. Isotropic objects are not affected.

The mechanisms that ensure the coherence of the swarms of anisotropic elementary modules respond by colluding with other mechanisms that also manage anisotropic elementary modules by jointly generating isotropic composite objects. The composite will be characterized by a single location swarm, but that swarm will reflect the landing locations of multiple hopping paths. The constituting hopping paths are anisotropic, but the result of the merge will be that the swarm is effectively isotropic. In physics the phenomenon of color neutralization is called "***color confinement***". This phenomenon has a binding effect. The process ***binds quarks into hadrons***. The color shifting quaternions play the role of the ***gluons***. That is why we will use the name "gluon" for the pairs of color shifting quaternions. The gluons give raise to ***a third basic field***. They are governed by a special mechanism that controls their presence and their activity. We will use symbol $\mathfrak{Z}$ for the gluon related field.

9.7   Free space

In the separable Hilbert space, the eigenvectors of the Cartesian-ordered reference operator $\mathcal{R}^{\textcircled{0}}$ that do not belong to a module subspace together span free space. The elementary modules reside on symmetry centers whose center locations float on the eigenspace of $\mathcal{R}^{\textcircled{0}}$.

At every progression instant only one element of the swarm $\{a_j^x\}$ is used. Thus "free space" surrounds all elements of the swarm. It forms most of the continuum $\mathfrak{C}$, which is deformed by the embedding of the currently selected swarm element.

10 Field dynamics

With respect to quaternionic differential calculus the basic fields behave in a similar way. This especially holds in the absence of continuity disrupting discrete artifacts. We will use a more general symbol for the investigated field in order to analyze behavior of the fields under differentiation and integration. In the appendix we will describe the difference between quaternionic differential calculus and Maxwell based differential calculus. In order to support that comparison we will define the derived subfields $\mathfrak{E}$ and $\mathfrak{B}$. Both $\mathfrak{C}$ and $\mathfrak{A}$ have such subfields!

In this chapter the differential equations are all quaternionic differential equations. They are no Maxwell equations. The Maxwell-like equations use progression rather than coordinate time. Progression conforms to proper time.

10.1 Differentiation

In the model that we selected, the dynamics of the fields can be described by quaternionic differential calculus. Apart from the eigenspaces of reference operators and the symmetry centers we encountered three basic fields that are defined by quaternionic functions and corresponding operators. One is the symmetry related field $\mathfrak{A}$, another is the embedding field $\mathfrak{C}$ and the third field $\mathfrak{Z}$ is caused by the activity of the gluons.

$\mathfrak{A}$ determines the dynamics of the symmetry centers. $\mathfrak{C}$ gets deformed and vibrated by the recurrent embedding of point-like elementary particles that each reside on an individual symmetry center. Field $\mathfrak{Z}$ gets deformed by the presence and the activity of gluons.

Apart from the way that they are affected by point-like artifacts that disrupt the continuity of the field, the fields obey, under not too violent conditions and over not too large ranges, the same differential calculus. The main difference between the fields is the nature of the artifacts that disturb the continuity of the fields.

Two quite similar, but still significantly different kinds of dynamic geometric differential calculus exist. One kind is the genuine quaternionic differential calculus. The other kind is known as Maxwell based differential calculus. These two kinds will appear to represent different views onto the basic fields. In order to perform the comparison we must extend the set of Maxwell equations. In principle this means that the Maxwell based set of differential equations is incomplete. However, in practice and in order to achieve certain goals the set of Maxwell equations is extended with equivalents of the gauge equations. In this chapter only the quaternionic differential calculus will be treated. The Maxwell based differential equations and the comparison of the two kinds are treated in the appendix.

10.2 Quaternionic differential calculus.

First we will investigate the validity range of our pack of pure quaternionic differential equations. We will only consider equations that do not surpass second order differentiation. This restricts application to not too violent changes of the investigated fields.

Under rather general conditions the change of a quaternionic function $f(q)$ can be described by:

$$df(q) \approx \sum_{\mu=0\ldots3}\left\{\frac{\partial f}{\partial q_\mu} + \sum_{\mu=0\ldots3}\frac{\partial}{\partial v}\frac{\partial f}{\partial q_\mu}dq^\nu\right\}dq^\mu = c_\mu(q)dq^\mu + c_{\mu\nu}(q)dq^\mu dq^\nu \tag{1}$$

Here the coefficients $c_\mu(q)$ and $c_{\mu\nu}(q)$ are full quaternionic functions. dq^μ are real numbers. e^ν are quaternionic base vectors.

This covers first and second order differential terms. We ignore the higher order differentials. Thus, these conditions cannot be considered to be general conditions! Under more moderate and sufficiently short range conditions the differential function is supposed to behave more linearly.

$$df(q) \approx \sum_{\mu=0\ldots3} \frac{\partial f}{\partial q_\mu} dq^\mu = c_\mu(q) dq^\mu \tag{2}$$

Under even stricter conditions the partial differential functions become real functions $c_0^\mu(q)$ that are attached to quaternionic base vectors:

$$df(q) = c_0^\tau \, dq_\tau + c_0^x \, \boldsymbol{i} \, dq_x + c_0^y \, \boldsymbol{j} \, dq_y + c_0^z \, \boldsymbol{k} \, dq_z = c_0^\mu(q) \, e_\mu \, dq_\mu \tag{3}$$

$$= \sum_{\mu=0}^{3} \left(\sum_{\varsigma=0}^{3} \frac{\partial f^\varsigma}{\partial q_\mu} e_\varsigma \right) e_\mu dq^\mu = \sum_{\mu=0\ldots3} \Phi_\mu e_\mu dq^\mu$$

$$\Phi_\mu = c_0^\mu = \sum_{\varsigma=0}^{3} \frac{\partial f^\varsigma}{\partial q_\mu} e_\varsigma = \frac{\partial f^\varsigma}{\partial q_\mu} e_\varsigma = \frac{\partial f}{\partial q_\mu} \tag{4}$$

Thus, in a rather flat continuum we can use the quaternionic nabla ∇. This is the situation that we want to explore with our set of pure quaternionic equations. ***The resulting conditions are very restrictive!*** These conditions are far from general conditions. However, these restrictions still tolerate point-like disturbances of the continuity of the original function f.

$$\nabla = \left\{ \frac{\partial}{\partial \tau}, \frac{\partial}{\partial x}, \frac{\partial}{\partial y}, \frac{\partial}{\partial z} \right\} = \frac{\partial}{\partial \tau} + \boldsymbol{i} \frac{\partial}{\partial x} + \boldsymbol{j} \frac{\partial}{\partial y} + \boldsymbol{k} \frac{\partial}{\partial z} = \nabla_0 + \boldsymbol{\nabla} \tag{5}$$

$$\nabla f = \sum_{\mu=0}^{3} \frac{\partial f}{\partial q_\mu} e_\mu \tag{6}$$

This form of the partial differential equation highlights the fact that in first order and second order partial differential equations ***the nabla operator can be applied as a multiplier***. This means that we can apply the quaternionic multiplication rule.

$$\Phi_0 = \nabla_0 \psi_0 - \langle \boldsymbol{\nabla}, \boldsymbol{\psi} \rangle \tag{7}$$

$$\Phi = \nabla_0 \psi + \nabla \psi_0 \pm \nabla \times \psi \tag{8}$$

The $\pm$ sign indicates that the nabla operator is also afflicted by symmetry properties of the applied quaternionic number system. The above equations represent only low order partial differential equations. In this form the equations can still describe point-like disruptions of the continuity of the field. We can take the conjugate:

$$\Phi^* = (\nabla \psi)^* = \nabla^* \psi^* \mp 2 \nabla \times \psi \tag{9}$$

$$\nabla^*(\nabla^* \psi^*)^* = \nabla^* \Phi = \nabla^* \nabla \psi \tag{10}$$

10.2.1 The first kind of second order quaternionic partial differential equation

This kind of double partial differentiation will then result in the following quaternionic **non-homogeneous second order partial differentiation equation**:

$$\xi = \xi_0 + \boldsymbol{\xi} = \nabla^* \nabla \psi = (\nabla_0 - \boldsymbol{\nabla})(\nabla_0 + \boldsymbol{\nabla})(\psi_0 + \boldsymbol{\psi}) \tag{1}$$

$$= \{\nabla_0 \nabla_0 + \langle \boldsymbol{\nabla}, \boldsymbol{\nabla} \rangle\}\psi = \frac{\partial^2 \psi}{\partial \tau^2} + \frac{\partial^2 \psi}{\partial x^2} + \frac{\partial^2 \psi}{\partial y^2} + \frac{\partial^2 \psi}{\partial z^2}$$

We can split the above equation in a real (scalar) part and an imaginary (vector) part.

Investigation of the details shows that the $\nabla^* \nabla$ operator has a rather simple consequence that is shown in formula (1)

$$\zeta_0 = \nabla_0 \phi_0 + \langle \boldsymbol{\nabla}, \boldsymbol{\phi} \rangle \tag{2}$$
$$= \nabla_0 \nabla_0 \varphi_0 - \nabla_0 \langle \boldsymbol{\nabla}, \boldsymbol{\varphi} \rangle + \langle \boldsymbol{\nabla}, \boldsymbol{\nabla} \rangle \varphi_0 + \nabla_0 \langle \boldsymbol{\nabla}, \boldsymbol{\varphi} \rangle \pm \langle \boldsymbol{\nabla}, \boldsymbol{\nabla} \times \boldsymbol{\varphi} \rangle$$
$$= (\nabla_0 \nabla_0 + \langle \boldsymbol{\nabla}, \boldsymbol{\nabla} \rangle)\varphi_0$$

$$\zeta = -\boldsymbol{\nabla}\phi_0 + \nabla_0 \boldsymbol{\phi} \mp \boldsymbol{\nabla} \times \boldsymbol{\phi} \tag{3}$$
$$= -\boldsymbol{\nabla}\nabla_0 \varphi_0 + \boldsymbol{\nabla}\langle \boldsymbol{\nabla}, \boldsymbol{\varphi} \rangle + \nabla_0 \boldsymbol{\nabla}\varphi_0 + \nabla_0 \nabla_0 \boldsymbol{\varphi} \pm \nabla_0 \boldsymbol{\nabla} \times \boldsymbol{\varphi}$$
$$\mp \boldsymbol{\nabla} \times \boldsymbol{\nabla}\varphi_0 \mp \boldsymbol{\nabla} \times \nabla_0 \boldsymbol{\varphi} - \boldsymbol{\nabla} \times \boldsymbol{\nabla} \times \boldsymbol{\varphi}$$
$$= -\boldsymbol{\nabla}\nabla_0 \varphi_0 + \boldsymbol{\nabla} \times \boldsymbol{\nabla} \times \boldsymbol{\varphi} + \langle \boldsymbol{\nabla}, \boldsymbol{\nabla} \rangle \boldsymbol{\varphi} + \nabla_0 \boldsymbol{\nabla}\varphi_0 + \nabla_0 \nabla_0 \boldsymbol{\varphi} \pm \nabla_0 \boldsymbol{\nabla} \times \boldsymbol{\varphi}$$
$$\mp \boldsymbol{\nabla} \times \boldsymbol{\nabla}\varphi_0 \mp \boldsymbol{\nabla} \times \nabla_0 \boldsymbol{\varphi} - \boldsymbol{\nabla} \times \boldsymbol{\nabla} \times \boldsymbol{\varphi}$$

$$= (\nabla_0 \nabla_0 + \langle \boldsymbol{\nabla}, \boldsymbol{\nabla} \rangle)\boldsymbol{\varphi}$$

Here ξ is a quaternionic function that for a part ρ describes the density distribution of a set of point-like artifacts that disrupt the continuity of function $\psi(q)$.

$$\rho = \rho_0 + \boldsymbol{\rho} = \langle \boldsymbol{\nabla}, \boldsymbol{\nabla} \rangle \psi = \frac{\partial^2 \psi}{\partial x^2} + \frac{\partial^2 \psi}{\partial y^2} + \frac{\partial^2 \psi}{\partial z^2} \tag{4}$$

$$\xi - \rho = \nabla_0 \nabla_0 \psi \tag{5}$$

In case of a single static point-like artifact, the solution ψ will describe the corresponding Green's function. Its actual form depends on the boundary conditions.

Function $\psi(q)$ describes the mostly continuous field ψ.

The second order partial differential equation that is based on the double quaternionic nabla **can be split into two continuity equations**, which are quaternionic first order partial differential equations:

$$\Phi = \nabla \psi \tag{6}$$

$$\rho = \nabla^* \Phi \tag{7}$$

If ψ and Φ are normalizable functions and $\|\psi\| = 1$, then with real m and $\|\zeta\| = 1$ follows:

$$\nabla \psi = m\, \zeta \tag{9}$$

10.2.2 The other second order partial differential equation

We encounter another quaternionic second order partial differential equation, but this one cannot be split into two first order quaternionic partial differential equations. It is based on d'Alembert's operator $\mathfrak{D} = (-\nabla_0 \nabla_0 + \langle \boldsymbol{\nabla}, \boldsymbol{\nabla} \rangle)$.

$$\zeta = \zeta_0 + \boldsymbol{\zeta} = \mathfrak{D}\varphi = \mathfrak{D}(\varphi_0 + \boldsymbol{\varphi}) = \{-\nabla_0 \nabla_0 + \langle \boldsymbol{\nabla}, \boldsymbol{\nabla} \rangle\}\varphi \tag{1}$$

Dirac has shown that it can be split into two biquaternionic partial differential equations. This fact is treated in the appendix.

In contrast to the first kind of second order quaternionic partial differential equation, the second kind accepts waves as solutions of the homogeneous version of the equation. The waves are **eigenfunctions** of differential operator $\mathfrak{D}$. All superpositions of such eigenfunctions are again solutions of the homogeneous equation and can be added to the solutions of the inhomogeneous equation. These superpositions form so called **wave packages**. When they move, wave packages tend to disperse.

$$\nabla_0 \nabla_0 f = \langle \nabla, \nabla \rangle f = -\omega^2 f \tag{2}$$

$$f(t, x) = a \exp\big(i\omega(ct - |x - x'|)\big); c = \pm 1 \tag{3}$$

This leads to a category of solutions that are known as solutions of the **Helmholtz equation**. These solutions characterize the behavior of constituents of **atomic modular systems**.

10.3 Fourier equivalents

In this quaternionic differential calculus, differentiation is implemented as multiplication.

This is revealed by the Fourier equivalents of the equations (4) through (10) in the previous paragraph:

$$\widetilde{\Phi} = \widetilde{\Phi}_0 + \widetilde{\boldsymbol{\Phi}} = p\,\tilde{\psi} = (p_0 + \boldsymbol{p})(\tilde{\psi}_0 + \widetilde{\boldsymbol{\psi}}) \tag{1}$$

The nabla ∇ is replaced by operator p. $\widetilde{\Phi}$ is the Fourier transform of Φ.

$$\widetilde{\Phi}_0 = p_0 \tilde{\psi}_0 - \langle \boldsymbol{p}, \widetilde{\boldsymbol{\psi}} \rangle \tag{2}$$

$$\widetilde{\boldsymbol{\Phi}} = p_0 \widetilde{\boldsymbol{\psi}} + \boldsymbol{p}\tilde{\psi}_0 \pm \boldsymbol{p} \times \widetilde{\boldsymbol{\psi}} \tag{3}$$

The equivalent of the quaternionic second order partial differential equation is:

$$\tilde{\xi} = \tilde{\xi}_0 + \widetilde{\boldsymbol{\xi}} = p^* p\,\tilde{\psi} = \{p_0 p_0 + \langle \boldsymbol{p}, \boldsymbol{p} \rangle\}\tilde{\psi} \tag{4}$$

$$\tilde{\rho} = \tilde{\rho}_0 + \widetilde{\boldsymbol{\rho}} = \langle \boldsymbol{p}, \boldsymbol{p} \rangle \tilde{\psi} \tag{5}$$

The continuity equations result in:

$$\widetilde{\Phi} = p\tilde{\psi} \tag{6}$$

$$\tilde{\rho} = p^* \widetilde{\Phi} \tag{7}$$

10.4 Poisson equations

The **screened Poisson equation** is a special condition of the non-homogeneous second order partial differential equation in which some terms are zero or have a special value.

$$\nabla^* \nabla \psi = \nabla_0 \nabla_0 \psi + \langle \boldsymbol{\nabla}, \boldsymbol{\nabla} \rangle \psi = \xi \tag{1}$$

$$\nabla_0 \nabla_0 \psi = -\lambda^2 \, \psi \tag{2}$$

$$\langle \boldsymbol{\nabla}, \boldsymbol{\nabla} \rangle \psi - \lambda^2 \psi = \xi \tag{3}$$

The 3D solution of this equation is determined by the screened Green's function $G(r)$.

Green functions represent solutions for point sources. In spherical symmetric boundary conditions the Green's function becomes:

$$G(r) = \frac{\exp(-\lambda \, r)}{r} \tag{4}$$

$$\psi = \iiint G(\boldsymbol{r} - \boldsymbol{r}') \, \rho(\boldsymbol{r}') \, d^3\boldsymbol{r}' \tag{5}$$

G(r) has the shape of the Yukawa potential [13]

In case of $\lambda = 0$ it resembles the Coulomb or gravitation potential of a point source.

If $\lambda \neq 0$, then a solution of equation (3) is:

$$\psi = a(\boldsymbol{x}) \exp(\pm i \, \omega \, \tau); \lambda = \pm i \, \omega \tag{6}$$

These solutions concern a screened Poisson equation that is based on the first version of the second order partial differential equation. The equation that is based on d'Alembert's operator delivers:

$$\mathfrak{D}\varphi = \mathfrak{D}(\varphi_0 + \boldsymbol{\varphi}) = \{-\nabla_0 \nabla_0 + \langle \boldsymbol{\nabla}, \boldsymbol{\nabla} \rangle\}\varphi = \zeta \tag{7}$$

$$\nabla_0 \nabla_0 \varphi = \frac{\partial^2 \varphi}{\partial \tau^2} = \lambda^2 \, \varphi$$

71

$$(\langle \boldsymbol{\nabla}, \boldsymbol{\nabla} \rangle - \lambda^2)\varphi = \frac{\partial^2 \varphi}{\partial x^2} + \frac{\partial^2 \varphi}{\partial y^2} + \frac{\partial^2 \varphi}{\partial z^2} - \lambda\varphi = \zeta \tag{8}$$

$$\varphi = a(\boldsymbol{x})\exp(\pm\lambda\tau) \tag{9}$$

The Green's function is the same, but solution (9) differs significantly from solution (6). The difference only concerns the temporal behavior of the field.

10.5 Special solutions of the homogeneous partial differential equations

The fact that the **wave equation** has waves as its solution is the cause that d'Alembert's equation has obtained this additional name. The fact that both homogeneous second order partial differential equations possess special solutions for odd numbers of participating dimensions is much less known.

Here we focus on these special solutions of the quaternionic homogeneous second order partial differential equations. These solutions are of special interest because for odd numbers of participating dimensions these equations have solutions in the form of **shape keeping fronts**.

The homogeneous equations run as:

$$\frac{\partial^2 \psi}{\partial x^2} + \frac{\partial^2 \psi}{\partial y^2} + \frac{\partial^2 \psi}{\partial z^2} \pm \frac{\partial^2 \psi}{\partial \tau^2} = \frac{1}{r^2}\frac{\partial}{\partial r}\left(r^2 \frac{\partial \psi}{\partial r}\right) \pm \frac{\partial^2 \psi}{\partial \tau^2} = 0 \tag{1}$$

Here we treat the two kinds of homogeneous equations together.

First we focus on the solutions that vary in one dimension. Thus:

$$\frac{\partial^2 \psi}{\partial z^2} \pm \frac{\partial^2 \psi}{\partial \tau^2} = 0 \tag{2}$$

We try a solution in the form $\varphi = f(\alpha z + \beta \tau)$:

$$\frac{\partial f}{\partial z} = \alpha f'; \frac{\partial^2 f}{\partial z} = \alpha \frac{\partial f'}{\partial z} = \alpha^2 f'' \tag{3}$$

$$\frac{\partial f}{\partial \tau} = \beta f'; \frac{\partial^2 f}{\partial \tau^2} = \beta \frac{\partial f'}{\partial \tau} = \beta^2 f'' \tag{4}$$

$$\alpha^2 f'' \pm \beta^2 f'' = 0 \tag{5}$$

This is solved when $\alpha^2 = \mp\beta^2$.

For the first kind of the second order partial differential equation this means: $\beta = \pm\alpha\,\boldsymbol{i}$, where $\boldsymbol{i}$ is a normalized imaginary quaternion. With $g(z) = f(\beta z)$ follows:

$$\varphi = g(z\,\boldsymbol{i} \pm \tau) \qquad (6)$$

The function g represents a shape keeping front. It is not a wave.

The imaginary $\boldsymbol{i}$ represents the base vector in the x, y plane. Its orientation θ may be a function of z.

That orientation determines the polarization of the one-dimensional shape keeping front. The **messengers** that are mentioned earlier are constituted of strings of these one-dimensional shape keeping fronts. The string members are equidistant. The messengers travel with a fixed speed. They feature a fixed shape and a fixed amplitude. The equidistance results in a characteristic frequency.

For the second kind of the second order partial differential equation this means: $\beta = \pm\alpha$. With $g(z) = f(\beta z)$ follows:

$$\varphi = g(z \pm \tau) \qquad (7)$$

Next we focus on the three dimensional spherical symmetric condition. In that case the equations can be separated by writing $\psi = r\,\varphi(r, \tau)$

$$\frac{\partial^2 \varphi}{\partial r^2} + \frac{2}{r}\frac{\partial \varphi}{\partial r} \pm \frac{\partial^2 \varphi}{\partial \tau^2} = 0 \implies \frac{\partial^2 \psi}{\partial r^2} \pm \frac{\partial^2 \psi}{\partial \tau^2} = 0 \qquad (8)$$

With other words ψ fulfills the conditions of the one-dimensional case. Thus solutions in the form $\varphi = f(\alpha r + \beta \tau)/r$ will fit.

For the first kind of the second order partial differential equation this means: $\beta = \pm\alpha\,\boldsymbol{i}$, where $\boldsymbol{i}$ is a normalized imaginary quaternion. With $g(x) = f(\beta x)$ follows:

$$\varphi = g(r\,\boldsymbol{i} \pm \tau)/r \qquad (9)$$

$\boldsymbol{i}$ represents a base vector in radial direction.

For the second kind of the second order partial differential equation this means: $\beta = \pm\alpha$. With $g(x) = f(\beta x)$ follows:

$$\varphi = g(x \pm \tau)/r \qquad (10)$$

These solutions feature a fixed speed and a fixed shape. However, their amplitude diminishes as $1/r$ with distance r from the sources. When integrated over a long enough period of progression the result takes the form of the fields Green's function.

The shape keeping fronts are not waves and do not form wave packages. Instead the shape keeping fronts occur in strings and do not disperse.

10.6 Special formulas

We list a series of interesting formulas that hold generally for the nabla operator ∇.

$$\nabla \langle k, x \rangle = k \tag{1}$$

k is constant.

$$\langle \nabla, \mathbf{x} \rangle = 3 \tag{2}$$

$$\nabla \times \mathbf{x} = \mathbf{0} \tag{3}$$

$$\nabla |\mathbf{x}| = \frac{\mathbf{x}}{|\mathbf{x}|} \tag{4}$$

$$\nabla \frac{1}{|\mathbf{x} - \mathbf{x}'|} = -\frac{\mathbf{x} - \mathbf{x}'}{|\mathbf{x} - \mathbf{x}'|^3} \tag{5}$$

$$\langle \nabla, \frac{\mathbf{x} - \mathbf{x}'}{|\mathbf{x} - \mathbf{x}'|^3} \rangle = \langle \nabla, \nabla \rangle \frac{1}{|\mathbf{x} - \mathbf{x}'|} = \langle \nabla, \nabla \frac{1}{|\mathbf{x} - \mathbf{x}'|} \rangle = 4\pi \, \delta(\mathbf{x} - \mathbf{x}') \tag{6}$$

Similar formulas apply to the quaternionic nabla and parameter values.

$$\nabla x = 1 - 3 \, ; \; \nabla^* x = 1 + 3 \, ; \; \nabla x^* = 1 + 3 \tag{7}$$

$$\nabla (x^* x) = x \tag{8}$$

$$\nabla |x| = \nabla \sqrt{(x^* x)} = \frac{x}{|x|} \tag{9}$$

$$\nabla \frac{1}{|x - x'|} = -\frac{x - x'}{|x - x'|^3} \tag{10}$$

$$\nabla^* \frac{x - x'}{|x - x'|^3} = \nabla \nabla^* \frac{1}{|x - x'|} = \left(\frac{\partial}{\partial \tau} \frac{\partial}{\partial \tau} + \langle \boldsymbol{\nabla}, \boldsymbol{\nabla} \rangle \right) \frac{1}{|x - x'|} \neq 4\pi \, \delta(x - x') \tag{11}$$

Instead:

$$(\nabla_0 \nabla_0 + \langle \boldsymbol{\nabla}, \boldsymbol{\nabla} \rangle) \frac{1}{|x|} = \frac{3\tau^2}{|x|^5} - \frac{1}{|x|^3} + \frac{3\tau^2}{|x|^5} = \frac{6\tau^2 - |x|^2}{|x|^5} = \frac{5\tau^2 - |\boldsymbol{x}|^2}{|x|^5} \tag{12}$$

$$(\nabla_0 \nabla_0 - \langle \boldsymbol{\nabla}, \boldsymbol{\nabla} \rangle) \frac{1}{|x|} = -\frac{1}{|x|^3} \tag{13}$$

$$\langle \boldsymbol{\nabla}, \boldsymbol{\nabla} \rangle \frac{1}{|\boldsymbol{x}|} = 4\pi \, \delta(\boldsymbol{x}) \tag{14}$$

Thus, with spherical boundary conditions, $\frac{1}{4\pi \, |x-x'|}$ is suitable as the Green's function for the Poisson equation, but $\frac{1}{4\pi \, |x-x'|}$ does not represent a Green's function for the quaternionic operator $(\nabla_0 \nabla_0 + \langle \boldsymbol{\nabla}, \boldsymbol{\nabla} \rangle)$!

For a homogeneous second order partial differential equation a Green's function is not required. Thus, the deficit of a green's function does not forbid the existence of a quaternionic homogeneous second order partial differential equation. Still equation (6) forms the base of the Poisson equation.

10.7 Differential field equations

By introducing new symbols $\mathfrak{E}$ and $\mathfrak{B}$ we will keep the quaternionic differential equations closer to the Maxwell differential equations. Still essential differences exist between these two sets of differential equations. This will be elucidated in detail in the appendix.

Like the quaternions themselves the quaternionic nabla can be split in a scalar part and a vector part. The quaternionic nabla acts as a multiplying operator and this means that the first order partial differential equation splits in five terms. Part of these terms are scalars. The other terms are vectors.

The following formulas are not Maxwell equations. At the utmost the formulas are Maxwell-like.

$$\phi = \nabla \, \varphi = (\nabla_0 + \boldsymbol{\nabla})(\varphi_0 + \boldsymbol{\varphi}) = \nabla_0 \varphi_0 - \langle \boldsymbol{\nabla}, \boldsymbol{\varphi} \rangle + \nabla_0 \boldsymbol{\varphi} + \boldsymbol{\nabla} \varphi_0 \pm \boldsymbol{\nabla} \times \boldsymbol{\varphi} \tag{1}$$

$$= \nabla_0 \varphi_0 - \langle \boldsymbol{\nabla}, \boldsymbol{\varphi} \rangle - \mathfrak{E} \pm \mathfrak{B}$$

$$\mathfrak{E} \overset{\text{def}}{=} -\nabla_0 \boldsymbol{\varphi} - \boldsymbol{\nabla}\varphi_0 \tag{2}$$

$$\nabla_0 \mathfrak{E} = -\nabla_0 \nabla_0 \, \boldsymbol{\varphi} - \nabla_0 \boldsymbol{\nabla}\varphi_0 \tag{3}$$

$$\langle \boldsymbol{\nabla}, \mathfrak{E} \rangle = -\nabla_0 \langle \boldsymbol{\nabla}, \boldsymbol{\varphi} \rangle - \langle \boldsymbol{\nabla}, \boldsymbol{\nabla} \rangle \varphi_0 \tag{4}$$

$$\mathfrak{B} \overset{\text{def}}{=} \boldsymbol{\nabla} \times \boldsymbol{\varphi} \tag{5}$$

These definitions imply:

$$\langle \mathfrak{E}, \mathfrak{B} \rangle = 0 \tag{6}$$

$$\nabla_0 \mathfrak{B} = -\boldsymbol{\nabla} \times \mathfrak{E} \tag{7}$$

$$\langle \boldsymbol{\nabla}, \mathfrak{B} \rangle = 0 \tag{8}$$

$$\boldsymbol{\nabla} \times \mathfrak{B} = \boldsymbol{\nabla}\langle \boldsymbol{\nabla}, \boldsymbol{\varphi} \rangle - \langle \boldsymbol{\nabla}, \boldsymbol{\nabla} \rangle \boldsymbol{\varphi} \tag{9}$$

The Maxwell equations ignore the real part of ϕ.

$$\phi_0 = \nabla_0 \phi_0 = \nabla_0 \nabla_0 \, \varphi_0 - \nabla_0 \langle \boldsymbol{\nabla}, \boldsymbol{\varphi} \rangle \tag{10}$$

$$\boldsymbol{\nabla}\phi_0 = \nabla_0 \, \boldsymbol{\nabla}\varphi_0 - \boldsymbol{\nabla}\langle \boldsymbol{\nabla}, \boldsymbol{\varphi} \rangle = \nabla_0 \, \boldsymbol{\nabla}\varphi_0 - \boldsymbol{\nabla} \times \boldsymbol{\nabla} \times \, \boldsymbol{\varphi} - \langle \boldsymbol{\nabla}, \boldsymbol{\nabla} \rangle \, \boldsymbol{\varphi} \tag{11}$$

$$\zeta = \zeta_0 + \boldsymbol{\zeta} = (\nabla_0 + \langle \boldsymbol{\nabla}, \boldsymbol{\nabla} \rangle)\varphi \tag{12}$$

$$\zeta_0 = (\nabla_0 \nabla_0 + \langle \boldsymbol{\nabla}, \boldsymbol{\nabla} \rangle)\varphi_0 = \nabla_0 \, \phi_0 - \langle \boldsymbol{\nabla}, \mathfrak{E} \rangle \tag{13}$$

$$\boldsymbol{\zeta} = (\nabla_0 \nabla_0 + \langle \boldsymbol{\nabla}, \boldsymbol{\nabla} \rangle)\boldsymbol{\varphi} = -\boldsymbol{\nabla}\phi_0 - \nabla_0 \mathfrak{E} - \boldsymbol{\nabla} \times \mathfrak{B} \tag{14}$$

More in detail the equations mean:

$$\zeta_0 = \nabla_0 \phi_0 + \langle \boldsymbol{\nabla}, \boldsymbol{\phi} \rangle \tag{15}$$

$$= \{ \nabla_0 \nabla_0 \varphi_0 - \nabla_0 \langle \boldsymbol{\nabla}, \boldsymbol{\varphi} \rangle \} + \{ \langle \boldsymbol{\nabla}, \boldsymbol{\nabla} \rangle \varphi_0 + \nabla_0 \langle \boldsymbol{\nabla}, \boldsymbol{\varphi} \rangle \pm \langle \boldsymbol{\nabla}, \boldsymbol{\nabla} \times \boldsymbol{\varphi} \rangle \}$$

$$= (\nabla_0 \nabla_0 + \langle \boldsymbol{\nabla}, \boldsymbol{\nabla} \rangle) \varphi_0$$

$$\boldsymbol{\zeta} = -\boldsymbol{\nabla} \phi_0 + \nabla_0 \boldsymbol{\phi} \mp \boldsymbol{\nabla} \times \boldsymbol{\phi} \tag{16}$$

$$= \{ -\boldsymbol{\nabla} \nabla_0 \varphi_0 + \boldsymbol{\nabla} \times \boldsymbol{\nabla} \times \boldsymbol{\varphi} + \langle \boldsymbol{\nabla}, \boldsymbol{\nabla} \rangle \boldsymbol{\varphi} \} + \{ \nabla_0 \boldsymbol{\nabla} \varphi_0 + \nabla_0 \nabla_0 \boldsymbol{\varphi} \pm \nabla_0 \boldsymbol{\nabla} \times \boldsymbol{\varphi} \}$$

$$\{ \mp \boldsymbol{\nabla} \times \boldsymbol{\nabla} \varphi_0 \mp \boldsymbol{\nabla} \times \nabla_0 \boldsymbol{\varphi} - \boldsymbol{\nabla} \times \boldsymbol{\nabla} \times \boldsymbol{\varphi} \}$$

$$= (\nabla_0 \nabla_0 + \langle \boldsymbol{\nabla}, \boldsymbol{\nabla} \rangle) \boldsymbol{\varphi} + \boldsymbol{\nabla} \times \boldsymbol{\nabla} \times \boldsymbol{\varphi} - \boldsymbol{\nabla} \times \boldsymbol{\nabla} \times \boldsymbol{\varphi}$$

$$\rho_0 = \langle \boldsymbol{\nabla}, \boldsymbol{\nabla} \rangle \varphi_0 = \zeta_0 - \nabla_0 \nabla_0 \varphi_0 \tag{17}$$

$$\boldsymbol{\rho} = \langle \boldsymbol{\nabla}, \boldsymbol{\nabla} \rangle \boldsymbol{\varphi} = \boldsymbol{\zeta} - \nabla_0 \boldsymbol{\nabla_0} \boldsymbol{\varphi} \tag{18}$$

10.8 Quaternionic differential operators

When applied to quaternionic functions, quaternionic differential operators result in another quaternionic function that uses the same parameter space.

The operators $\nabla_0, \boldsymbol{\nabla}, \nabla = \nabla_0 + \boldsymbol{\nabla}, \nabla^* = \nabla_0 - \boldsymbol{\nabla}, \langle \boldsymbol{\nabla}, \boldsymbol{\nabla} \rangle, \nabla \nabla^* = \nabla^* \nabla = \nabla_0 \nabla_0 + \langle \boldsymbol{\nabla}, \boldsymbol{\nabla} \rangle$ and $\mathfrak{D} = -\nabla_0 \nabla_0 + \langle \boldsymbol{\nabla}, \boldsymbol{\nabla} \rangle$ are all quaternionic differential operators.

∇ is the quaternionic nabla operator.

∇^* is its quaternionic conjugate.

The Dirac nabla operators $\mathcal{D} = \mathbb{i} \, \nabla_0 + \boldsymbol{\nabla}$ and $\mathcal{D}^* = \mathbb{i} \, \nabla_0 - \boldsymbol{\nabla}$ convert quaternionic functions into biquaternionic functions. The equation

$$\mathcal{D} \mathcal{D}^* f = \mathfrak{D} f = -\nabla_0 \nabla_0 + \langle \boldsymbol{\nabla}, \boldsymbol{\nabla} \rangle \, f = g \tag{19}$$

represents a wave equation and is a pure quaternionic equation! The Dirac operator and the Dirac equation are treated in detail in the appendix.

10.9 Poynting vector

The definitions of $\mathfrak{E}$ and $\mathcal{B}$ invite the definition of the Poynting vector $\boldsymbol{S}$:

$$\boldsymbol{S} = \mathfrak{E} \times \mathcal{B} \tag{1}$$

$$u = \tfrac{1}{2} (\langle \mathfrak{E}, \mathfrak{E} \rangle + \langle \mathcal{B}, \mathcal{B} \rangle) \tag{2}$$

$$\frac{\partial u}{\partial \tau} = \langle \boldsymbol{\nabla}, \boldsymbol{S} \rangle + \langle \boldsymbol{J}, \mathfrak{E} \rangle \tag{3}$$

Where ρ represents the presence of charges will $\boldsymbol{J}$ represent the flow of charges.

11 Double differentiation

11.1 Right and left sided nabla

The quaternionic nabla can be split into a right sided version and a left sided version. Without further indication we consider the right version as the current version. The version is determined by the imaginary part and is linked with the handedness of the product rule.

$$\nabla_r f = e^\mu \frac{\partial f}{\partial x_\mu} = e^\mu e^\nu \frac{\partial f_\nu}{\partial x_\mu} = e^\mu e^\nu \nabla_\mu f_\nu = \nabla f$$

$$\nabla_l f = \frac{\partial f}{\partial x_\mu} e^\mu = e^\nu e^\mu \frac{\partial f_\nu}{\partial x_\mu} = e^\nu e^\mu \nabla_\mu f_\nu = (e^\mu e^\nu)^* \nabla_\mu f_\nu = (\nabla_r f)^* = (\nabla f)^* = \nabla f - 2\boldsymbol{\nabla} \times \boldsymbol{f}$$

$$\nabla_r(\nabla_l f) = e^\rho e^\nu e^\mu \nabla_\rho \nabla_\mu f_\nu$$

11.2 Double partial differentiation

The partial differential equations hide that they are part of a differential equation.

$$\nabla' \nabla f = \xi = \sum_{\nu=0}^{3} e'_\nu \frac{\partial}{\partial q'_\nu} \left(\sum_{\mu=0}^{3} e_\mu \frac{\partial f}{\partial q_\mu} \right) = \left(e'_\nu e_\mu \frac{\partial^2}{\partial q_\mu \partial q'_\nu} \right) f \tag{1}$$

11.3 Single difference

Single difference is defined by

$$df(q) = \sum_{\mu=0}^{3} \sum_{\varsigma=0}^{3} \frac{\partial f^\varsigma}{\partial q_\mu} e_\mu e_\varsigma \; dq^\mu = \sum_{\nu=0}^{3} \phi_\nu e_\nu dq^\nu \tag{2}$$

$$\frac{\partial f^\varsigma}{\partial q_\mu} e_\mu e_\varsigma = \begin{bmatrix} \dfrac{\partial f^0}{\partial q_0} & \dfrac{\partial f^1}{\partial q_0} \boldsymbol{i} & \dfrac{\partial f^2}{\partial q_0} \boldsymbol{j} & \dfrac{\partial f^3}{\partial q_0} \boldsymbol{k} \\ \dfrac{\partial f^0}{\partial q_1} \boldsymbol{i} & \dfrac{\partial f^1}{\partial q_1} & \dfrac{\partial f^2}{\partial q_1} \boldsymbol{k} & -\dfrac{\partial f^3}{\partial q_1} \boldsymbol{j} \\ \dfrac{\partial f^0}{\partial q_2} \boldsymbol{j} & -\dfrac{\partial f^1}{\partial q_2} \boldsymbol{k} & \dfrac{\partial f^2}{\partial q_2} & \dfrac{\partial f^3}{\partial q_2} \boldsymbol{i} \\ \dfrac{\partial f^0}{\partial q_3} \boldsymbol{k} & \dfrac{\partial f^1}{\partial q_3} \boldsymbol{j} & -\dfrac{\partial f^2}{\partial q_3} \boldsymbol{i} & \dfrac{\partial f^3}{\partial q_3} \end{bmatrix} \tag{3}$$

$$
= \begin{bmatrix} \dfrac{\partial f^0}{\partial q_0} & -\mathcal{E}_x \boldsymbol{i} & -\mathcal{E}_y \boldsymbol{j} & -\mathcal{E}_z \boldsymbol{k} \\[2mm] \mathcal{E}_x \boldsymbol{i} & \dfrac{\partial f^1}{\partial q_1} & -\mathcal{B}_{z1} \boldsymbol{k} & -\mathcal{B}_{y2} \boldsymbol{j} \\[2mm] \mathcal{E}_y \boldsymbol{j} & -\mathcal{B}_{z2} \boldsymbol{k} & \dfrac{\partial f^2}{\partial q_2} & -\mathcal{B}_{x1} \boldsymbol{i} \\[2mm] \mathcal{E}_z \boldsymbol{k} & -\mathcal{B}_{y1} \boldsymbol{j} & -\mathcal{B}_{x2} \boldsymbol{i} & \dfrac{\partial f^3}{\partial q_3} \end{bmatrix}
$$

Here

$$
\mathcal{B}_x = \mathcal{B}_{x1} - \mathcal{B}_{x2}; \; \mathcal{B}_y = \mathcal{B}_{y1} - \mathcal{B}_{y2}; \; \mathcal{B}_z = \mathcal{B}_{z1} - \mathcal{B}_{z2} \tag{4}
$$

$$
\dot{f} = \frac{df}{d\lambda} = \sum_{\mu=0}^{3} \phi_\mu e_\mu \frac{dq^\mu}{d\lambda} = \sum_{\mu=0}^{3} \phi_\mu e_\mu \dot{q}^\mu \tag{5}
$$

The scalar λ is can be a linear function of τ or a scalar function of q.

$$
\dot{q} \stackrel{\text{def}}{=} \frac{dq}{d\lambda} = e_\mu \frac{dq^\mu}{d\lambda} = e_\mu \dot{q}^\mu \tag{6}
$$

Double difference is defined by:

$$
d^2 f(q) = \sum_{\nu=0}^{3} e'_\nu \left(\sum_{\mu=0}^{3} \frac{\partial^2 f^\varsigma}{\partial q_\mu \partial q'_\nu} e_\mu dq^\mu \right) e_\varsigma dq'^\nu \tag{7}
$$

$$
\ddot{f} \stackrel{\text{def}}{=} \frac{d^2 f(q)}{d\lambda^2} = e_\varrho \ddot{f}^\varrho = \sum_{\nu=0}^{3} e'_\nu \left(\sum_{\mu=0}^{3} \frac{\partial^2 f^\varsigma}{\partial q_\mu \partial q'_\nu} e_\mu \frac{dq^\mu}{d\lambda} \right) e_\varsigma \frac{dq'^\nu}{d\lambda} \tag{8}
$$

$$
= \sum_{\nu=0}^{3} e'_\nu \left(\sum_{\mu=0}^{3} \frac{\partial^2 f^\varsigma}{\partial q_\mu \partial q'_\nu} e_\mu \dot{q}^\mu \right) e_\varsigma \dot{q}'^\nu = \left(\dot{q}^\mu \dot{q}'^\nu \frac{\partial^2}{\partial q_\mu \partial q'_\nu} e'_\nu e_\mu \right) f = \zeta_{\nu\mu} f
$$

$$
\zeta_{\nu\mu} = e'_\nu e_\mu \, \dot{q}'^\nu \, \dot{q}^\mu \frac{\partial^2}{\partial q_\mu \partial q'_\nu} = e'_\nu e_\mu \Upsilon_{\nu\mu} \tag{9}
$$

$$
\tag{10}
$$

$$\Upsilon_{\nu\mu} = \dot{q}'^{\nu} \, \dot{q}^{\mu} \, \frac{\partial^2}{\partial q_{\mu} \partial q'_{\nu}}$$

If we apply $\phi = \nabla f$ as the first differential operation and $\xi = \nabla^* \phi$ as the second differential operation, then $e = \{1, +i, +j, +k\}$ and $e' = \{1 - i, -j, -k\}$ and

$$\Upsilon_{\nu\mu} = \begin{bmatrix} +\Upsilon_{00} & +\Upsilon_{01}i & +\Upsilon_{02}j & +\Upsilon_{03}k \\ -\Upsilon_{10}i & \circledast \, \Upsilon_{11} & +\Upsilon_{12}k & +\Upsilon_{13}j \\ -\Upsilon_{20}j & -\Upsilon_{21}k & \circledast \, \Upsilon_{22} & -\Upsilon_{23}i \\ -\Upsilon_{30}k & -\Upsilon_{31}j & +\Upsilon_{32}i & \circledast \, \Upsilon_{33} \end{bmatrix} \tag{11}$$

Here the switch $\circledast$ distinguishes between quaternionic differential calculus and Maxwell based differential calculus. See the appendix.

11.4 Deformed space

If the investigated field represents deformed space $\mathfrak{C}$, then the field $\mathfrak{R}$, which represents the parameter space of function $\mathfrak{C}(q)$ represents the virgin state of that deformed space.

Further, the equation $\frac{d^2\mathfrak{C}(q)}{d\lambda^2} = 0$ represents a local condition in which $\mathfrak{C}$ is not affected by external influences. Here λ can be any linear combination of progression τ or it can represent the equivalent of local quaternionic distance:

$$\lambda = a \, q_0 + b$$

or

$$\lambda = |q|$$

12 Actions of the fields

For all fields the homogeneous second order partial differential equations are the same. Thus, the differences between fields are located in the inhomogeneous part. The influences of disturbances of the continuity of the field are gathered in this inhomogeneous part. Without these disturbances most of the fields would be flat and their defining function would be equal to its parameter space.

In this view, many of the fields are more or less blurred representations of discrete distributions, where the elements of the distribution are target values of a function that has rational quaternions as its parameter space. In some cases the discrete distribution represents a dynamic location density distribution. In fact two views are possible, either the field influences the discrete objects that correspond to location swarms or the swarms define the fields via their location density distribution. Smoothed fields are afflicted with extra blur.

Apart from the symmetry related fields $\mathfrak{A}^x$ that are raised by the charges of the symmetry centers and the field $\mathfrak{Z}$,that describes the gluons, at least one other field basic exists. That field is the embedding field $\mathfrak{C}$. It represents the live space of the modules and modular systems. The origins of these fields differ fundamentally. The embedding field smoothly follows a distribution of discrete quaternionic values, which are eigenvalues of a series of operators. Some of these values do not fit properly in the set of values that surrounds them. In the special condition that these disparities appear in coherent swarms, we have indicated the swarm as the representative of an elementary particle. The disparities are due to difference in the symmetries of the underlying domains. These symmetries determine how the values cooperate in convolutions. If the disparities were not present, then the embedding field would be equal to the parameter space $\mathcal{R}$ and that continuum would follow parameter space $\mathfrak{R}$.

The embedding field is not directly affected by the symmetry related charges of the symmetry centers. It is indirectly affected, because the symmetry related fields affect the location of the symmetry centers that house the objects that can deform the embedding field. In principle each disruption of the continuity of the field, thus each element of the swarm that represents an elementary particle, affects the embedding field $\mathfrak{C}$. The smoothed version $\mathfrak{U}$ of the embedding field is far less vigilant. Also the symmetry related field $\mathfrak{A}$,which is coupled to the geometric center of the symmetry center reacts much less vigilant. The gluon field is related to locations where pairs of color shifting quaternions disturb the generation process of the anisotropic coherent swarms and causes the generation of hadrons, which are conglomerates of quarks.

The embedding field $\mathfrak{C}$ is affected by the embedding of artifacts that are picked by a dedicated controlling mechanism that uses a symmetry center $\mathfrak{S}_n^x$. as a resource. After selection of the location of the artifact, the controlling mechanism embeds this artifact into the embedding continuum $\mathfrak{C}$. This continuum is represented by the continuum eigenspace of operator $\mathfrak{C}$.

Another interpretation is that this field describes the location swarms that are generated by the controlling mechanisms.

Each of these mechanisms operates in a cyclic and stochastic fashion. The embedding events occur in the direct neighborhood of the geometric center of the corresponding symmetry center. The result is a recurrently regenerated coherent location swarm that also represent a stochastic hopping path. The swarm is centered around the geometric center of the symmetry center. Hopping means that the controlling mechanism generates at the utmost one embedding location per progression step. This means that the hopping object can be considered as a point-like artifact. At the embedding instant the artifact actually resides at the location that is represented by an element of the location swarm. Thus, the swarm represents the spatial map of a set of potential detection locations. The swarm is generated within the symmetry center $\mathfrak{S}_n^x$ and is encapsulated by ∂H_n^x. The actions of the

mechanisms deform the field $\mathfrak{C}$ inside the floating regions H_n^x. The deformation of $\mathfrak{C}$ reaches beyond the region H_n^x.

In this way, the mechanism creates an elementary module, which is able to deform the embedding field $\mathfrak{C}$ and inherits the symmetry related charge from the symmetry center. The deformation represents the local contribution to the embedding field by the elementary module that owns the swarm.

On the other hand the geometric center of the symmetry center houses the electric charge that influences field $\mathfrak{A}$. This view can be reversed. It is possible to consider the path that the geometric center of the symmetry center takes under the influence of both fields. This view requires an estimate of the results of the actions of these fields. This will be achieved via the ***path integral***. First we will investigate the influence of the embedding field $\mathfrak{C}$. In a later phase we will add the results of the much less vigilant actions of the symmetry related field $\mathfrak{A}$.

As indicated beforehand a third basic field is the result of the activity of gluons. That activity disturbs the generation of anisotropic elementary modules. The controlling mechanisms react by assembling several partially generated anisotropic elementary modules into an isotropic composite. In this composite multiple symmetry centers are involved. Also these symmetry centers join. Outside of the joined encapsulation the composite appears isotropic. The composite still may carry electric charge. But it no longer carries color charge. Inside the capsule multiple hopping paths walk and form a common location swarm.

12.1 Path of the symmetry center

The symmetry center $\mathfrak{S}_n^x$ that conforms to encapsulated region H_n^x, keeps its private symmetry flavor. At the passage through the boundary the symmetry flavor of the background parameter space $\mathfrak{R}^{\circledcirc}$ flips from history to future. As a consequence the symmetry related charge of the symmetry center will flip.

The eigenspace of operator σ_n^x is represented by a tube that contains a series of sheets that each represent a static status quo. As long as the tube crosses the boundary the corresponding elementary module exists.

The passage of the symmetry center through the rim may be interpreted as the annihilation of the historic symmetry center and the creation of a new symmetry center with a reverse symmetry flavor that will extend its live in the future.

The passage of the symmetry centers through the rim goes together with annihilation and creation phenomena for the objects that reside on these platforms. Thus, this passage is related to the conversion or the annihilation or the creation of elementary modules. However, most of these occurrences do not lead to the complete conversion of the concerned object into another behavior mode. These exceptional occurrences are known as pair production and pair annihilation. Thus, in most cases the behavior mode of the module persists.

In the quaternionic space-progression model the existence of symmetry centers is independent of progression. With other words the number of symmetry centers is a model constant. The passage through the rim does not influence this number. Only the characteristics of the combination of the symmetry center and the background parameter space are affected by the passage.

12.2 Multi-mix path algorithm

In this primary investigation we ignore the actions of the symmetry related potential. They are far less vigilant than the direct results of the embedding of individual locations. The name "***multi-mix***

algorithm" stands for similar algorithm that is known as "***path integral***". "path integral" is in fact a misnomer. The algorithm concerns a sequence of multiplications. Due to the fact that during the regeneration of the considered object the displacement of the object is rather stable, will part of the multiplication factors reduce to unity. The other factors are close to unity. The result is that the sequence reduces to a sequence of additions of a large number of small contributions. These contributions are the actions of the individual hops of an elementary module.

Elementary modules reside on an individual symmetry center. A dedicated mechanism controls its recurrent generation and embeds the object into the embedding field. The path of the symmetry center is the averaged path of the embedded object. The embedded object is hopping along the elements of the generated location swarm. The landing locations of the hops are generated by the controlling mechanism in a stochastic fashion, but such that at first approximation the swarm as a whole can be considered to be moving as one unit. This is possible when the swarm is characterized by a continuous location density distribution, which owns a displacement generator. That is the case when the location density distribution owns a Fourier transform. This fact enables the description of the path of the swarm by a "multi-mix algorithm". The hopping of the embedded object can be described by a sequence of factors that after multiplication represent the whole path. Each factor represents three sub-factors.

The procedure that underlies the multi-mix algorithm depends on the fact that the multiplication of factors that are all very close to unity can be replaced by a summation.

1. The first sub-factor represents the jump from configuration space to momentum space. This sub-factor is given by the inner product of the Hilbert vector that represents the current location and the Hilbert vector that represents the momentum of the swarm. This second Hilbert vector is assumed to be constant during the current regeneration of the location swarm.
2. The second sub-factor represents the effect of the hop in momentum space.
3. The third sub-factor represents the jump back from momentum space to configuration space.

In the sequence of factors the third sub-factor of the current term compensates the effect of the first sub-factor of next term. Their product equals unity.

What results is a sequence of factors that are very close to unity and that represent the effects of the hops in momentum space. Due to the fact that the momentum is considered to be constant, the logarithms of the terms can be taken and added in an overall sum. In this way, the multiplication is equal to the sum of the logarithms of the factors.

This summation approaches what is known as the "path integral". In our interpretation it is not an integral, but instead it is a finite summation. In more detail the procedure can be described as follows.

We suppose that momentum $\boldsymbol{p}_n$ is constant during the particle generation cycle in which the controlling mechanism produces the swarm $\{a_i\}$. Every hop gives a contribution to the path. These contributions can be divided into three steps per contributing hop:

1. Change to Fourier space. This involves as sub-factor the inner product $\langle a_i | p_n \rangle$.
2. Evolve during an infinitesimal progression step into the future.
   a. Multiply with the corresponding displacement generator $\boldsymbol{p}_n$.
   b. The generated step in configuration space is $(\boldsymbol{a}_{i+1} - \boldsymbol{a}_i)$.
   c. The action contribution factor in Fourier space is $\langle \boldsymbol{p}_n, \boldsymbol{a}_{i+1} - \boldsymbol{a}_i \rangle$.

3. Change back to configuration space. This involves as sub-factor the inner product $\langle p_n | a_{i+1} \rangle$

The combined term contributes a factor $\langle a_i | p_n \rangle \exp(\langle \boldsymbol{p}_n, \boldsymbol{a}_{i+1} - \boldsymbol{a}_i \rangle) \langle p_n | a_{i+1} \rangle$.

Two subsequent steps give:

$$\langle a_i | p_n \rangle \exp(\langle \boldsymbol{p}_n, \boldsymbol{a}_{i+1} - \boldsymbol{a}_i \rangle) \langle p_n | a_{i+1} \rangle \langle a_{i+1} | p_n \rangle \exp(\langle \boldsymbol{p}_n, \boldsymbol{a}_{i+2} - \boldsymbol{a}_{i+1} \rangle) \langle p_n | a_{i+2} \rangle \tag{1}$$

$$= \langle a_i | p_n \rangle \exp(\langle \boldsymbol{p}_n, \boldsymbol{a}_{i+2} - \boldsymbol{a}_i \rangle) \langle p_n | a_{i+2} \rangle$$

The red terms in the middle turn into unity. The other terms also join.

Over a full particle generation cycle with N steps this results in:

$$\prod_{i=1}^{N-1} \langle a_i | p_n \rangle \exp(\langle \boldsymbol{p}_n, \boldsymbol{a}_{i+1} - \boldsymbol{a}_i \rangle) \langle p_n | a_{i+1} \rangle \tag{2}$$

$$= \langle a_1 | p_n \rangle \exp(\langle \boldsymbol{p}_n, \boldsymbol{a}_N - \boldsymbol{a}_1 \rangle) \langle p_n | a_N \rangle = \langle a_1 | p_n \rangle \exp\left(\sum_{i=2}^{N} \langle \boldsymbol{p}_n, \boldsymbol{a}_{i+1} - \boldsymbol{a}_i \rangle \right) \langle p_n | a_N \rangle$$

$$= \langle a_1 | p_n \rangle \exp(L \, d\tau) \langle p_n | a_N \rangle$$

$$L \, d\tau = \sum_{i=2}^{N-1} \langle \boldsymbol{p}_n, \boldsymbol{a}_{i+1} - \boldsymbol{a}_i \rangle = \langle \boldsymbol{p}_n, d\boldsymbol{q} \rangle \tag{3}$$

$$L = \langle \boldsymbol{p}_n, \dot{\boldsymbol{q}} \rangle \tag{4}$$

L is known as the *Lagrangian*.

Equation (4) holds for the special condition in which $\boldsymbol{p}_n$ is constant. If $\boldsymbol{p}_n$ is not constant, then the Hamiltonian H varies with location. In the next equations we ignore subscript $_n$.

$$\frac{\partial H}{\partial q_i} = -\dot{p}_i \tag{5}$$

$$\frac{\partial H}{\partial p_i} = \dot{q}_i \tag{6}$$

$$\frac{\partial L}{\partial q_i} = \dot{p} \tag{7}$$

$$\frac{\partial L}{\partial \dot{q}_i} = p_i \tag{8}$$

$$\frac{\partial H}{\partial \tau} = -\frac{\partial H}{\partial \tau} \tag{9}$$

$$\frac{d}{d\tau}\frac{\partial L}{\partial \dot{q}_i} = \frac{\partial L}{\partial q_i} \tag{10}$$

$$H + L = \sum_{i=1}^{3} \dot{q}_i p_i \tag{11}$$

Here we used proper time τ rather than coordinate time t.

The effect of the hopping path is that the geometric center of the symmetry center is moved over a small resulting distance $\boldsymbol{a}_N - \boldsymbol{a}_1$. Together with "charge" $(N \cdot Q_n)$ this move determines the next version of momentum $\boldsymbol{p}_n$.

The result is that both the symmetry related fields $\mathfrak{A}^x$ and the embedding field $\mathfrak{C}$ influence the location of the geometric center of the symmetry center $\mathfrak{S}_n^x$.

In this investigation we ignored the influence of the symmetry related field $\mathfrak{A}$. This field influences momentum $\boldsymbol{p}_n$ and the corresponding eigenvector $|p_n\rangle$. This means that the product of the red colored middle terms is no longer equal to unity. Instead the product differs slightly from unity and the effect can be included in the path integral. In this way a small slowly varying extra contribution is added to each subsequent term in the summation. This extra contribution is a smooth function of progression and thus, it is a smooth function of the index of the term.

The result of the "multi-mix algorithm" is expectable. The "step" of the swarm equals the sum of the steps of the hops. The "multi-mix algorithm" is introduced in order to show the similarity with the "path integral". The "path integral" is taken over all possible paths. Usually the "path integral" algorithm is introduced by starting from the Lagrangian. Here we started the "multi-mix algorithm" from the hopping path and the "multi-mix algorithm" results in the Lagrangian.

12.3 Gluon action

The presence of gluons causes the disruption of the generation of anisotropic swarms of artifacts and the governing mechanisms will join their activity by generating isotropic swarms of artifacts that will represent conglomerates of the intended elementary modules. As a consequence separate anisotropic elementary modules will hardly ever reach the condition that they are represented by a private swarm. Instead the isotropic swarms will appear as persistent results. Thus, gluons combine multiple hopping paths into a single coherent swarm. This means that the "multi-mix algorithm" must be applied to each of the hopping paths and the result must be attached to a common location center. The number of hops in a hopping path can be used as a location weighting factor.

12.4 Grouped isotropic artifacts

Next we consider grouped artifacts that cause discontinuities in the realm of a symmetry center. The concerned field is the embedding field. Since we do no longer focus on symmetry related charges, we will omit the superscript ^{x}.

We consider the case that the locations of the artifacts form a coherent swarm $\{c_n\}$ that can be characterized by a continuous location density distribution $\rho(\boldsymbol{q})$.

$$\chi(\boldsymbol{q}) = \sum_{n=0}^{N} \iiint_V \rho(\boldsymbol{q}) \, Q_n \, \delta(\boldsymbol{q} - \boldsymbol{c}_n) = -\frac{1}{4\pi} \sum_{n=0}^{N} \iiint_V \rho(\boldsymbol{q}) Q_n \, \langle \boldsymbol{\nabla}, \boldsymbol{\nabla} \frac{1}{|\boldsymbol{q} - \boldsymbol{c}|} \rangle \tag{1}$$

If we use the spherical symmetric **Gaussian location distribution** of artifacts $\rho(r)$ that was introduced earlier as **test function**,

$$\rho(r) = \langle \boldsymbol{\nabla}, \boldsymbol{\nabla} \rangle \mathfrak{T}(r) = -\frac{Q}{\left(\sigma\sqrt{2\pi}\right)^3} \exp\left(-\frac{r^2}{2\sigma^2}\right) \tag{2}$$

then a potential in the form of

$$\mathfrak{T}(r) = -\frac{Q}{4\pi} \frac{ERF\left(r/_{\sigma\sqrt{2}}\right)}{r} \tag{3}$$

results.

At somewhat larger distances the potential behaves like a single charge potential.

$$\chi(r) \approx \frac{-Q}{4\pi r} \tag{4}$$

This gives an idea of what happens when a mechanism that acts within the realm of a symmetry center produces a coherent swarm of artifacts that will be embedded into a field that gets deformed by these artifacts.

Despite the fact that it is constituted from a myriad of singular contributions, the potential in equation (3) is a continuous function and its gradient at the center point equals zero! Thus the corresponding deformation has a "wide-spread" binding effect.

12.5 Acceleration of the symmetry center

Due to their actions, the fields $\mathfrak{A}$ and $\mathfrak{C}$ may accelerate the location of the symmetry center on which an elementary module resides. This occurs via the interaction of these fields with the contributions that the symmetry center and the recurrently embedded elementary module add to the influences of these fields.

The symmetry center and with it the residing elementary module float over the background parameter space $\mathfrak{R}$. This means that these items also float over the fields $\mathfrak{A}$ and $\mathfrak{C}$.

12.5.1 The symmetry related field

The symmetry related charge Q_n^x of the symmetry center $\mathfrak{S}_n^x$ contributes the local scalar potential φ_{n_0} to the symmetry related field $\mathfrak{A}$.

$$\varphi_{n_0}(\boldsymbol{q}) = \frac{Q_n^x}{|\boldsymbol{q} - \boldsymbol{c}_n^x|} \tag{1}$$

On the other hand

$$\boldsymbol{E}_n(\boldsymbol{q}) = \boldsymbol{\nabla}\varphi_{n_0} = \frac{Q_n^x(\boldsymbol{q} - \boldsymbol{c}_n^x)}{|\boldsymbol{q} - \boldsymbol{c}_n^x|^3} \tag{2}$$

Another symmetry center $\mathfrak{S}_m^x$ contributes potential φ_{m_0} to the symmetry related field $\mathfrak{A}$. The force $\boldsymbol{F}_{nm}$ between the two symmetry centers equals:

$$\boldsymbol{F}_{nm} = \boldsymbol{E}_n Q_m^x = \frac{Q_n^x Q_m^x (\boldsymbol{c}_n^x - \boldsymbol{c}_m^x)}{|\boldsymbol{c}_n^x - \boldsymbol{c}_m^x|^3} = -\boldsymbol{F}_{mn} = -\boldsymbol{E}_m Q_n^x \tag{3}$$

This need not correspond to an actual acceleration. On the other hand, if relative to the parameter space $\mathfrak{R}$, the movement of the symmetry center $\mathfrak{S}_n^x$ is uniform with speed $\boldsymbol{v}_n$, then the scalar potential φ_{n_0} corresponds to a vector potential $\boldsymbol{\varphi}_n = \varphi_{n_0} \boldsymbol{v}_n$. If relative to the parameter space $\mathfrak{R}$, the symmetry center actually accelerates, then this goes together with an extra field $\boldsymbol{E}_n = \dot{\boldsymbol{\varphi}}_n = \varphi_{n_0} \dot{\boldsymbol{v}}_n$ that represents the corresponding change of field $\mathfrak{A}$. Thus. If the two forces $\boldsymbol{F}_{nm}$ and $\boldsymbol{F}_{mn}$ do not hold each other in equilibrium, then the field $\mathfrak{A}$ will change dynamically with this extra contribution.

12.5.2 The embedding field

The location swarms that are generated by dedicated controlling mechanisms produce a local potential that also can accelerate the symmetry center on which the location swarm resides relative to the parameter space $\mathfrak{R}$. We analyze the situation by assuming that the swarm is represented by a Gaussian location distribution. Thus, we use the corresponding artifact as a test particle. The corresponding local potential that contributes to field $\mathfrak{C}$ equals

$$\chi_n(r) = -\frac{Q_n}{4\pi} \frac{ERF\left(r/\sigma\sqrt{2}\right)}{r} \tag{1}$$

Here Q_n represents the strength of the local potential. At somewhat larger distances the potential behaves as a single "charge" potential.

$$\chi_n(\boldsymbol{q}) \approx \frac{-Q_n}{4\pi|\boldsymbol{q} - \boldsymbol{c}_n^x|} \tag{2}$$

This virtual "charge" is located at the center of the symmetry center $\mathfrak{S}_n^x$. The scalar potential $\chi_n(\boldsymbol{q})$ adds to the embedding field $\mathfrak{C}$. The result is that $\mathfrak{C}$ gets deformed.

The local scalar potential $\chi_n(\boldsymbol{q})$ corresponds to a derived field $\mathcal{E}_n(\boldsymbol{q})$.

$$\mathcal{E}_n(\boldsymbol{q}) = \boldsymbol{\nabla}\chi_n = -\frac{Q_n(\boldsymbol{q} - \boldsymbol{c}_n^x)}{|\boldsymbol{q} - \boldsymbol{c}_n^x|^3} \tag{3}$$

Another symmetry center $\mathfrak{S}_m^x$ contributes potential $\chi_m(\boldsymbol{q})$ to the embedding field $\mathfrak{C}$. The force $\boldsymbol{F}_{nm}$ between the two symmetry centers equals:

$$\boldsymbol{F}_{nm} = \mathcal{E}_n Q_m = -\frac{Q_n Q_m(\boldsymbol{c}_n^x - \boldsymbol{c}_m^x)}{|\boldsymbol{c}_n^x - \boldsymbol{c}_m^x|^3} = -\boldsymbol{F}_{mn} = -\mathcal{E}_m Q_n \tag{4}$$

This need not correspond to an actual acceleration. The force raising field $\mathcal{E}_n$ is treated in detail in a special section of this paper.

If the platform $\mathfrak{S}_m^x$ on which the swarm resides moves with uniform speed $\boldsymbol{v}$, then the local potential corresponds to a local vector potential.

$$\boldsymbol{\mathcal{X}}_n = \chi_n \boldsymbol{v} \tag{5}$$

If this platform accelerates, then this goes together with an extra contribution to field $\mathcal{E}_n$ that counteracts the acceleration.

$$\mathcal{E}_n = \dot{\boldsymbol{\mathcal{X}}}_n = \chi_n \dot{\boldsymbol{v}} \tag{6}$$

This effect is known as ***inertia***.

12.6 The smoothed embedding field

The embedding field $\mathfrak{C}$ is described by a mostly continuous function $\mathfrak{C}(q)$. The convolution of $\mathfrak{C}(q)$ with a blurring function transforms this function in an everywhere continuous function $\mathfrak{U}(q)$. Space cavities exist where both $\mathfrak{C}(q)$ and $\mathfrak{U}(q)$ are not defined. The blurring function integrates over the regeneration cycle of elementary modules in the progression part of the domain. If in the spatial domain the test function $\mathfrak{T}(q)$ is used as the blurring function for isolated discontinuities and a Gaussian distribution is used for coherent swarms of discontinuities, then the function $\mathfrak{U}(q)$ defines the smoothed embedding field $\mathfrak{U}$. This field takes the role of a model-wide potential. In physics this is the role of the gravitation potential. In this model we consider $\mathfrak{U}$ to represent the equivalent of ***universe***, however it represents a blurred universe.

The local contribution to the embedding field $\mathfrak{C}$ by the elementary particle has a smoothed versions which is the equivalent of its individual potential. It contributes to field $\mathfrak{U}$.

12.7 Spurious artifacts

Due to their minor effect, spurious artifacts will be hidden for observers due to the blanket that is spread over the corresponding field by the smoothed version of this field that the observers will see. Only recurrent regeneration of the artifact can generate a reasonable detection probability.

13 Free elementary modules

Free elementary modules obey special differential equations.

The landing locations of the hops that form the hopping path and the location swarm trigger the Palestra and that trigger starts a spherical shape keeping front that we named a clamp. The integration of the clamp over the regeneration cycle period of the swarm results in the Green's function of the field, which represents an averaged response of the Palestra on the trigger. The convolution of the Green's function with the location density distribution of the swarm results in the contribution of the elementary module to the Palestra $\mathfrak{C}$. For free elementary modules this contribution equals the Palestra.

The clamp is a solution of the homogeneous second order partial differential equation under isotropic conditions.

$$\nabla \nabla^* \psi = \frac{1}{r^2} \frac{\partial}{\partial r}\left(r^2 \frac{\partial \psi}{\partial r}\right) + \frac{\partial^2 \psi}{\partial \tau^2} = 0 \tag{1}$$

$$\psi = \frac{f(\boldsymbol{i}\,r - c\,t)}{r} + \frac{g(\boldsymbol{i}\,r + c\,t)}{r} \tag{2}$$

We only use the left term and average over the cycle period.

This results in the Green's function:

$$G(r) = 1/r \tag{3}$$

The integration converts the field ψ into the Palestra C.

Next we convolute the Green's function with the location density distribution of the swarm.

Locally, the result equals the Palestra. The integration converts the homogeneous equation into an inhomogeneous equation in which the added term equals the Palestra.

$$\frac{1}{r^2} \frac{\partial}{\partial r}\left(r^2 \frac{\partial C}{\partial r}\right) + \frac{\partial^2 C}{\partial \tau^2} = G(r) \circ \rho(r) = C(r) \tag{4}$$

This equation can be split into two first order partial differential equations.

$$\nabla \nabla^* C = C \tag{5}$$

$$\varphi = \nabla^* C \tag{6}$$

$$\nabla \varphi = C \tag{7}$$

14 Force raising subfields

The change of a field is represented by a partial differential equation

$$\Phi = \nabla\,\psi = \Phi_0 + \boldsymbol{\Phi} = (\nabla_0 + \boldsymbol{\nabla})(\psi_0 + \boldsymbol{\psi}) \tag{1}$$

$$\Phi_0 = \nabla_0\psi_0 - \langle \boldsymbol{\nabla}, \boldsymbol{\psi}\rangle \tag{2}$$

$$\boldsymbol{\Phi} = \nabla_0\boldsymbol{\psi} + \boldsymbol{\nabla}\psi_0 \pm \boldsymbol{\nabla}\times\boldsymbol{\psi} = -\mathfrak{E} \pm \mathfrak{B} \tag{3}$$

Here we consider a situation in which the total field change is zero and more in detail:

$$\mathfrak{E} = \mathfrak{B} = 0 \tag{4}$$

A change of the scalar field ψ_0 can be compensated by a divergence of the vector field $\boldsymbol{\psi}$. Similarly, a change of the vector field $\boldsymbol{\psi}$ can be compensated by a gradient of the scalar field ψ_0. The term $E = \nabla_0\boldsymbol{\psi}$ represents a **force raising field**.

The Green's function $G(\boldsymbol{r})$ of the field can be considered as the result of the integration of a clamp over a long enough period. Parameter $\boldsymbol{r}$ is the displacement from the location of the trigger.

$$G(\boldsymbol{r}) = \frac{1}{4\pi|\boldsymbol{r}|} \tag{5}$$

However, $G(\boldsymbol{r})$ can also be considered as the effect on the field of a relative steady artifact. In that case the Green's function can be interpreted as the scalar potential $\varphi(\boldsymbol{r})$ of the artifact. The strength of the influence is characterized by a real number valued charge Q_1.

$$\varphi(\boldsymbol{r}) = Q_1\,G(\boldsymbol{r}) = \frac{Q_1}{4\pi|\boldsymbol{r}|} \tag{6}$$

As such, every clamp represents a unit charge. Also symmetry related charges represent point-like artifacts that characterize the strength of the corresponding potential.

If the point-like artifact moves rather than hops and this movement occurs with a uniform speed $\boldsymbol{v}$, then the scalar potential turns into a vector potential $\boldsymbol{A}(\boldsymbol{r})$.

$$\boldsymbol{A}(\boldsymbol{r}) = \varphi(\boldsymbol{r})\boldsymbol{v} = \frac{Q_1}{4\pi|\boldsymbol{r}|}\boldsymbol{v} \tag{7}$$

In the above formulas plays $\varphi(\boldsymbol{r})$ the role of ψ_0 and $\boldsymbol{A}(\boldsymbol{r})$ plays the role of $\boldsymbol{\psi}$. If the point-like artifact accelerates, then the change of the vector potential goes together with the existence of a new vector field $\boldsymbol{E}(\boldsymbol{r})$ that acts as a force raising field. This follows from the fact that the total change of the field stays zero.

$$\nabla_0 \boldsymbol{\psi} + \boldsymbol{\nabla}\psi_0 = \dot{\boldsymbol{A}}(\boldsymbol{r}) + \boldsymbol{\nabla}\left(\frac{Q_1}{4\pi|\boldsymbol{r}|}\right) = \dot{\boldsymbol{A}}(\boldsymbol{r}) - \frac{Q_1\,\dot{\boldsymbol{v}}}{4\pi|\boldsymbol{r}|^3}\boldsymbol{r} = \boldsymbol{0} \tag{8}$$

If the acceleration occurs in radial direction, then this results in a force raising field $\boldsymbol{E}(\boldsymbol{r})$:

$$\boldsymbol{E}(\boldsymbol{r}) = \dot{\boldsymbol{A}}(\boldsymbol{r}) = \frac{Q_1}{4\pi|\boldsymbol{r}|^2}\dot{\boldsymbol{v}} \tag{9}$$

With respect to this force raising field another point-like charge with charge value Q_2 that is also embedded in the original field will sense a force $\boldsymbol{F}(\boldsymbol{r})$ that equals the product of the force raising field and the charge of the second embedded point-like object.

$$\boldsymbol{F}(\boldsymbol{r}_2 - \boldsymbol{r}_1) = Q_2\,\boldsymbol{E}(\boldsymbol{r}_2 - \boldsymbol{r}_1) = \frac{Q_1 Q_2}{4\pi|\boldsymbol{r}_2 - \boldsymbol{r}_1|}\dot{\boldsymbol{v}} \tag{10}$$

A force raising field $\boldsymbol{E} = \boldsymbol{\nabla}\psi_0$ is a component of a base field $\boldsymbol{\psi}$ that can exert a force onto a charged object. The force raising field counteracts the change of the field when another component $\boldsymbol{\psi}$ of that field is changed $\nabla_0 \boldsymbol{\psi}$.

For example, inertia is the result of a force raising field that counteracts the acceleration of massive objects.

15 Information transfer

In the model, information transfer between discrete objects is implemented by the fields with which they interact. Interaction means that the location of the object or the state of the object is affected by the field and/or that the field is deformed by the presence of the object. The state of the object is its assembly of discernable properties. These properties may depend on the mechanism that governs the behavior and the existence of the object.

Solutions of the second order partial differential equation of the field play an important role in these interactions. Especially the messengers play a major role in the transfer of information. In this model photons are implemented by strings of messengers.

15.1 Messengers

Messengers are configured by solutions of the quaternionic second order partial differential equation. For odd numbers of participating dimensions some of the solutions of the homogeneous second order partial differential equation are combinations of shape keeping fronts. In three dimensions the spherical shape keeping fronts diminish their amplitude as $1/r$ with distance r of the trigger point. One-dimensional wave fronts **keep their amplitude**. As a consequence these shape keeping fronts can travel huge distances through the field that supports them. Each shape keeping front can carry a bit of information and/or energy. In order to reach these distances the carrying field must exist long enough and it must reach far enough.

The symmetry related field $\mathfrak{A}$ does not fulfil the requirements for long distance travel. It depends on the nearby existence of symmetry related charges and its amplitude also diminishes as 1/r with distance from the charge.

The embedding field $\mathfrak{C}$ is a better candidate for long distance transfer of energy and information. $\mathfrak{C}$ exists always and everywhere. One-dimensional shape keeping fronts vibrate the $\mathfrak{C}$ field, but do not deform this field. They just follow existing deformations.

Creating a string of one-dimensional shape keeping fronts requires a recurrent shape keeping front generation process. Such processes do not underlay the generation of symmetry related charges that support the $\mathfrak{A}$ field. However, such processes exist during the recurrent embedding of artifacts that occurs in the $\mathfrak{C}$ field.

Recurrent regeneration of spherical shape keeping fronts is capable to deform the corresponding field. It has similar effects as a stationary deformation by a point-like artifact has.

15.2 Frenet Serret path

The fixed speed of the messengers represents an interesting case. The change of a field has five components that cover four dimensions. However the path $\gamma(\tau)$ of an object in the spatial part of that field can be characterized by three mutually independent figures.

The first figure is called the **unit tangent vector $e_1(\tau)$**. The vector is directed along the tangent that departs at a selected location τ on that path.

$$e_1(\tau) = \gamma'(\tau)/\|\gamma'(\tau)\| \tag{1}$$

The second figure is called the **normal vector $e_2(\tau)$**.

$$f(\tau) = \gamma''(\tau) - \langle \gamma''(\tau), e_1(\tau) \rangle \, e_1(\tau) \tag{2}$$

$$e_2(\tau) = \frac{f(\tau)}{\|f(\tau)\|} \tag{3}$$

The size $\|\boldsymbol{f}(\tau)\|$ of vector $\boldsymbol{f}(\tau)$ is not equal to unity and the direction of $\boldsymbol{f}(\tau)$ is perpendicular to the unit tangent vector. The inverse of the size is an indication of the local curvature of the field that acts as the transport medium for the messenger. It is called the local **curvature** κ of the path $\boldsymbol{\gamma}(\tau)$.

$$\kappa = \frac{1}{\langle \boldsymbol{f}(\tau), \boldsymbol{e}_2(\tau)\rangle}$$

The third figure is called the **bi-normal vector $\boldsymbol{e}_3(\tau)$.**

$$\boldsymbol{g}(\tau) = \boldsymbol{\gamma}'''(\tau) - \langle\boldsymbol{\gamma}'''(\tau),\boldsymbol{e}_1(\tau)\rangle\,\boldsymbol{e}_1(\tau) - \langle\boldsymbol{\gamma}'''(\tau),\boldsymbol{e}_2(\tau)\rangle\,\boldsymbol{e}_2(\tau)$$

$$\boldsymbol{e}_3(\tau) = \frac{\boldsymbol{g}(\tau)}{\|\boldsymbol{g}(\tau)\|} = \boldsymbol{e}_1(\tau) \times \boldsymbol{e}_2(\tau)$$

The size $\|\boldsymbol{g}(\tau)\|$ of vector $\boldsymbol{g}(\tau)$ is not equal to unity and the direction of $\boldsymbol{g}(\tau)$ is perpendicular to both the unit tangent vector and the normal vector. The size is an indication of the local **curl** of the field that acts as the transport medium for the messenger. It is called the torque t of the path $\boldsymbol{\gamma}(\tau)$.

Since the speed $\|\boldsymbol{\gamma}'(\tau)\|$ is constant the right-side term in equation (2) is zero. We take the speed equal to unity. This reduces the path to a natural path, which is described by three orthonormal frame vectors. $\boldsymbol{T}, \boldsymbol{N}$ and $\boldsymbol{B}$.

$$\boldsymbol{T}(\tau) = \boldsymbol{\gamma}'(\tau)$$

$$\boldsymbol{T}'(\tau) = \kappa\,\boldsymbol{N}(\tau)$$

$$\boldsymbol{N}'(\tau) = -\kappa\,\boldsymbol{T}(\tau) + t\,\boldsymbol{B}(\tau)$$

$$\boldsymbol{B}'(\tau) = -t\,\boldsymbol{N}(\tau)$$

$$\boldsymbol{B} = \boldsymbol{T} \times \boldsymbol{N}$$

Due to the curvature and the curl of the carrying field the path becomes a **geodesic**. Within the geodesic and along the path the messenger travels with constant speed. It means that along the geodesic the progression steps are equal to the spatial steps and the carrying field deforms in order to support the sidesteps due to the non-zero curvature κ and the non-zero torque t of the path of the messenger.

15.3 Photons

The fixed speed of shape keeping fronts translates in the same fixed speed for the messengers. A string of one-dimensional shape keeping fronts can carry a quantized amount of energy. Photons appear to be the physical realizations of the messengers. The relation $E = h\,\nu$ and the fixed speed of photons indicate that at least at relative short range the string of shape keeping fronts takes a fixed amount of progression steps for its creation, for its passage and for its absorption.

However, observations of long range effects over cosmological distances reveal that these relations do not hold over huge distances. Red-shift of patterns of "old" photons that are emitted by atoms and arrive from distant galaxies indicate that the spatial part of field $\mathfrak{C}$ is extending as a function of progression.

With the interpretation of photons as strings of shape keeping fronts this means that the duration of emission and the duration of absorption are also functions of progression. As a consequence, some of the emitted wave fronts are "missed" at later absorption. The detected photon corresponds to a lower energy and a lower frequency than the emitted photon has. According to relation $E = h\,\nu$ that holds locally, the detected photon appears to be red-shifted. The energy of the "missed" shape

keeping fronts is converted into other kinds of energy or the missed shape keeping fronts keep proceeding as lower energy photons. Spurious shape keeping fronts may stay undetected.

15.4 Consequences for our model

Thus, the quaternionic second order partial differential equation may be valid in the vicinity of the images of symmetry centers inside $\mathfrak{C}$, but does not properly describe the long range behavior of $\mathfrak{C}$. Due to its restricted range and the non-recurrent generation of its charges, the $\mathfrak{A}$ field does not show the equivalents of photons and red-shift phenomena.

The long range phenomena of photons indicate that the parameter space $\mathfrak{R}^{\circledcirc}$ of $\mathfrak{C}$ may actually own an origin. For higher progression values and for most of the spatial reach of field $\mathfrak{C}$, that origin is located at huge distances. Information coming from low progression values arrives with photons that have travelled huge distances. They report about a situation in which symmetry centers were located on average at much smaller inter-distances.

Instead of photons the $\mathfrak{A}$ field may support waves, such as radio waves and microwaves. These waves are solutions of the wave equation, which is part of Maxwell based differential calculus.

On the other hand, the wave equation also has shape keeping fronts as its solutions.

15.5 Energy-mass equivalence

The indication that self-coherence at least partly is caused by the enormous number of elements in the swarms that represent elementary particles and for another part it is caused by the effects of inertia inside the swarm leads on the one hand to the assumption that the mass of elementary particles is directly proportional to the number of elements inside the swarm. The creation and annihilation events of elementary modules then lead to the conclusion that during these events the solutions of the homogeneous second order differential equations convert from spherical three dimensional solutions to linear one-dimensional solutions or vice versa. This process occurs step by step. What happens during each step, is restricted by the reservation of symmetry conditions. During the life of the elementary module what happens can and will be integrated over the regeneration cycle of the swarm that represents the elementary module. The integration converts the spherical solutions into the Green's function of the field. It converts the homogeneous second order partial differential equation into an inhomogeneous equation. The new term represents the Green's function.

The one-dimensional solutions will be combined in a one-dimensional string of equidistant elements. For each element of the swarm and thus for each solution in the form of a spherical shape keeping front, an element of the string of equidistant one-dimensional shape and amplitude keeping fronts is generated. At particle annihilation, the photons leave in a direction that is perpendicular to the direction in which the swarm is/was moving. This indicates that some other object that is active in a third direction is also involved in the process.

16 At the start of progression

At progression value $\tau = 0$, the mechanisms that generate the artifacts, which cause discontinuities in the embedding manifold $\mathfrak{C}$ have not yet done any work. It means that this manifold was flat and its defining function equaled its parameter space at instance $\tau = 0$.

At $\tau = 0$ nothing arrives from the past.

The model offers the possibility that the domain Ω expands as a function of τ. In that case it is possible that domain Ω covers a growing amount of symmetry centers.

17 Low dose rate imaging

17.1 Preface

The author started his career in high-tech industry in the development of image intensifier devices. His job was to help optimizing the imaging quality of these image intensifier devices. This concerned both image intensifiers for night vision applications and x-ray image intensifiers that were aimed at medical applications. Both types of devices target low dose rate application conditions. These devices achieve image intensification in quite different ways. Both types can be considered to operate in a linear way. The qualification of the image intensifier is based on the fact that human image perception is optimized for low dose rate conditions.

At low dose rates the author never perceived waves in the intensified images. At the utmost he saw hail storms of impinging discrete particles and the corresponding detection patterns can simulate interference patterns. The conclusion is, that the waves that might be present in the observed image are probability waves. Individual photons are perceived as detected quanta. They are never perceived as waves.

17.2 Human perception

With respect to visual perception the human visual trajectory closely resembles the visual trajectory of all vertebrates. This was discovered by Hubel and Weisel. They got a Noble price for their work.

The sensitivity of the human eye covers a huge range. The visual trajectory implements several special measures that help extending that range. At high dose rates the pupil of the eye acts as a diaphragm that partly closes the lens and in this way it increases the sharpness of the picture on the retina. At such dose rates the cones perform the detection job. The cones are sensitive to colors and offer a quick response. In unaided conditions, the rods take over at low dose rates and they do not differentiate between colors. In contrast to the cones the rods apply a significant integration time. This integration diminishes the effects of quantum noise that becomes noticeable at low dose rates. The sequence of optimizations do not stop at the retina. In the trajectory from the retina to the fourth cortex of the brain several dedicated decision centers decode the received image by applying masks that trigger on special aspects of the image. For example a dedicated mask can decide whether the local part of the image is an edge, in which direction this edge is oriented and in which direction the edge moves. Other masks can discern circular spots. Via such masks the image is encoded before the information reaches the fourth cortex. Somewhere in the trajectory the information of the right eye crosses the information that is contained in the left eye. The difference is used to construct three dimensional vision. Quantum noise can easily disturb the delicate encoding process. That is why the decision centers do not pass their information when its signal to noise ratio is below a given level. That level is influenced by the physical and mental condition of the observer. At low dose rates, this signal to noise ratio barrier prevents a psychotic view. The higher levels of the brain thus do not receive a copy of the image that was detected at the retina. Instead that part of the brain receives a set of quite trustworthy encoded image data that will be deciphered in an associative way. It is expected that other parts of the brain for a part act in a similar noise blocking way.

The evolution of the vertebrates must have installed this delicate visual data processing subsystem in a period in which these vertebrates lived in rather dim circumstances, where visual perception of low dose rate images was of vital importance.

This indicates that the signal to noise ratio in the image that arrives at the eyes pupil has significant influence on the perceptibility of the low dose image. At high dose rates the signal to noise ratio hardly plays a role. In those conditions the role of the spatial blur is far more important.

It is fairly easy to measure the signal to noise ratio in the visual channel by applying a DC meter and an RMS meter. However, at very low dose rates, the damping of both meters might pose problems. What quickly becomes apparent is the relation of the signal to noise ratio and the number of the quanta that participate in the signal. The measured relation is typical for stochastic quantum generation processes that are classified as Poisson processes.

It is also easy to comprehend that when the signal is spread over a spatial region, the number of quantal that participate per surface unit is diminishing. Thus spatial blur has two influences. It lowers the local signal and at the other hand it increase the integration surface. Lowering the signal decreases the number of quanta. Enlarging the integration surface will increase the number of involved quanta. Thus, these two effects partly compensate each other. An optimum perceptibility condition exists that maximizes the signal to noise ratio in the visual trajectory.

The blur is caused by the Point Spread Function. This function represents a spatially varying binomial process that attenuates the efficiency of the original Poisson process. This creates a new Poisson process that features a spatially varying efficiency. Several components in the imaging chain may contribute to the Point Spread Function such that the effective Point Spread Function equals the convolution of the Point Spread Functions of the components. Mathematically it can be shown that for linear image processors the Optical Transfer Functions form an easier applicable characteristic than the Point Spread Functions, because the Fourier transform that converts the Point Spread Function into the Optical Transfer Function converts the convolutions into simple multiplications.

The Optical Transfer Function is influenced by several factors. Examples are the color distribution, the angular distribution and the phase homogeneity of the impinging radiation. Also veiling glare may hamper the imaging quality.

The fact that the signal to noise ratio appears to be a deciding factor in the perception process has led to a second way of characterizing the relevant influences. The Detective Quantum Efficiency (DQE) characterizes the efficiency of the usage of the available quanta. It compares the actual situation with the hypothetical situation in which all generated quanta would be used in the information channel. Again the measured signal noise ratio is compared to the ideal situation in which the stochastic generator is a Poisson process and no binomial processes will attenuate that primary Poisson process. This means that blurring and temporal integration must play no role in the determination of the DQE and the measured device will be compared to quantum detectors that will capture all available quanta. It also means that intensification processes will not add extra relative variance to the signal. The application of micro channel plates will certainly add extra relative variation. This effect will be accounted as a deterioration of the detection efficiency and not as a change of the stochastic process from a Poisson process to an exponential process. Mathematically this is an odd procedure, but it is a valid approach when the measurements are used to objectively evaluate perceptibility.

17.3 Mechanisms

The fact that the objective qualification of perceptibility can be performed by the Optical Transfer Function in combination with the Detective Quantum Efficiency indicates that the generation of the quanta is governed by a Poisson process that is coupled to a binomial process, where the binomial process is implemented by a spatial Point Spread Function.

The mechanisms that ensure dynamical coherence appear to apply stochastic processes whose signal to noise ratio is proportional to the square root of the number of generated quanta.

Quite probably the quantum generation process belongs to the category of Poisson point processes and in particular to the subcategory that are known as log Gaussian Cox point processes.

18 Discussion

This paper shifts the mystery that in current physical theories exist about the wave function to the mysteries that exist about the characteristic function of the stochastic processes that give the hopping path and the corresponding location swarm their location density distribution. The existence of that characteristic function means that this location density distribution must possess a Fourier transform and that as a consequence the swarm can be considered to behave as one unit. Some guesses are made about the nature of the stochastic processes. Nothing is said about how the corresponding mechanisms cooperate. This paper suggests that the mechanisms implement self-coherence and that this self-coherence relates to inertia.

This paper only considers the divergence based version of the generalized Stokes theorem. The consequences for the curl based version are not investigated in detail. From fluid dynamics it is known that artifacts that are embedded in a fluid may suffer from the vorticity of the embedding field [x].

This paper does not investigate the consequences of polar ordering. It probably relates to the spin properties of elementary modules. In that case the polar ordering of symmetry centers regulates the distinction between fermions and bosons. The half integer spin particles may use ordering of the azimuth, where the integer spin particles use the ordering of the polar angle. However, this does not explain the difference in behavior between these categories. The paper also does not investigate the origin of the Pauli principle, which is closely related to the notion of spin.

The concept of exterior derivative is carefully crafted by skillful mathematicians, such that it becomes independent of the selection of parameter spaces. However, in a situation like the situation that is investigated by the Hilbert Book Test Model in which several parameter spaces float on top of a background parameter space, the selection of the ordering of the parameter spaces does matter. The symmetry flavors of the coupled parameter spaces determine the values of the integrals that account for the contributions of the artifacts. It is represented by the symmetry related charges of these artifacts. These symmetry related charges are supposed to be located at the geometric centers of the symmetry centers.

As happens so often, physical reality reveals facts (such as the symmetry related charges) that cannot easily be discovered by skilled mathematicians. The standard model contains a short list of electric charges that correspond to the symmetry related charges. The standard model does not give an explanation for the existence of this short list. In the Hilbert Book Test Model it becomes clear that the electric charge and the color charge are a properties of connected parameter spaces and not a property of the objects that use these parameter spaces. Instead, these objects inherit the charge properties from the platform on which they reside.

Both the symmetry related fields and the embedding continuum affect the geometric location of the symmetry center. They do that in different ways.

If electric charges are properties of the connection between spaces, then the fields to which these charges contribute implement the forces between these connections. No extra objects are needed to implement these forces!

100

It is sensible to expect that depending on the type of their "charges" all basic fields are capable of attracting or repelling the spaces on which these "charges" reside. This behavior is described by the differential and integral equations that are obeyed by the considered field.

The model does not dive deep into the binding process. In that respect regular physical theories go much further.

The Hilbert Book Test Model is no more and no less than a mathematical test case. The paper does not pretend that physical reality behaves like this model. But the methods used and the results obtained in this paper might learn more about how models of physical reality can be structured and how these can behave.

19 Lessons

Some interesting lessons can be derived from the model. At the first place the model introduces a commandment:

"Thou shalt construct in a modular way".

This commandment enforces the constructors to **construct in a very economical way** that applies as littles resource as is possible. A problem occurs when the resources are limited.

In the beginning, the evolution is controlled by pure stochastic processes. In that evolution process increasingly complicated modular systems will be generated. This process depends on the availability of nearby resources. As soon as in a local environment the evolution reaches a level that intelligent species (read types) are formed, these species can take active part in the evolution process. In that environment the stochastic modular design method turns into an intelligent design method.

After investigation of the lifeforms that he discovered at the islands in the oceans and at the beaches of southern continents, Darwin concluded that only the fittest species can reach a longer existence in the evolution process. A similar rule exist for the modules and modular systems. However this rule must be extended, because the survival struggle does not so much concern the individuals. Instead, it concerns the survival of module types and that survival is supported when the type promotes the survival of the community of the type to which the individual belongs. This often must include the care of the survival of the types that are used by the considered type as a resource. If a community grows so large that its resources become endangered, then the complete community is endangered. Thus a second commandment follows the primal commandment:

"Each individual must take care of the resources of the community of which that individual is a member".

20 References

[1] https://en.wikipedia.org/wiki/Mathematical_formulation_of_quantum_mechanics

[2] The lattices of quantum logic and classical logic are treated in detail in: http://vixra.org/abs/1411.0175 .

[3] Quantum logic was introduced by Garret Birkhoff and John von Neumann in their 1936 paper. G. Birkhoff and J. von Neumann, *The Logic of Quantum Mechanics*, Annals of Mathematics, Vol. 37, pp. 823–843

[4] The Hilbert space was discovered in the first decades of the 20-th century by David Hilbert and others. http://en.wikipedia.org/wiki/Hilbert_space.

[5] In the second half of the twentieth century Constantin Piron and Maria Pia Solèr proved that the number systems that a separable Hilbert space can use must be division rings. See: "Division algebras and quantum theory" by John Baez. http://arxiv.org/abs/1101.5690 and http://www.ams.org/journals/bull/1995-32-02/S0273-0979-1995-00593-8/ and http://arxiv.org/abs/quant-ph/0510095

[6] In 1843 quaternions were discovered by Rowan Hamilton. http://en.wikipedia.org/wiki/History_of_quaternions

[7] Warren D. Smith, Quaternions, octonions, and now, 16-ons and 2n-ons; http://scorevoting.net/WarrenSmithPages/homepage/nce2.pdf

[8] Quaternionic function theory and quaternionic Hilbert spaces are treated in: http://vixra.org/abs/1411.0178 .

[9] Paul Dirac introduced the bra-ket notation, which popularized the usage of Hilbert spaces. Dirac also introduced its delta function, which is a generalized function. Spaces of generalized functions offered continuums before the Gelfand triple arrived.

Dirac, P.A.M. (1982) [1958]. Principles of Quantum Mechanics. International Series of Monographs on Physics (4th ed.). Oxford University Press. p. 255. ISBN 978-0-19-852011-5.

[10] In the sixties Israel Gelfand and Georgyi Shilov introduced a way to model continuums via an extension of the separable Hilbert space into a so called Gelfand triple. The Gelfand triple often gets the name rigged Hilbert space. It is a non-separable Hilbert space. http://www.encyclopediaofmath.org/index.php?title=Rigged_Hilbert_space .

[11] https://en.wikipedia.org/wiki/Stokes%27_theorem#General_formulation.

[12] Stokes

[13] Justin Shaw, Invariant Vector Calculus. http://www.math.uwaterloo.ca/~j9shaw/Invariant%20Vector%20Calculus.pdf.

[13] Fermion Symmetry Flavors. http://vixra.org/abs/1512.0225

[14] https://en.wikipedia.org/wiki/Poisson%27s_equation#Potential_of_a_Gaussian_charge_density

[14] Foundation of a Mathematical Model of Physical Reality. http://vixra.org/abs/1511.0074

Appendix

1 Lattices

A lattice is a set of elements $a, b, c, \dots$ that is closed for the connections $\cap$ and $\cup$. These connections obey:

- The set is **partially ordered**.
  - This means that with each pair of elements a, b belongs an element c, such that $a \subset c$ and $b \subset c$.
- The set is a $\cap$ **half lattice.**
  - This means that with each pair of elements a, b an element c exists, such that $c = a \cap b$.
- The set is a $\cup$ half lattice.
  - This means that with each pair of elements a, b an element c exists, such that $c = a \cup b$.
- The set is a lattice.
  - This means that the set is both a $\cap$ half lattice and a $\cup$ half lattice.

The following relations hold in a lattice:

$$a \cap b = b \cap a \tag{1}$$

$$(a \cap b) \cap c = a \cap (b \cap c) \tag{2}$$

$$a \cap (a \cup b) = a \tag{3}$$

$$a \cup b = b \cup a \tag{4}$$

$$(a \cup b) \cup c = a \cup (b \cup c) \tag{5}$$

$$a \cup (a \cap b) = a \tag{6}$$

The lattice has a **partial order inclusion** $\subset$:

$$a \subset b \Longleftrightarrow a \cap b = a \tag{7}$$

A **complementary lattice** contains two elements n and e with each element a a complementary element a' such that:

$$a \cap a' = n \tag{8}$$

$$a \cap n = n \tag{9}$$

$$a \cap e = a \qquad (10)$$

$$a \cup a' = e \qquad (11)$$

$$a \cup e = e \qquad (12)$$

$$a \cup n = a \qquad (13)$$

An **orthocomplemented lattice** contains two elements n and e and with each element a an element a'' such that:

$$a \cup a'' = e \qquad (14)$$

$$a \cap a'' = n$$

$$(a'')'' = a \qquad (15)$$

$$a \subset b \Leftrightarrow b'' \subset a'' \qquad (16)$$

e is the **unity element**; n is the **null element** of the lattice

A **distributive lattice** supports the distributive laws:

$$a \cap (b \cup c) = (a \cap b) \cup (a \cap c) \qquad (17)$$

$$a \cup (b \cap c) = (a \cup b) \cap (a \cup c) \qquad (18)$$

A **modular lattice** supports:

$$(a \cap b) \cup (a \cap c) = a \cap (b \cup (a \cap c)) \qquad (19)$$

A **weak modular lattice** supports instead:

There exists an element d such that

$$a \subset c \Leftrightarrow (a \cup b) \cap c = a \cup (b \cap c) \cup (d \cap c) \qquad (20)$$

106

where d obeys:

$$(a \cup b) \cap d = d \tag{21}$$

$$a \cap d = n \tag{22}$$

$$b \cap d = n \tag{23}$$

$$(a \subset g) \, and \, (b \subset g) \Leftrightarrow d \subset g \tag{24}$$

In an **atomic lattice** holds

$$\exists_{p \in L} \forall_{x \in L} \{x \subset p \Rightarrow x = n\} \tag{25}$$

$$\forall_{a \in L} \forall_{x \in L} \{(a < x < a \cap p) \Rightarrow (x = a \, or \, x = a \cap p)\} \tag{26}$$

p is an atom

Quaternion geometry and arithmetic

Quaternions and quaternionic functions offer the advantage of a very compact notation of items that belong together [8].

Quaternions can be considered as the combination of a real scalar and a 3D vector that has real coefficients. The vector forms the imaginary part of the quaternion. Quaternionic number systems are division rings. It means that all non-zero members have a unique inverse. Other division rings are real numbers and complex numbers. The separable Hilbert space only uses the rational subsets of these number systems.

Bi-quaternions exist whose parts exist of a complex scalar and a 3D vector that has complex coefficients. Octonions and bi-quaternions do not form division rings. This paper does not use them. However, one exception is tolerated: in considering the Dirac equation, bi-quaternionic functions and bi-quaternionic differential operators are used. The Dirac equation is treated in the appendix.

1.1   Notation

We indicate the real part of quaternion a by the suffix a_0.

We indicate the imaginary part of quaternion a by bold face $\boldsymbol{a}$.

$$a = a_0 + \boldsymbol{a} \tag{1}$$

We indicate the quaternionic conjugate by a superscript in the form of a star.

$$a^* = a_0 - \boldsymbol{a} \tag{2}$$

We introduce the **complex base number** i via

$$i \cdot i = -1 \tag{3}$$

In bi-quaternionic equations, i commutes with all quaternions.

$$i \cdot a = a \cdot i \tag{4}$$

However, the product is no longer a quaternion. Instead, it is a bi-quaternion. Bi-quaternions are indicated by a beret.

$$\widehat{c} = a + i \cdot b \tag{5}$$

Here a and b are both regular quaternions. Complex conjugation is acting as:

$$\mathring{\imath}^{\bullet} = -\mathring{\imath} \tag{6}$$

Complex conjugation is indicated with a superscript in the form of a filled circle.

$$\widehat{c}^{\bullet} = a - \mathring{\imath} \cdot b \tag{7}$$

Here we see bi-quaternions as hyper-complex numbers with quaternionic coefficients. These numbers do not form a division ring. These numbers are not equivalent to octonions. This paper does not apply Clifford algebra, Jordan algebra or other than the pure division ring algebra's, because the author considers them to conceal more than they elucidate.

1.2   Quaternionic sum

$$c = c_0 + \boldsymbol{c} = a + b \tag{1}$$

$$c_0 = a_0 + b_0 \tag{2}$$

$$\boldsymbol{c} = \boldsymbol{a} + \boldsymbol{b} \tag{3}$$

1.3   Quaternionic product

$$f = f_0 + \boldsymbol{f} = d \cdot e \tag{1}$$

$$f_0 = d_0 \cdot e_0 - \langle \boldsymbol{d}, \boldsymbol{e} \rangle \tag{2}$$

$$\boldsymbol{f} = d_0 \cdot \boldsymbol{e} + e_0 \cdot \boldsymbol{d} \pm \boldsymbol{d} \times \boldsymbol{e} \tag{3}$$

Thus the product contains five parts. The $\pm$ sign indicates the influence of right or left handedness of the version of the quaternionic number system.

$\langle \boldsymbol{d}, \boldsymbol{e} \rangle$ is the inner product of $\boldsymbol{d}$ and $\boldsymbol{e}$.

$\boldsymbol{d} \times \boldsymbol{e}$ is the outer product of $\boldsymbol{d}$ and $\boldsymbol{e}$.

We usually omit the multiplication sign $\cdot$.

1.3.1   Handedness

We introduce by superscript $^{\emptyset}$ a switch in handedness of the quaternion. This does not touch the real part.

$$f^\emptyset = d^\emptyset \cdot e^\emptyset = d_0 \cdot e_0 - \langle \boldsymbol{d}^\emptyset, \boldsymbol{e}^\emptyset \rangle + d_0 \cdot \boldsymbol{e}^\emptyset + e_0 \cdot \boldsymbol{d}^\emptyset \mp \boldsymbol{d}^\emptyset \times \boldsymbol{e}^\emptyset \tag{1}$$

$$\boldsymbol{d}^\emptyset \times \boldsymbol{e}^\emptyset = -\boldsymbol{d} \times \boldsymbol{e} \tag{2}$$

$d \cdot e^\emptyset$ and $d^\emptyset \cdot e$ **are undefined**!

Thus a right handed quaternion cannot be multiplied with a left handed quaternion. Quaternionic conjugation switches the handedness. In addition:

$$(a \cdot b)^* = b^* \cdot a^* \tag{3}$$

A continuous quaternionic function does not switch its handedness. Embedding a conflicting quaternion in the target space of a function produces a local artifact that produces a local discontinuity. This also holds for other aspects of the quaternion symmetries.

1.4   Norm

$$|a| = \sqrt{a_0 a_0 + \langle \boldsymbol{a}, \boldsymbol{a} \rangle} = \sqrt{a \cdot a^*} \tag{1}$$

1.5   Norm of quaternionic functions

Square-integrable functions are normalizable. The norm is defined by:

$$\|\psi\|^2 = \int_V |\psi|^2 \, dV \tag{1}$$

$$= \int_V \{ |\psi_0|^2 + |\boldsymbol{\psi}|^2 \} dV$$

$$= \|\psi_0\|^2 + \|\boldsymbol{\psi}\|^2$$

1.6 Quaternionic rotation

In multiplication quaternions do not commute. Thus, in general $a\,b/a \neq b$. In this multiplication the imaginary part of b that is perpendicular to the imaginary part of a is rotated over an angle φ that is twice the complex phase of a.

$a = |a|\exp(\mathbf{i}\varphi)$

The transform aba^{-1} rotates the imaginary part $\pmb{b}$ of b around an axis along the imaginary part $\pmb{a}$ of a over an angle 2φ that is twice the argument φ of a in the complex field spanned by $\pmb{a}$ and $\mathbf{1}$

$\perp$ means perpendicular
$\parallel$ means parallel
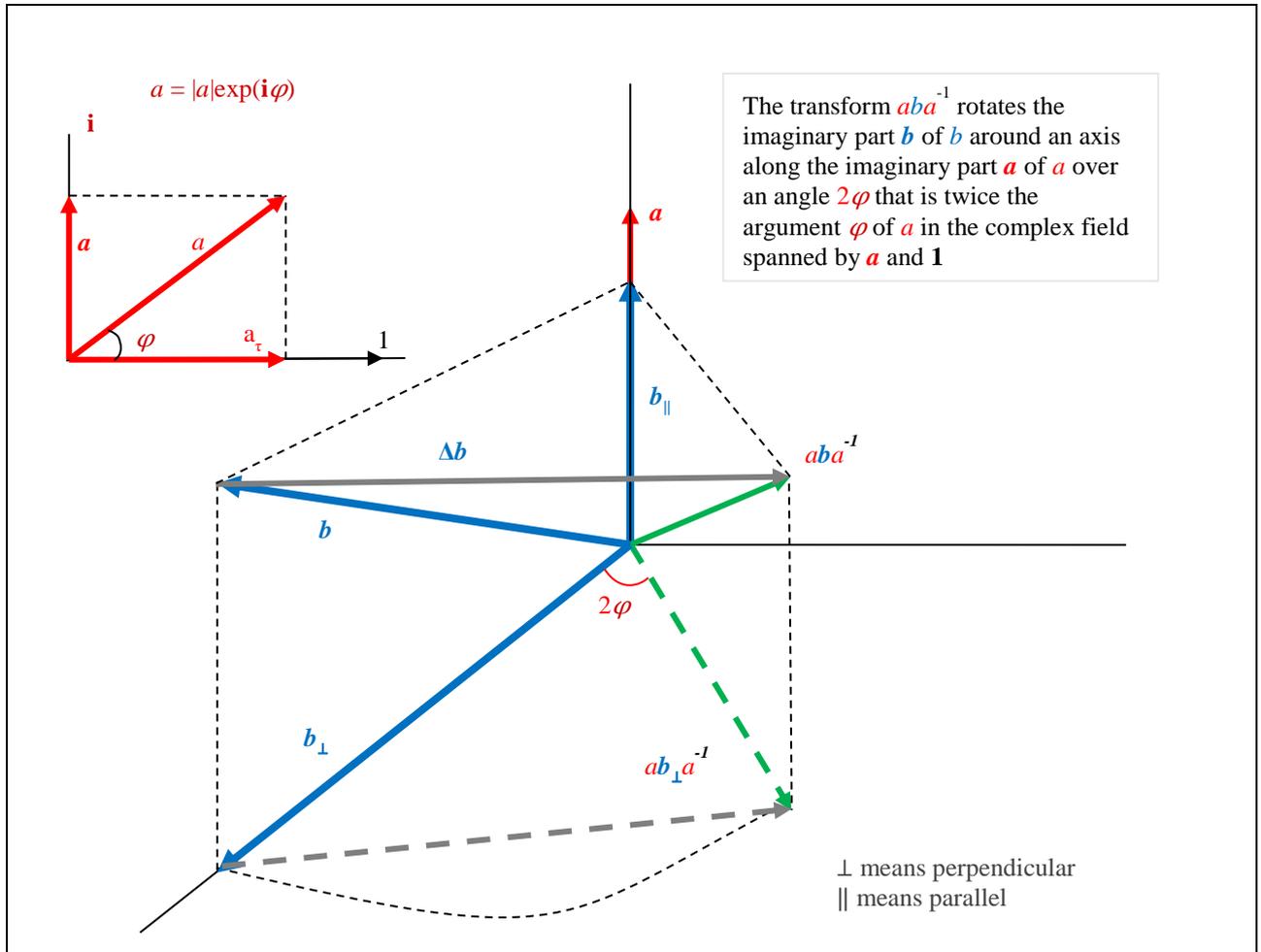
This means that if $\varphi = \pi/4$, then the rotation $c = a\,b/a$ shifts $\pmb{b}_\perp$ to another dimension. This fact puts quaternions that feature the same size of the real part as the size of the imaginary part is in a special category. They can switch states of tri-state systems. In addition, they can switch the color charge of quarks.

2 The quaternionic separable Hilbert space

We will specify the characteristics of a generalized quaternionic infinite dimensional separable Hilbert space $\mathfrak{H}$. The adjective "quaternionic" indicates that the inner products of vectors and the eigenvalues of operators are taken from the number system of the quaternions. Separable Hilbert spaces can be using real numbers, complex numbers or quaternions. These three number systems are division rings. In fact the quaternionic number system comprises all division rings.

2.1 Notations and naming conventions

$\{f_x\}_x$ means ordered set of f_x . It is a way to define discrete functions.

The use of bras and kets differs slightly from the way Dirac uses them.

$|f\rangle$ is a ket vector.

$\langle f|$ is a bra vector.

A is an operator.

$A^\dagger$ is the adjoint operator of operator A.

$|$ on its own, is a nil operator.

We will use capitals for operators and lower case Greek characters for quaternions and eigenvalues. We use Latin characters for ket vectors, bra vectors and eigenvectors. Imaginary and anti-Hermitian objects will be indicated in **bold** text. Real numbers get subscript $_0$.

Due to the non-commutative product of quaternions, special care must be paid to the ordering of factors inside products. In this paper a particular ordering is selected. It is one out of a lager set of possibilities.

2.2 Quaternionic Hilbert space

The Hilbert space $\mathfrak{H}$ is a **linear space**. That means for the elements $|f\rangle$, $|g\rangle$ and $|h\rangle$ of $\mathfrak{H}$ and quaternionic numbers α and β a linear space is defined. $|f\rangle$, $|g\rangle$ and $|h\rangle$ are ket vectors.

2.2.1 Ket vectors

For **ket** vectors hold

$$|f\rangle + |g\rangle = |g\rangle + |f\rangle = |g + f\rangle \tag{1}$$

$$(|f\rangle + |g\rangle) + |h\rangle = |f\rangle + (|g\rangle + |h\rangle) \tag{2}$$

$$|\alpha f\rangle = |f\rangle\,\alpha \; ; \;\; |f\rangle = |\alpha f\rangle\,\alpha^{-1} \tag{3}$$

$$|(\alpha + \beta)\,f\rangle \;=\; |f\rangle\,\alpha \,+\, |f\rangle\,\beta \tag{4}$$

$$(|f\rangle + |g\rangle)\,\alpha \;=\; |f\rangle\,\alpha \,+\, |g\rangle\,\alpha \tag{5}$$

$$|f\rangle\,0 \;=\; |0\rangle \tag{6}$$

$$|f\rangle\,1 \;=\; |f\rangle \tag{7}$$

2.2.2 Bra vectors

The **bra** vectors form the dual Hilbert space $\mathfrak{H}^\dagger$ of $\mathfrak{H}$.

$$\langle f| + \langle g| \;=\; \langle g| + \langle f| \;=\; \langle f + g| \tag{1}$$

$$(\langle f| + \langle g|) + \langle h| \;=\; \langle f| + (\langle g| + \langle h|) \tag{2}$$

$$\langle \alpha f| = \alpha^*\langle f| \; ; \;\; \langle f| = (\alpha^*)^{-1}\,\langle \alpha f| \tag{3}$$

$$\langle f\,(\alpha + \beta)| = \alpha^*\langle f| + \beta^*\,\langle f| \tag{4}$$

Notice the quaternionic conjugation that affects the coefficients of bra vectors.

$$(\langle f| + \langle g|)\alpha \;=\; \langle f|\,\alpha \,+\, \langle g|\,\alpha \tag{5}$$

$$0\,\langle f| \;=\; \langle 0| \tag{6}$$

$$1\,\langle f| \;=\; \langle f| \tag{7}$$

2.2.3 Scalar product

The scalar product couples Hilbert space $\mathfrak{H}^\dagger$ to its dual $\mathfrak{H}$.

$$\langle f|g \rangle = \langle g|f \rangle^* \tag{1}$$

$$\langle f+g|h \rangle = \langle f|h \rangle + \langle g|h \rangle \tag{2}$$

$$\langle \alpha f|g \rangle = \alpha^* \langle f|g \rangle = \alpha^* \langle g|f \rangle^* = \langle g|\alpha f \rangle^* \tag{5}$$

$$\langle f|\alpha g \rangle = \langle f|g \rangle \, \alpha = \langle g|f \rangle^* \, \alpha = \langle \alpha g|f \rangle^* \tag{6}$$

$\langle f|$ is a bra vector. $|g\rangle$ is a ket vector. α is a quaternion. $\langle f|g\rangle$ is quaternion valued.

If the Hilbert space represents both dual spaces, then the scalar product is also called an ***inner product***.

2.2.4 Separable

In mathematics a topological space is called separable if it contains a countable dense subset; that is, there exists a sequence $\{|x_n\rangle\}_{n=1}^{\infty}$ of elements of the space such that every nonempty open subset of the space contains at least one element of the sequence.

Every continuous function on the separable space $\mathfrak{H}$ is determined by its values on this countable dense subset.

2.2.5 ***Base vectors***

The Hilbert space $\mathfrak{H}$ is **separable**. That means that a countable row of elements $\{|f_n\rangle\}$ exists that **spans** the whole space.

If $\langle f_n|f_m \rangle = \delta(m,n) = [1$ when $n = m;$ 0 otherwise$]$ then $\{|f_n\rangle\}$ forms an **orthonormal base** of the Hilbert space.

A ket base $\{|k\rangle\}$ of $\mathfrak{H}$ is a minimal set of ket vectors $|k\rangle$ that together span the Hilbert space $\mathfrak{H}$.

Any ket vector $|f\rangle$ in $\mathfrak{H}$ can be written as a linear combination of elements of $\{|k\rangle\}$.

$$|f\rangle = \sum_k (|k\rangle \, \langle k|f\rangle) \tag{1}$$

A bra base $\{\langle b|\}$ of $\mathfrak{H}^{\dagger}$ is a minimal set of bra vectors $\langle b|$ that together span the Hilbert space $\mathfrak{H}^{\dagger}$.

Any bra vector $\langle f|$ in $\mathfrak{H}^{\dagger}$ can be written as a linear combination of elements of $\{\langle b|\}$.

$$\langle f| = \sum_k (\langle k|f\rangle \, \langle b|) \tag{2}$$

Usually base vectors are taken such that their norm equals 1. Such a base is called an orthonormal base.

2.2.6 *Operators*

Operators act on a subset of the elements of the Hilbert space.

2.2.6.1 Linear operators

An operator Q is linear when for all vectors $|f\rangle$ and $|g\rangle$ for which Q is defined and for all quaternionic numbers α and β:

$$|Q \ \alpha \ f\rangle + |Q \ \beta \ g\rangle = |Q \ f\rangle\alpha + |Q \ g\rangle\beta = \tag{1}$$

$$Q(|\alpha \ f\rangle + |\beta \ g\rangle) = Q(|f\rangle\alpha + |g\rangle\beta)$$

Operator B is **colinear** when for all vectors $|f\rangle$ for which B is defined and for all quaternionic numbers α there exists a quaternionic number γ such that:

$$|\alpha \ B \ f\rangle = |B \ f\rangle \gamma\alpha\gamma^{-1} \overset{\text{def}}{=} |B \ \gamma\alpha\gamma^{-1} \ f\rangle \tag{2}$$

If $|f\rangle$ is an eigenvector of operator A with quaternionic eigenvalue a,

$$A|f\rangle = |f\rangle a$$

then $|b \ f\rangle$ is an eigenvector of A with quaternionic eigenvalue $b^{-1}a \ b$.

$$A|b \ f\rangle = |A \ b \ f\rangle = |A \ f\rangle b = |f\rangle a \ b = |b \ f\rangle b^{-1}a \ b$$

$A^\dagger$ is the **adjoint** of the **normal** operator A.

$$\langle f \ |A \ g\rangle = \langle f \ A^\dagger|g\rangle = \langle g \ |A^\dagger \ f\rangle^* \tag{4}$$

$$A^{\dagger\dagger} = A \tag{5}$$

$$(A + B)^\dagger = B^\dagger + A^\dagger \tag{6}$$

115

$$(A \cdot B)^\dagger \ = \ B^\dagger A^\dagger \tag{7}$$

If $A = A^\dagger$, then A is a **self adjoint** operator.

| is a nil operator.

2.2.6.2 Operator construction

The construct $|f\rangle\langle g|$ acts as a linear operator. $|g\rangle\langle f|$ is its adjoint operator.

The **reverse bra-ket method** uses an orthonormal base $\{|q_i\rangle\}$ that belongs to quaternionic eigenvalues $\{q_i\}$ and a quaternionic function $F(q)$ and in this way a linear operator F can be defined such that for all vectors $|g\rangle$ and $|h\rangle$ holds:

$$\langle g|F\,h\rangle = \sum_i \{\langle g|q_i\rangle F(q_i)\langle q_i|h\rangle\} \tag{7}$$

$$F \stackrel{\text{def}}{=} \sum_i \{|q_i\rangle f(q_i)\langle q_i|\} \tag{8}$$

If no confusion arises, then the same symbol is used for the function F(q), the operator F and the set of eigenvalues F. For the orthonormal base $\{|q_i\rangle\}$ holds:

$$\langle q_j|q_k\rangle = \delta_{jk} \tag{9}$$

We will use

$$F \stackrel{\text{def}}{=} |q_i\rangle F(q_i)\langle q_i| \tag{10}$$

as a shorthand for equations (7) and (8).

$$F^\dagger \stackrel{\text{def}}{=} |q_i\rangle F(q_i)^*\langle q_i| \tag{11}$$

$$|q_i\rangle F(q_i)\langle q_i| = |q_i\,F(q_i)\rangle\langle q_i| = |q_i\rangle\langle F(q_i)^*\,q_i| \tag{12}$$

The eigenspace of reference operator $\mathcal{R}$ defined by

116

$$\mathcal{R} \stackrel{\text{def}}{=} \sum_i \{|q_i\rangle q_i \langle q_i|\} \tag{13}$$

represents the countable ***parameter space*** of discrete function $F(q_i)$.

F and $\mathcal{R}$ are constructed operators.

If collection $\{q_i\}$ covers all rational members of a quaternionic number system then this definition specifies a reference operator for which the eigenspace represents the parameter space of all discrete functions that can be defined with this number system.

Quaternionic number systems exist in several versions that only differ in the way that the elements are ordered. We will identify these different versions with special superscripts. When relevant, this will also be done with the number systems, with the operators, with the eigenvectors and with the eigenvalues.

$$\mathcal{R}^{⓪} \stackrel{\text{def}}{=} \sum_i \left\{|q_i^{⓪}\rangle q_i^{⓪} \langle q_i^{⓪}|\right\} \tag{14}$$

$\mathcal{R}^{⓪}$ is a member of a set of reference operators $\{\mathcal{R}^x\}$. The superscript ^{x} specifies the symmetry flavor of the number system $\{q^x\}$.

The superscript ^{x} can be ⓪, ①, ②, ③, ④, ⑤, ⑥, ⑦, ⑧, ⑨, ⑩, ⑪, ⑫, ⑬, ⑭, or ⑮.

Often, we will use the same character for identifying eigenvectors, eigenvalues and the corresponding operator.

Definition 8 specifies a normal operator. The set of eigenvectors of a normal operator form an orthonormal base of the Hilbert space.

A self adjoint operator has real numbers as eigenvalues. If T is a normal operator, then $T_0 = (T + T^{\dagger})/2$ is a self adjoint operator and $\boldsymbol{T} = (T - T^{\dagger})/2$ is an imaginary normal operator. Self adjoint operators are also Hermitian operators. Imaginary normal operators are also anti-Hermitian operators.

2.2.6.3 Normal operators
The most common definition of continuous operators is:

A **continuous** operator is an operator that creates images such that the inverse images of open sets are open.

Similarly, a **continuous** operator creates images such that the inverse images of closed sets are closed.

If $|a\rangle$ is an eigenvector of normal operator A with eigenvalue a then

$$\langle a|A|a\rangle \ = \ \langle a|a|a\rangle \ = \ \langle a|a\rangle\, a \tag{1}$$

indicates that the eigenvalues are taken from the same number system as the inner products.

A normal operator is a continuous linear operator.

A normal operator in $\mathfrak{H}$ creates an image of $\mathfrak{H}$ onto $\mathfrak{H}$. It transfers closed subspaces of $\mathfrak{H}$ into closed subspaces of $\mathfrak{H}$.

The normal operators N have the following property.

$$N\colon \mathfrak{H} \ \Rightarrow \ \mathfrak{H} \tag{2}$$

Thus the normal operator N maps separable Hilbert space $\mathfrak{H}$ onto itself.

N commutes with its **(Hermitian) adjoint** $N^{\dagger}$:

$$NN^{\dagger} \ = \ N^{\dagger}N \tag{2}$$

Normal operators are important because the spectral theorem holds for them.

Examples of normal operators are

- **unitary** operators: $U^{\dagger} = U^{-1}$, unitary operators are bounded;
- **Hermitian** operators (i.e., self-adjoint operators): $N^{\dagger} = N$;
- **Anti-Hermitian** or anti-self-adjoint operators: $N^{\dagger} = -N$;
- **Anti-unitary** operators: $U^{\dagger} = -U^{-1}$, anti-unitary operators are bounded;
- **positive operators**: $N = MM^{\dagger}$
- **orthogonal projection** operators: $P^{\dagger} = P = P^{2}$.

For normal operators hold:

$$AB = A_0 B_0 - \langle \boldsymbol{A}, \boldsymbol{B}\rangle + A_0 \boldsymbol{B} + \boldsymbol{A} B_0 \pm \boldsymbol{A} \times \boldsymbol{B} \tag{3}$$

$$N_0 = \tfrac{1}{2}\left(N + N^{\dagger}\right) \tag{4}$$

$$\boldsymbol{N} = \tfrac{1}{2}\left(N - N^{\dagger}\right) \tag{5}$$

$$NN^{\dagger} = N_0 N_0 + \langle \boldsymbol{N}, \boldsymbol{N}\rangle = N_0^2 - \boldsymbol{N}^2 \tag{6}$$

For every compact self-adjoint operator T on a real, complex or quaternionic Hilbert space $\mathfrak{H}$, there exists an orthonormal basis of $\mathfrak{H}$ consisting of eigenvectors of T. More specifically, the orthogonal complement of the kernel (null space) of T admits, either a finite orthonormal basis of eigenvectors of T, or a countable infinite orthonormal basis of eigenvectors of T, with corresponding eigenvalues $\{\lambda_n\} \subset \mathbb{R}$, such that $\lambda_n \to 0$. Due to the fact that $\mathfrak{H}$ is separable the set of eigenvectors of T can be extended with a base of the kernel in order to form a complete orthonormal base of $\mathfrak{H}$.

If T is compact on an infinite dimensional Hilbert space $\mathfrak{H}$, then T is not invertible, hence $\sigma(T)$, the spectrum of T, always contains 0. The spectral theorem shows that $\sigma(T)$ consists of the eigenvalues $\{\lambda_n\}$ of T, and of 0 (if 0 is not already an eigenvalue). The set $\sigma(T)$ is a compact subset of the real line, and the eigenvalues are dense in $\sigma(T)$.

A normal operator has a set of eigenvectors that spans the whole Hilbert space $\mathfrak{H}$.

In quaternionic Hilbert space a normal operator has quaternions as eigenvalues.

The set of eigenvalues of a normal operator is NOT compact. This is due to the fact that $\mathfrak{H}$ is separable. Therefore the set of eigenvectors is countable. As a consequence the set of eigenvalues is countable. Further, in general the eigenspace of normal operators has no finite diameter.

A continuous bounded linear operator on $\mathfrak{H}$ has a compact eigenspace. The set of eigenvalues has a closure and it has a finite diameter.

2.2.6.5   Eigenspace
The set of eigenvalues $\{q\}$ of the operator Q form the eigenspace of Q.

2.2.6.6   Eigenvectors and eigenvalues
For the eigenvector $|q\rangle$ of normal operator Q holds

$$|Q\,q\rangle = |q\,q\rangle = |q\rangle q \tag{1}$$

$$\langle q\,Q^\dagger| = \langle q\,q| = q^*\langle q| \tag{2}$$

$$\forall_{|f\rangle \in \mathfrak{H}} \left[\{\langle f|Q\,q\rangle\}_q = \{\langle f|q\rangle q\}_q = \left\{\langle q\,Q^\dagger|f\rangle^*\right\}_q = \{(q^*\langle q|f\rangle)^*\}_q \right] \tag{3}$$

The eigenvalues of 2^n-on normal operator are 2^n-ons. For Hilbert spaces the eigenvalues are restricted to elements of a division ring.

$$Q = \sum_{j=0}^{n-1} I_j Q_i \qquad (4)$$

The Q_j are self-adjoint operators.

$$Q = \sum_{j=0}^{n-1} I_j Q_i$$

2.2.6.7   Unitary operators

For unitary operators holds:

$$U^\dagger = U^{-1} \tag{1}$$

Thus

$$UU^\dagger = U^\dagger U = I \tag{2}$$

Suppose $U = I + C$ where U is unitary and C is compact. The equations *(2)* and $C = U - I$ show that C is normal. The spectrum of C contains 0, and possibly, a finite set or a sequence tending to 0. Since $U = I + C$, the spectrum of U is obtained by shifting the spectrum of C by 1.

The unitary transform can be expressed as:

$$U = exp(\tilde{I}\,\Phi/\hbar) \tag{3}$$

$$\hbar = h/(2\,\pi) \tag{4}$$

Φ is Hermitian. The constant h refers to the granularity of the eigenspace.

Unitary operators have eigenvalues that are located in the unity sphere of the 2^n-ons field.

The eigenvalues have the form:

$$u = exp(\boldsymbol{i}\,\varphi/\hbar) \tag{5}$$

φ is real. $\boldsymbol{i}$ is a unit length imaginary number in 2^n-on space. It represents a direction.

u spans a sphere in 2^n-on space. For constant $\boldsymbol{i}$, u spans a circle in a complex subspace.

2.2.6.7.1   *Polar decomposition*

Normal operators N can be split into a real operator A and a unitary operator U. U and A have the same set of eigenvectors as N.

$$N = \|N\|\, U = A\,U = U\,A = A\,exp\left(\tilde{I}\frac{\Phi}{\hbar}\right) = exp\left(\Phi_r + \tilde{I}\frac{\Phi}{\hbar}\right) \tag{1}$$

Φ_r is a positive normal operator.

121

Suppose that two operators X and N have the commutation relation:

$$[N, X] = c\, X \tag{1}$$

for some scalar c. If $|n\rangle$ is an eigenstate of N with eigenvalue equation,

$$|N\, n\rangle = |n\rangle\, n \tag{2}$$

then the operator X acts on $|n\rangle$ in such a way as to shift the eigenvalue by c:

$$|N\, X\, n\rangle = |(X\, N\ +\ [N, X])n\rangle = |(X\, N\ +\ c\, X)n\rangle \tag{3}$$
$$= |X\, N\, n\rangle + |X\, n\rangle\, c = |X\, n\rangle\, n + |X\, n\rangle\, c = |X\, n\rangle(n + c)$$

In other words, if $|n\rangle$ is an eigenstate of N with eigenvalue n then $|X\, n\rangle$ is an eigenstate of N with eigenvalue $n + c$.

The operator X is a *raising operator* for N if c is real and positive, and a *lowering operator* for N if c is real and negative.

If N is a Hermitian operator then c must be real and the Hermitian adjoint of X obeys the commutation relation:

$$[N,\ X^{\dagger}] = -\, c\ X^{\dagger} \tag{4}$$

In particular, if X is a lowering operator for N then $X^{\dagger}$ is a raising operator for N and vice-versa.

2.2.7   Unit sphere of $\mathfrak{H}$

The ket vectors in $\mathfrak{H}$ that have their norm equal to one form together the **unit sphere** Θ of $\mathfrak{H}$.

The orthonormal base vectors are all member of the unit sphere.

2.2.8   Bra-ket in four dimensional space

The Bra-ket formulation can also be used in transformations of the four dimensional curved spaces.

The bra $\langle f|$ is then a covariant vector and the ket $|g\rangle$ is a contra-variant vector. The inner product acts as a metric.

$$s = \langle f|g\rangle \tag{1}$$

The effect of a linear transformation L is then given by

$$s_L = \langle f|Lg\rangle \tag{2}$$

The effect of a the transpose transformation $L^{\dagger}$ is then given by

$$\langle fL^\dagger \,|g\rangle = \langle f|Lg\rangle \tag{3}$$

For a unitary transformation U holds:

$$\langle Nf|Ng\rangle = \langle f|N^\dagger Ng\rangle = \langle f|NN^\dagger g\rangle = \langle NN^\dagger f|g\rangle = \langle N^\dagger Nf|g\rangle \tag{4}$$

$$\langle Uf|Ug\rangle = \langle f|g\rangle \tag{5}$$

$$\langle \nabla f|\nabla g\rangle = \langle f|\nabla^\dagger \nabla g\rangle = \langle f|\nabla\nabla^\dagger g\rangle = \langle \nabla\nabla^\dagger f|g\rangle = \langle \nabla^\dagger \nabla f|g\rangle \tag{6}$$

Notice that

$$\nabla\nabla^\dagger = \nabla^\dagger\nabla = \nabla_0\nabla_0 + \langle \mathbf{\nabla}, \mathbf{\nabla}\rangle = \nabla_0^2 - \mathbf{\nabla}^2 \tag{7}$$

2.2.9 Closure

The closure of $\mathfrak{H}$ means that converging rows of vectors converge to a vector of $\mathfrak{H}$.

In general converging rows of eigenvalues of Q do not converge to an eigenvalue of Q.

Thus, the set of eigenvalues of Q is open.

At best the density of the coverage of the set of eigenvalues is comparable with the set of 2^n-ons that have rational numbers as coordinate values.

With other words, compared to the set of real numbers the eigenvalue spectrum of Q has holes.

The set of eigenvalues of operator Q includes 0. This means that Q does not have an inverse.

The rigged Hilbert space $\mathcal{H}$ can offer a solution, but then the direct relation with quantum logic is lost.

2.2.10 Canonical conjugate operator P

The existence of a canonical conjugate represents a stronger requirement on the continuity of the eigenvalues of canonical eigenvalues.

Q has eigenvectors $\{|q\rangle\}_q$ and eigenvalues q_s.

P has eigenvectors $\{|p\rangle\}_p$ and eigenvalues p_s.

For each eigenvector $|q\rangle$ of Q we define an eigenvector $|p\rangle$ and eigenvalues p_s of P such that:

$$\langle q|p\rangle = \langle p|q\rangle^* = exp\,(i\,p_s\,q_s/\hbar) \tag{1}$$

$\hbar = h/(2\pi)$ is a scaling factor. $\langle q|p \rangle$ is a quaternion. $\pmb{i}$ is a unit length imaginary quaternion. q_s and p_s are quaternionic (eigen)values corresponding to $|q\rangle$ and $|p\rangle$.

2.2.11 Displacement generators

Variance of the scalar product gives:

$$\pmb{i}\,\hbar\,\delta\langle q|p\rangle \;=\; -p_s\langle q|p\rangle\delta q \tag{1}$$

$$\pmb{i}\,\hbar\,\delta\langle p|q\rangle \;=\; -q_s\langle p|q\rangle\delta p \tag{2}$$

In the rigged Hilbert space $\mathcal{H}$ the variance can be replaced by differentiation.

Partial differentiation of the function $\langle q|p\rangle$ gives:

$$\pmb{i}\,\hbar\,\frac{\partial}{\partial q_s}\langle q|p\rangle \;=\; -p_s\langle q|p\rangle \tag{3}$$

$$\pmb{i}\,\hbar\,\frac{\partial}{\partial p_s}\langle p|q\rangle = -q_s\langle p|q\rangle \tag{4}$$

3   Gelfand triple

The separable Hilbert space only supports countable orthonormal bases and countable eigenspaces. The rigged Hilbert space $\mathcal{H}$ that **belongs to** an infinite dimensional separable Hilbert space $\mathfrak{H}$ is a Gelfand triple. It supports non-countable orthonormal bases and continuum eigenspaces.

A rigged Hilbert space is a pair $(\mathfrak{H}, \Phi)$ with $\mathfrak{H}$ a Hilbert space, Φ a dense subspace, such that Φ is given a topological vector space structure for which the inclusion map i is continuous.

Identifying $\mathfrak{H}$ with its dual space $\mathfrak{H}^\dagger$, the adjoint to i is the map

$$i^*\colon \mathfrak{H} = \mathfrak{H}^\dagger \to \Phi^\dagger \tag{1}$$

The duality pairing between Φ and $\Phi^\dagger$ has to be compatible with the inner product on $\mathfrak{H}$, in the sense that:

$$\langle u, v \rangle_{\Phi \times \Phi^\dagger} = (u, v)_{\mathfrak{H}} \tag{2}$$

whenever $u \in \Phi \subset \mathfrak{H}$ and $v \in \mathfrak{H} = \mathfrak{H}^\dagger \subset \Phi^\dagger$.

The specific triple $(\Phi \subset \mathfrak{H} \subset \Phi^\dagger)$ is often named after the mathematician Israel Gelfand).

Note that even though Φ is isomorphic to $\Phi^\dagger$ if Φ is a Hilbert space in its own right, this isomorphism is *not* the same as the composition of the inclusion i with its adjoint $i^\dagger$

$$i^\dagger i\colon \Phi \subset \mathfrak{H} = \mathfrak{H}^\dagger \to \Phi^\dagger \tag{3}$$

3.1   Understanding the Gelfand triple

The Gelfand triple of a real separable Hilbert space can be understood via the enumeration model of the real separable Hilbert space. This enumeration is obtained by taking the set of eigenvectors of a normal operator that has rational numbers as its eigenvalues. Let the smallest enumeration value of the rational enumerators approach zero. Even when zero is reached, then still the set of enumerators is countable. Now add all limits of converging rows of rational enumerators to the enumeration set. After this operation the enumeration set has become a continuum and has the same cardinality as the set of the real numbers. This operation converts the Hilbert space $\mathfrak{H}$ into its Gelfand triple $\mathcal{H}$ and it converts the normal operator in a new operator that has the real numbers as its eigenspace. It means that the orthonormal base of the Gelfand triple that is formed by the eigenvectors of the new normal operator has the cardinality of the real numbers. It also means that linear operators in this Gelfand triple have eigenspaces that are continuums and have the cardinality of the real numbers[1]. The same reasoning holds for complex number based Hilbert spaces and quaternionic Hilbert spaces and their respective Gelfand triples.

---

[1] This story also applies to the complex and the quaternionic Hilbert spaces and their Gelfand triples.

A similar insight can be obtained via the ***reverse bra-ket method***. The (mostly) continuous function F(q) can relate a continuum parameter space {q} to a closed set $\{|q\rangle\}$ of Hilbert vectors that form an orthonormal base of the rigged Hilbert space $\mathcal{H}$. In this way a normal operator F is defined via:

$$\langle x|F\, y\rangle = \int_q \langle x|q\rangle F(q)\langle q|y\rangle \ dq \tag{1}$$

The relation between the infinite dimensional separable Hilbert space and its non-separable companion follows from:

$$\langle x|F\, y\rangle = \sum_{i=0}^{i=\infty} \langle x|q_i\rangle F(q_i)\langle q_i|y\rangle \approx \int_q \langle x|q\rangle F(q)\langle q|y\rangle \ dq \tag{2}$$

This can be interpreted by the view that the separable Hilbert space is embedded within its non-separable companion.

Formula (2) also reveals how summation of sets $\{q_i\}$ is related to integration of corresponding continuums {q}.

4   Quaternionic and Maxwell field equations

In this section, we will compare two sets of differential equations. Both sets use pure space as part of the parameter space.

- Quaternionic differential equations
  - These equations use progression as one of its parameters.
- Maxwell based differential equations
  - These equations use quaternionic distance as one of its parameters.

In this chapter we will use a switch $\circledast = \pm 1$ that selects between two different sets of differential calculus. One set concerns low order quaternionic differential calculus. The other set concerns Maxwell based differential calculus. The switch will be used to highlight the great similarity and the significant differences between these sets.

By introducing new symbols $\mathfrak{E}$ and $\mathfrak{B}$ we will turn the quaternionic differential equations into Maxwell-like quaternionic differential equations. We introduced a simple switch $\circledast = \pm 1$ that apart from the difference between the parameter spaces, will turn one set of equations into the other set.

Maxwell based differential calculus splits quaternionic functions into a scalar function and a vector function. Instead of the quaternionic nabla $\nabla = \nabla_0 + \boldsymbol{\nabla}$ the Maxwell based equations use the scalar operator $\nabla_0 = \frac{\partial}{\partial t}$ and the vector nabla $\boldsymbol{\nabla}$ as separate operators. Maxwell equations use a switch α that controls the structure of a gauge equation.

$$\varkappa = \alpha \frac{\partial}{\partial t} \, \varphi_0 + \langle \boldsymbol{\nabla}, \boldsymbol{\varphi} \rangle \tag{1}$$

For Maxwell based differential calculus is $\alpha = +1$ and $\nabla_0 = \frac{\partial}{\partial t}$. The switch value is $\circledast$ -1.

For quaternionic differential calculus is $\alpha = -1$ and $\nabla_0 = \frac{\partial}{\partial \tau}$. The switch value is $\circledast = +1$.

In the book EMFT the scalar field $\varkappa$ is taken as a gauge with

   $\alpha = 1$; Lorentz gauge

   $\alpha = 0$; Coulomb gauge

   $\alpha = -1$; Kirchhoff gauge.

We will use the definition of a scalar field $\varkappa$:

$$\varkappa \overset{\text{def}}{=} \alpha \, \nabla_t \varphi_0 + \langle \boldsymbol{\nabla}, \boldsymbol{\varphi} \rangle \Longleftrightarrow \phi_0 = \nabla_\tau \varphi_0 - \langle \boldsymbol{\nabla}, \boldsymbol{\varphi} \rangle \tag{2}$$

In Maxwell based differential calculus the scalar field $\varkappa$ is ignored or it is taken equal to zero. As will be shown, zeroing $\varkappa$ is not necessary for the derivation of the Maxwell based wave equation [14].

Maxwell equations split the considered functions in scalar functions and vector functions. The Maxwell differential operators are also split and as a consequence they cannot be treated as multiplying operators. We keep them together with curly brackets.

$$\phi = \{\phi_0, \boldsymbol{\phi}\} = \{\nabla_0, \boldsymbol{\nabla}\}\{\varphi_0, \boldsymbol{\varphi}\} \tag{3}$$

$$\phi_0 = \nabla_0\,\varphi_0 - \circledast\,\langle \boldsymbol{\nabla}, \boldsymbol{\varphi}\rangle \tag{4}$$

$$\boldsymbol{\phi} = \nabla_0\boldsymbol{\varphi} + \boldsymbol{\nabla}\varphi_0 \pm \boldsymbol{\nabla}\times\boldsymbol{\varphi} \tag{5}$$

Equations (4) and (5) are not genuine Maxwell equations. We introduce them here as extra Maxwell equations. Choice $\circledast = -1$ conforms to the Lorenz gauge. We define extra symbols $\mathfrak{E}$ and $\mathfrak{B}$ for parts of the first order partial differential equation.

$$\mathfrak{E} \overset{\text{def}}{=} -\nabla_0\boldsymbol{\varphi} - \boldsymbol{\nabla}\varphi_0 \tag{6}$$

$$\nabla_0\mathfrak{E} = -\nabla_0\nabla_0\,\boldsymbol{\varphi} - \nabla_0\boldsymbol{\nabla}\varphi_0 \tag{7}$$

$$\langle \boldsymbol{\nabla}, \mathfrak{E}\rangle = -\nabla_0\langle \boldsymbol{\nabla}, \boldsymbol{\varphi}\rangle - \langle \boldsymbol{\nabla}, \boldsymbol{\nabla}\rangle\varphi_0 \tag{8}$$

$$\mathfrak{B} \overset{\text{def}}{=} \boldsymbol{\nabla}\times\boldsymbol{\varphi} \tag{9}$$

These definitions imply:

$$\langle \mathfrak{E}, \mathfrak{B}\rangle = 0 \tag{10}$$

$$\nabla_0\mathfrak{B} = -\boldsymbol{\nabla}\times\mathfrak{E} \tag{11}$$

$$\langle \boldsymbol{\nabla}, \mathfrak{B}\rangle = 0 \tag{12}$$

$$\boldsymbol{\nabla}\times\mathfrak{B} = \boldsymbol{\nabla}\langle \boldsymbol{\nabla}, \boldsymbol{\varphi}\rangle - \langle \boldsymbol{\nabla}, \boldsymbol{\nabla}\rangle\boldsymbol{\varphi} \tag{13}$$

128

Also the following two equations are not genuine Maxwell equations, but they relate to the gauge equation.

$$\nabla_0 \phi_0 = \nabla_0 \nabla_0 \, \varphi_0 - \circledast \, \nabla_0 \langle \boldsymbol{\nabla}, \boldsymbol{\varphi} \rangle \tag{14}$$

$$\boldsymbol{\nabla} \phi_0 = \nabla_0 \, \boldsymbol{\nabla} \varphi_0 - \circledast \, \boldsymbol{\nabla} \langle \boldsymbol{\nabla}, \boldsymbol{\varphi} \rangle = \nabla_0 \, \boldsymbol{\nabla} \varphi_0 - \circledast \, \boldsymbol{\nabla} \times \boldsymbol{\nabla} \times \, \boldsymbol{\varphi} - \circledast \, \langle \boldsymbol{\nabla}, \boldsymbol{\nabla} \rangle \, \boldsymbol{\varphi} \tag{15}$$

$$\zeta = (\nabla_0 + \circledast \, \langle \boldsymbol{\nabla}, \boldsymbol{\nabla} \rangle) \varphi = \zeta_0 + \boldsymbol{\zeta} \Leftrightarrow \{\zeta_0, \boldsymbol{\zeta}\} = \{\nabla_0, -\boldsymbol{\nabla}\} \{\phi_0, \boldsymbol{\phi}\} \tag{16}$$

$$\zeta_0 = (\nabla_0 \nabla_0 + \circledast \, \langle \boldsymbol{\nabla}, \boldsymbol{\nabla} \rangle) \varphi_0 = \nabla_0 \, \phi_0 - \circledast \, \langle \boldsymbol{\nabla}, \mathfrak{E} \rangle \tag{17}$$

$$\boldsymbol{\zeta} = (\nabla_0 \nabla_0 + \circledast \, \langle \boldsymbol{\nabla}, \boldsymbol{\nabla} \rangle) \boldsymbol{\varphi} = -\boldsymbol{\nabla} \phi_0 - \nabla_0 \mathfrak{E} - \circledast \, \boldsymbol{\nabla} \times \mathcal{B} \tag{18}$$

More in detail the equations mean:

$$\zeta_0 = \nabla_0 \phi_0 + \circledast \, \langle \boldsymbol{\nabla}, \boldsymbol{\phi} \rangle \tag{19}$$
$$= \{\nabla_0 \nabla_0 \varphi_0 - \circledast \, \nabla_0 \langle \boldsymbol{\nabla}, \boldsymbol{\varphi} \rangle\} + \{\circledast \, \langle \boldsymbol{\nabla}, \boldsymbol{\nabla} \rangle \varphi_0 + \circledast \, \nabla_0 \langle \boldsymbol{\nabla}, \boldsymbol{\varphi} \rangle \pm \circledast \, \langle \boldsymbol{\nabla}, \boldsymbol{\nabla} \times \boldsymbol{\varphi} \rangle\}$$
$$= (\nabla_0 \nabla_0 + \circledast \, \langle \boldsymbol{\nabla}, \boldsymbol{\nabla} \rangle) \varphi_0$$

$$\zeta_0 = \nabla_0 \, \phi_0 - \circledast \, \langle \boldsymbol{\nabla}, \mathfrak{E} \rangle \tag{20}$$
$$= \{\nabla_0 \nabla_0 \, \varphi_0 - \circledast \, \nabla_0 \langle \boldsymbol{\nabla}, \boldsymbol{\varphi} \rangle\} + \{\circledast \, \nabla_0 \langle \boldsymbol{\nabla}, \boldsymbol{\varphi} \rangle + \circledast \, \langle \boldsymbol{\nabla}, \boldsymbol{\nabla} \rangle \varphi_0\}$$
$$= (\nabla_0 \nabla_0 + \circledast \, \langle \boldsymbol{\nabla}, \boldsymbol{\nabla} \rangle) \varphi_0$$

$$\boldsymbol{\zeta} = -\boldsymbol{\nabla} \phi_0 + \nabla_0 \boldsymbol{\phi} \mp \boldsymbol{\nabla} \times \boldsymbol{\phi} \tag{21}$$
$$= \{-\boldsymbol{\nabla} \nabla_0 \varphi_0 + \circledast \, \boldsymbol{\nabla} \times \boldsymbol{\nabla} \times \boldsymbol{\varphi} + \circledast \, \langle \boldsymbol{\nabla}, \boldsymbol{\nabla} \rangle \boldsymbol{\varphi}\} + \{\nabla_0 \boldsymbol{\nabla} \varphi_0 + \nabla_0 \nabla_0 \boldsymbol{\varphi} \pm \nabla_0 \boldsymbol{\nabla} \times \boldsymbol{\varphi}\}$$
$$\{\mp \boldsymbol{\nabla} \times \boldsymbol{\nabla} \varphi_0 \mp \boldsymbol{\nabla} \times \nabla_0 \boldsymbol{\varphi} - \boldsymbol{\nabla} \times \boldsymbol{\nabla} \times \boldsymbol{\varphi}\}$$
$$= (\nabla_0 \nabla_0 + \circledast \, \langle \boldsymbol{\nabla}, \boldsymbol{\nabla} \rangle) \boldsymbol{\varphi} + \circledast \, \boldsymbol{\nabla} \times \boldsymbol{\nabla} \times \boldsymbol{\varphi} - \boldsymbol{\nabla} \times \boldsymbol{\nabla} \times \boldsymbol{\varphi}$$

$$\boldsymbol{\zeta} = -\boldsymbol{\nabla} \phi_0 - \nabla_0 \mathfrak{E} - \circledast \, \boldsymbol{\nabla} \times \mathcal{B} \tag{22}$$
$$= \{-\boldsymbol{\nabla} \nabla_0 \varphi_0 + \circledast \, \boldsymbol{\nabla} \times \boldsymbol{\nabla} \times \boldsymbol{\varphi} + \circledast \, \langle \boldsymbol{\nabla}, \boldsymbol{\nabla} \rangle \boldsymbol{\varphi}\} + \{\nabla_0 \nabla_0 \, \boldsymbol{\varphi} + \nabla_0 \boldsymbol{\nabla} \varphi_0\} - \circledast \, \boldsymbol{\nabla} \times \boldsymbol{\nabla} \times \boldsymbol{\varphi}$$
$$= (\nabla_0 \nabla_0 + \circledast \, \langle \boldsymbol{\nabla}, \boldsymbol{\nabla} \rangle) \boldsymbol{\varphi}$$

Equation (21) reveals why Maxwell based differential equations use the gauge $\varkappa$ rather than accept equation (4) as a genuine Maxwell equation.

$$\rho_0 = \circledast \langle \boldsymbol{\nabla}, \boldsymbol{\nabla} \rangle \varphi_0 = \zeta_0 - \nabla_0 \nabla_0 \varphi_0 \tag{23}$$

$$\boldsymbol{\rho} = \circledast \langle \boldsymbol{\nabla}, \boldsymbol{\nabla} \rangle \boldsymbol{\varphi} = \boldsymbol{\zeta} - \nabla_0 \boldsymbol{\nabla_0} \boldsymbol{\varphi} \tag{24}$$

Thus a simple change of a parameter and the control switch $\circledast$ turn quaternionic differential equations into equivalent Maxwell differential equations and vice versa. This makes clear that both sets represent two different views from the same subject, which is a field that can be stored in the eigenspace of an operator that resides in the Gelfand triple.

Still the comparison shows an anomaly in equation (21) that represents a significant difference between the two sets of differential equations that goes beyond the difference between the parameter spaces. A possible clue will be given in the section on the Dirac equation. This clue comes down to the conclusion that the Maxwell based equations do not lead via the coupling of two first order quaternionic partial differential equations to a regular second order partial quaternionic differential equation, but instead the wave equation represents a coupling between two solutions of different first order biquaternionic differential equations that use different parameter spaces. In the Dirac equation these solutions represent either particle behavior or antiparticle behavior.

5   Genuine Maxwell wave equations

The scalar part of the genuine Maxwell based differential equals zero. This is oppressed by the Lorenz gauge.

The genuine Maxwell differential equations deliver different inhomogeneous wave equations:

$$\mathfrak{E} \stackrel{\text{def}}{=} -\nabla_0 \varphi - \nabla \varphi_0 \tag{1}$$

$$\mathfrak{B} \stackrel{\text{def}}{=} \nabla \times \boldsymbol{\varphi} \tag{2}$$

The following definitions follow from the definitions of $\mathfrak{E}$ and $\mathfrak{B}$.

$$\nabla_0 \mathfrak{E} \stackrel{\text{def}}{=} -\nabla_0 \nabla_0 \, \boldsymbol{\varphi} - \nabla_0 \nabla \varphi_0 \tag{3}$$

$$\langle \nabla, \mathfrak{E} \rangle \stackrel{\text{def}}{=} -\nabla_0 \langle \nabla, \boldsymbol{\varphi} \rangle - \langle \nabla, \nabla \rangle \varphi_0 \tag{4}$$

$$\nabla_0 \mathfrak{B} \stackrel{\text{def}}{=} -\nabla \times \mathfrak{E} \tag{5}$$

$$\langle \nabla, \mathfrak{B} \rangle \stackrel{\text{def}}{=} \mathbf{0} \tag{6}$$

$$\nabla \times \mathfrak{B} \stackrel{\text{def}}{=} \nabla \langle \nabla, \boldsymbol{\varphi} \rangle - \langle \nabla, \nabla \rangle \boldsymbol{\varphi} \tag{7}$$

The Lorenz gauge means:

$$\nabla_0 \boldsymbol{\varphi_0} + \langle \nabla, \boldsymbol{\varphi} \rangle = 0 \tag{8}$$

The genuine Maxwell based wave equations are:

$$(\nabla_0 \nabla_0 - \langle \nabla, \nabla \rangle) \varphi_0 = \rho_0 = \langle \nabla, \mathfrak{E} \rangle \tag{9}$$

$$(\nabla_0 \nabla_0 - \langle \nabla, \nabla \rangle) \boldsymbol{\varphi} = J = \nabla \times \mathfrak{B} - \nabla_0 \mathfrak{E} \tag{10}$$

6   Dirac equation

6.1   The Dirac equation in original format

In its original form the Dirac equation is a complex equation that uses spinors, matrices and partial derivatives.

Instead of the usual $\left\{ \frac{\partial f}{\partial t}, i\frac{\partial f}{\partial x}, j\frac{\partial f}{\partial y}, k\frac{\partial f}{\partial z} \right\}$ we want to use operators $\nabla = \{\nabla_0, \boldsymbol{\nabla}\}$

The subscript $_0$ indicates the scalar part. Bold face indicates the vector part.

The operator ∇ relates to the applied parameter space. This means that the parameter space is also configured of combinations $x = \{x_0, \boldsymbol{x}\}$ of a scalar x_0 and a vector $\boldsymbol{x}$. Also the functions $f = \{f_0, \boldsymbol{f}\}$ can be split in scalar functions f_0 and vector functions $\boldsymbol{f}$.

The local parameter $t = x_0$ represents the scalar part of the applied parameter space.

Dirac was searching for a split of the Klein-Gordon equation into two first order differential equations.

$$\frac{\partial^2 f}{\partial t^2} - \frac{\partial^2 f}{\partial x^2} - \frac{\partial^2 f}{\partial y^2} - \frac{\partial^2 f}{\partial z^2} = -m^2 f \tag{1}$$

$$(\nabla_0 \nabla_0 - \langle \boldsymbol{\nabla}, \boldsymbol{\nabla} \rangle) f = \mathfrak{D} f = -m^2 f \tag{2}$$

Here $\mathfrak{D} = \nabla_0 \nabla_0 - \langle \boldsymbol{\nabla}, \boldsymbol{\nabla} \rangle$ is the d'Alembert operator.

Dirac used a combination of matrices and spinors in order to reach this result. He applied the Pauli matrices in order to simulate the behavior of vector functions under differentiation.

The unity matrix I and the Pauli matrices $\sigma_1, \sigma_2, \sigma_3$ are given by [15]:

$$I = \begin{bmatrix} 1 & 0 \\ 0 & 1 \end{bmatrix}, \quad \sigma_1 = \begin{bmatrix} 0 & 1 \\ 1 & 0 \end{bmatrix}, \quad \sigma_2 = \begin{bmatrix} 0 & -\mathfrak{i} \\ \mathfrak{i} & 0 \end{bmatrix}, \quad \sigma_3 = \begin{bmatrix} 1 & 0 \\ 0 & -1 \end{bmatrix} \tag{3}$$

For one of the potential orderings of the quaternionic number system, the Pauli matrices together with the unity matrix I relate to the quaternionic base vectors 1, $\boldsymbol{i}, \boldsymbol{j}$ and $\boldsymbol{k}$

$$1 \mapsto I, \quad \boldsymbol{i} \mapsto \mathfrak{i}\,\sigma_1, \quad \boldsymbol{j} \mapsto \mathfrak{i}\,\sigma_2, \quad \boldsymbol{k} \mapsto \mathfrak{i}\,\sigma_3 \tag{4}$$

$$\sigma_1 \sigma_2 - \sigma_2 \sigma_1 = 2\,\mathfrak{i}\,\sigma_3; \ \sigma_2 \sigma_3 - \sigma_3 \sigma_2 = 2\,\mathfrak{i}\,\sigma_1; \ \sigma_3 \sigma_1 - \sigma_1 \sigma_3 = 2\,\mathfrak{i}\,\sigma_2 \tag{5}$$

$$\sigma_1 \sigma_1 = \sigma_2 \sigma_2 = \sigma_3 \sigma_3 = I \tag{6}$$

The different ordering possibilities of the quaternionic number system correspond to different symmetry flavors. Half of these possibilities offer a right handed external vector product. The other half offer a left handed external vector product.

We will regularly use:

$$\langle \text{i\!i} \, \boldsymbol{\sigma}, \boldsymbol{\nabla} \rangle = \boldsymbol{\nabla} \, ; \text{i\!i} = \sqrt{-1} \tag{7}$$

With

$$p_\mu = -\text{i\!i} \, \nabla_\mu \tag{8}$$

follow

$$p_\mu \sigma_\mu = -\text{i\!i} \, e_\mu \nabla_\mu \tag{9}$$

$$\langle \boldsymbol{\sigma}, \boldsymbol{p} \rangle \leftrightarrow \text{i\!i} \, \boldsymbol{\nabla} \tag{10}$$

6.2   Dirac's approach

The original Dirac equation uses 4x4 matrices $\boldsymbol{\alpha}$ and β. [7]:

$\boldsymbol{\alpha}$ and β *are* matrices that implement the quaternion arithmetic behavior including the possible symmetry flavors of quaternionic number systems and continuums.

$$\alpha_\mu = \begin{bmatrix} 0 & \sigma_\mu \\ \sigma_\mu & 0 \end{bmatrix} \tag{1}$$

$$\beta = \begin{bmatrix} 1 & 0 \\ 0 & -1 \end{bmatrix} \tag{2}$$

$$\beta\beta = I \tag{3}$$

133

The interpretation of the Pauli matrices as representation of a special kind of angular momentum has led to the half integer eigenvalue of the corresponding spin operator.

Dirac's selection leads to

$$(p_0 - \langle \boldsymbol{\alpha}, \boldsymbol{p} \rangle - \beta mc)\{\varphi\} = 0 \tag{4}$$

$\{\varphi\}$ is a four component spinor.

Which splits into

$$(p_0 - \langle \boldsymbol{\sigma}, \boldsymbol{p} \rangle - mc)\varphi_A = 0 \tag{5}$$

and

$$(p_0 - \langle \boldsymbol{\sigma}, \boldsymbol{p} \rangle + mc)\varphi_B = 0 \tag{6}$$

φ_A and φ_B are spinor components. Thus the original Dirac equation splits into:

$$(\nabla_0 - \boldsymbol{\nabla} - \mathbb{i} \, mc)\varphi_A = 0 \tag{7}$$

$$(\nabla_0 - \boldsymbol{\nabla} + \mathbb{i} \, mc)\varphi_B = 0 \tag{8}$$

This split does not lead easily to a second order partial differential equation that looks like the Klein Gordon equation.

6.3   Relativistic formulation

Instead of Dirac's original formulation, usually the relativistic formulation is used [16].

That formulation applies gamma matrices, instead of the alpha and beta matrices. This different choice influences the form of the equations that result for the two spinor components.

$$\gamma_\mu = \beta \, \alpha_\mu = \begin{bmatrix} 0 & \sigma_1 \\ -\sigma_\mu & 0 \end{bmatrix}; \mu = 1,2,3 \tag{1}$$

$$\tag{2}$$

$$\gamma_0 = \beta = \begin{bmatrix} 1 & 0 \\ 0 & -1 \end{bmatrix}$$

$$\gamma_5 = i_0 \gamma_0 \gamma_1 \gamma_2 \gamma_3 = \begin{bmatrix} 0 & 1 \\ 1 & 0 \end{bmatrix} \tag{3}$$

The matrix γ_5 anti-commutes with all other gamma matrices.

Several different sets of gamma matrices are possible. The choice above leads to a "Dirac equation" of the form

$$\left(i\, \gamma^\mu \nabla_\mu - mc \right)\varphi = 0 \tag{7}$$

More extended:

$$\left(\gamma_0 \frac{\partial}{\partial t} + \langle \boldsymbol{\gamma}, \boldsymbol{\nabla} \rangle - \frac{m}{i\, \hbar} \right) \{\psi\} = 0 \tag{8}$$

$$\left(\begin{bmatrix} 1 & 0 \\ 0 & -1 \end{bmatrix} \frac{\partial}{\partial t} + \begin{bmatrix} 0 & \langle \boldsymbol{\sigma}, \boldsymbol{\nabla} \rangle \\ -\langle \boldsymbol{\sigma}, \boldsymbol{\nabla} \rangle & 0 \end{bmatrix} - \frac{m}{i\, \hbar} \begin{bmatrix} 1 & 0 \\ 0 & 1 \end{bmatrix} \right) \begin{bmatrix} \varphi_A \\ \varphi_B \end{bmatrix} = 0 \tag{9}$$

$$\left(i \begin{bmatrix} 1 & 0 \\ 0 & -1 \end{bmatrix} \frac{\partial}{\partial t} + \begin{bmatrix} 0 & \boldsymbol{\nabla} \\ -\boldsymbol{\nabla} & 0 \end{bmatrix} - \frac{m}{\hbar} \begin{bmatrix} 1 & 0 \\ 0 & 1 \end{bmatrix} \right) \begin{bmatrix} \varphi_A \\ \varphi_B \end{bmatrix} = 0 \tag{10}$$

$$i\, \frac{\partial}{\partial t} \varphi_A + \boldsymbol{\nabla} \varphi_B - \frac{m}{i\, \hbar} \varphi_A = 0 \tag{11}$$

$$-i\, \frac{\partial}{\partial t} \varphi_B - \boldsymbol{\nabla} \varphi_A - \frac{m}{i\, \hbar} \varphi_B = 0 \tag{12}$$

Also this split does not easily lead to a second order partial differential equation that looks like the Klein Gordon equation.

6.4   A better choice
Another interpretation of the Dirac approach replaces γ_0 with γ_5 [17]:

$$\left(\gamma_5 \frac{\partial}{\partial t} - \gamma_1 \frac{\partial}{\partial x} - \gamma_2 \frac{\partial}{\partial y} - \gamma_3 \frac{\partial}{\partial z} - \frac{m}{i\, \hbar} \right) \{\psi\} = 0 \tag{1}$$

$$\tag{2}$$

$$\left(\gamma_5 \frac{\partial}{\partial t} - \langle \boldsymbol{\gamma}, \boldsymbol{\nabla} \rangle - \frac{m}{\text{î}\,\hbar}\right)\{\psi\} = 0$$

$$\left(\begin{bmatrix} 0 & 1 \\ 1 & 0 \end{bmatrix}\frac{\partial}{\partial t} - \begin{bmatrix} 0 & \langle \boldsymbol{\sigma}, \boldsymbol{\nabla} \rangle \\ -\langle \boldsymbol{\sigma}, \boldsymbol{\nabla} \rangle & 0 \end{bmatrix} - \frac{m}{\text{î}\,\hbar}\begin{bmatrix} 1 & 0 \\ 0 & 1 \end{bmatrix}\right)\begin{bmatrix} \psi_A \\ \psi_B \end{bmatrix} = 0 \tag{3}$$

This invites splitting of the four component spinor equation into two equations for the two components ψ_A and ψ_B of the spinor:

$$\text{î}\,\nabla_0 \psi_A + \text{î}\,\langle \boldsymbol{\sigma}, \boldsymbol{\nabla} \rangle \psi_A = \frac{m}{\hbar}\,\psi_B \tag{4}$$

$$\text{î}\,\nabla_0 \varphi_B - \text{î}\,\langle \boldsymbol{\sigma}, \boldsymbol{\nabla} \rangle \psi_B = \frac{m}{\hbar}\,\psi_A \tag{5}$$

$$(\text{î}\,\nabla_0 + \boldsymbol{\nabla})\psi_A = \frac{m}{\hbar}\,\psi_B \tag{6}$$

$$(\text{î}\,\nabla_0 - \boldsymbol{\nabla})\psi_B = \frac{m}{\hbar}\,\psi_A \tag{7}$$

This looks far more promising. We can insert the right part of the first equation into the left part of the second equation.

$$(\text{î}\,\nabla_0 - \boldsymbol{\nabla})(\text{î}\,\nabla_0 + \boldsymbol{\nabla})\psi_A = (-\nabla_0\nabla_0 - \boldsymbol{\nabla}\boldsymbol{\nabla})\psi_A = (\langle \boldsymbol{\nabla}, \boldsymbol{\nabla} \rangle - \nabla_0\nabla_0)\psi_A \tag{8}$$

$$= \frac{m}{\hbar}(\text{î}\,\nabla_0 - \boldsymbol{\nabla})\,\psi_B = \frac{m^2}{\hbar^2}\,\psi_A$$

$$(\langle \boldsymbol{\nabla}, \boldsymbol{\nabla} \rangle - \nabla_0\nabla_0)\psi_A = \frac{m^2}{\hbar^2}\,\psi_A \tag{9}$$

$$(\text{î}\,\nabla_0 + \boldsymbol{\nabla})(\text{î}\,\nabla_0 - \boldsymbol{\nabla})\psi_B = (-\nabla_0\nabla_0 - \boldsymbol{\nabla}\boldsymbol{\nabla})\psi_B = (\langle \boldsymbol{\nabla}, \boldsymbol{\nabla} \rangle - \nabla_0\nabla_0)\psi_B \tag{10}$$

$$= \frac{m}{\hbar}(\text{î}\,\nabla_0 + \boldsymbol{\nabla})\,\psi_A = \frac{m^2}{\hbar^2}\,\psi_B$$

$$\left(\langle \boldsymbol{\nabla}, \boldsymbol{\nabla} \rangle - \nabla_0 \nabla_0 \right) \psi_B = \frac{m^2}{\hbar^2}\, \psi_B \tag{11}$$

This is what Dirac wanted to achieve. The two first order differential equations couple into a second order differential equation that is equivalent to a Klein Gordon equation. The homogeneous version of this second order partial differential equation is a wave equation and offers solutions that are waves.

The nabla operator acts differently onto the two component spinors ψ_A and ψ_B.

6.5   The quaternionic nabla and the Dirac nabla

The modified Pauli matrices together with a 2×2 identity matrix implement the equivalent of a quaternionic number system with a selected symmetry flavor.

$$I = \begin{bmatrix} 1 & 0 \\ 0 & 1 \end{bmatrix}; \; \mathring{\mathbb{i}}\,\sigma_1 = \begin{bmatrix} 0 & \mathring{\mathbb{i}} \\ \mathring{\mathbb{i}} & 0 \end{bmatrix}; \; \mathring{\mathbb{i}}\,\sigma_2 = \begin{bmatrix} 0 & 1 \\ -1 & 0 \end{bmatrix}; \; \mathring{\mathbb{i}}\,\sigma_3 = \begin{bmatrix} \mathring{\mathbb{i}} & 0 \\ 0 & -\mathring{\mathbb{i}} \end{bmatrix} \tag{1}$$

The modified Pauli matrices together with the I_0 matrix implements another structure, which is not a version of a quaternionic number system.

$$I_0 = \begin{bmatrix} \mathring{\mathbb{i}} & 0 \\ 0 & \mathring{\mathbb{i}} \end{bmatrix}; \; \mathring{\mathbb{i}}\,\sigma_1 = \begin{bmatrix} 0 & \mathring{\mathbb{i}} \\ \mathring{\mathbb{i}} & 0 \end{bmatrix}; \; \mathring{\mathbb{i}}\,\sigma_2 = \begin{bmatrix} 0 & 1 \\ -1 & 0 \end{bmatrix}; \; \mathring{\mathbb{i}}\,\sigma_3 = \begin{bmatrix} \mathring{\mathbb{i}} & 0 \\ 0 & -\mathring{\mathbb{i}} \end{bmatrix} \tag{2}$$

Both the quaternionic nabla and the Dirac nabla implement a way to let these differential operators act as multipliers.

The quaternionic nabla is defined as

$$\nabla = \nabla_0 + \boldsymbol{\nabla} = e^\mu \nabla_\mu = \nabla_0 + \mathring{\mathbb{i}}\,\langle \boldsymbol{\sigma}, \boldsymbol{\nabla} \rangle \tag{3}$$

$$\nabla^* = \nabla_0 - \boldsymbol{\nabla} \tag{4}$$

For scalar functions and for vector functions hold:

$$\nabla^* \nabla = \nabla \nabla^* = \nabla_0 \nabla_0 + \langle \boldsymbol{\nabla}, \boldsymbol{\nabla} \rangle \tag{5}$$

The Dirac nabla is defined as

$$\mathcal{D} = \mathring{\mathbb{1}}\,\nabla_0 + \boldsymbol{\nabla} = \mathring{\mathbb{1}}\,\nabla_0 + \mathring{\mathbb{1}}\,\langle \boldsymbol{\sigma}, \boldsymbol{\nabla}\rangle \tag{6}$$

$$\mathcal{D}^* = \mathring{\mathbb{1}}\,\nabla_0 - \boldsymbol{\nabla} \tag{7)}$$

$$\mathcal{D}^*\mathcal{D} = \mathcal{D}\,\mathcal{D}^* = -\nabla_0\nabla_0 + \langle \boldsymbol{\nabla}, \boldsymbol{\nabla}\rangle \tag{8}$$

6.5.1 Prove

We use

$$\nabla_0 \boldsymbol{\nabla} f_0 = \boldsymbol{\nabla}\nabla_0 f_0 \tag{1}$$

$$\nabla_0 \boldsymbol{\nabla} \boldsymbol{f} = \boldsymbol{\nabla}\nabla_0 \boldsymbol{f} = -\nabla_0 \langle \boldsymbol{\nabla}, \boldsymbol{f}\rangle + \nabla_0 \boldsymbol{\nabla} \times \boldsymbol{f} \tag{2}$$

$$\boldsymbol{\nabla}\boldsymbol{\nabla} f_0 = -\langle \boldsymbol{\nabla}, \boldsymbol{\nabla}\rangle f_0 + \boldsymbol{\nabla} \times \boldsymbol{\nabla} f_0 = -\langle \boldsymbol{\nabla}, \boldsymbol{\nabla}\rangle f_0 \tag{3}$$

$$\boldsymbol{\nabla}(\boldsymbol{\nabla} \boldsymbol{f}) = -\boldsymbol{\nabla}\langle \boldsymbol{\nabla}, \boldsymbol{f}\rangle + \boldsymbol{\nabla} \times \boldsymbol{\nabla} \times \boldsymbol{f} = -\langle \boldsymbol{\nabla}, \boldsymbol{\nabla}\rangle \boldsymbol{f} = (\boldsymbol{\nabla}\boldsymbol{\nabla})\boldsymbol{f} \tag{4}$$

$$\boldsymbol{\nabla} \times \boldsymbol{\nabla} \times \boldsymbol{f} = \boldsymbol{\nabla}\langle \boldsymbol{\nabla}, \boldsymbol{f}\rangle - \langle \boldsymbol{\nabla}, \boldsymbol{\nabla}\rangle \boldsymbol{f} \tag{5}$$

$$\langle \boldsymbol{\nabla}, \boldsymbol{\nabla} \times \boldsymbol{f}\rangle = 0 \tag{6}$$

$$\boldsymbol{\nabla} \times \boldsymbol{\nabla} f_0 = \boldsymbol{0} \tag{7}$$

This results in

$$(\alpha\nabla_0 + \boldsymbol{\nabla})f_0 = \alpha\nabla_0 f_0 + \boldsymbol{\nabla} f_0 \tag{8}$$

$$(\alpha\nabla_0 - \boldsymbol{\nabla})(\alpha\nabla_0 + \boldsymbol{\nabla})f_0 \tag{9}$$

$$= \alpha^2 \nabla_0\nabla_0 + \alpha\nabla_0\boldsymbol{\nabla} f_0 - \alpha\boldsymbol{\nabla}\nabla_0 f_0 + \langle \boldsymbol{\nabla}, \boldsymbol{\nabla}\rangle f_0 - \boldsymbol{\nabla} \times \boldsymbol{\nabla} f_0$$

$$= \alpha^2 \nabla_0\nabla_0 + \langle \boldsymbol{\nabla}, \boldsymbol{\nabla}\rangle f_0$$

$$(\alpha \nabla_0 + \boldsymbol{\nabla})\boldsymbol{f} = \alpha \nabla_0 \boldsymbol{f} - \langle \boldsymbol{\nabla}, \boldsymbol{f} \rangle + \boldsymbol{\nabla} \times \boldsymbol{f} \tag{10}$$

$$(\alpha \nabla_0 - \alpha \nabla_0 \boldsymbol{f} - \langle \boldsymbol{\nabla}, \boldsymbol{f} \rangle + \boldsymbol{\nabla} \times \boldsymbol{f})(\alpha \nabla_0 + \boldsymbol{\nabla})\boldsymbol{f}$$

$$(\alpha \nabla_0 - \boldsymbol{\nabla})(\alpha \nabla_0 + \boldsymbol{\nabla})f_0 \tag{11}$$

$$= \alpha^2 \nabla_0 \nabla_0 \boldsymbol{f} - \alpha \nabla_0 \langle \boldsymbol{\nabla}, \boldsymbol{f} \rangle + \alpha \nabla_0 \boldsymbol{\nabla} \times \boldsymbol{f} + \alpha \nabla_0 \langle \boldsymbol{\nabla}, \boldsymbol{f} \rangle$$

$$- \alpha \nabla_0 \boldsymbol{\nabla} \times \boldsymbol{f} + \boldsymbol{\nabla} \langle \boldsymbol{\nabla}, \boldsymbol{f} \rangle + \langle \boldsymbol{\nabla}, \boldsymbol{\nabla} \times \boldsymbol{f} \rangle - \boldsymbol{\nabla} \times \boldsymbol{\nabla} \times \boldsymbol{f}$$

$$= \alpha^2 \nabla_0 \nabla_0 \boldsymbol{f} + \langle \boldsymbol{\nabla}, \boldsymbol{\nabla} \rangle \boldsymbol{f}$$

6.5.2   Discussion

For $\alpha = 1$ the equations

$$(\nabla^* \nabla \, f_0 = \nabla \nabla^* \, f_0 = \nabla_0 \nabla_0 + \langle \boldsymbol{\nabla}, \boldsymbol{\nabla} \rangle) \, f_0 \tag{1}$$

$$(\nabla^* \nabla \, \boldsymbol{f} = \nabla \nabla^* \, \boldsymbol{f} = \nabla_0 \nabla_0 + \langle \boldsymbol{\nabla}, \boldsymbol{\nabla} \rangle) \, \boldsymbol{f} \tag{2}$$

work for both parts of a quaternionic function $f = f_0 + \boldsymbol{f}$.

For $\alpha = ⅈ$ the equations

$$(\mathcal{D}^* \mathcal{D} \, f_0 = \mathcal{D} \mathcal{D}^* \, f_0 = -\nabla_0 \nabla_0 + \langle \boldsymbol{\nabla}, \boldsymbol{\nabla} \rangle) \, f_0 \tag{3}$$

$$(\mathcal{D}^* \mathcal{D} \, \boldsymbol{f} = \mathcal{D} \mathcal{D}^* \boldsymbol{f} = -\nabla_0 \nabla_0 + \langle \boldsymbol{\nabla}, \boldsymbol{\nabla} \rangle) \, \boldsymbol{f} \tag{4}$$

work separately for scalar function f_0.and vector function $\boldsymbol{f}$. The right sides of the equations work for quaternionic functions. Thus

$$(g = \mathcal{D}f = -\nabla_0 \nabla_0 + \langle \boldsymbol{\nabla}, \boldsymbol{\nabla} \rangle) \, f \tag{5}$$

is a valid equation for quaternionic functions f and g.

Thus the d'Alembert operator $\mathfrak{D} = -\nabla_0 \nabla_0 + \langle \boldsymbol{\nabla}, \boldsymbol{\nabla} \rangle$ is a valid quaternionic operator.

The nabla operators reflects the structure of the parameter space of the functions on which they work. Thus the quaternionic nabla operator reflects a quaternionic number system. The Dirac nabla operator reflects the structure of the parameters of the two component spinors that figure in the modified Dirac equation.

Between the two spinor components ψ_A and ψ_B, the scalar part of the parameter space appears to change sign with respect to the vector part.

Applied to a quaternionic function, the quaternionic nabla results again in a ***quaternionic*** function.

$$\phi = \phi_0 + \boldsymbol{\phi} = (\nabla_0 + \boldsymbol{\nabla})(f_0 + \boldsymbol{f}) = \nabla_0 f_0 - \langle \boldsymbol{\nabla}, \boldsymbol{f} \rangle + \boldsymbol{\nabla} f_0 + \nabla_0 \boldsymbol{f} + \boldsymbol{\nabla} \times \boldsymbol{f} \qquad (6)$$

Applied to a quaternionic function, the Dirac nabla results in a ***biquaternionic*** function.

$$(\mathbb{i}\,\nabla_0 + \boldsymbol{\nabla})(f_0 + \boldsymbol{f}) = \nabla_0\,\mathbb{i}\,f_0 - \langle \boldsymbol{\nabla}, \boldsymbol{f} \rangle + \boldsymbol{\nabla} f_0 + \mathbb{i}\,\nabla_0 \boldsymbol{f} + \boldsymbol{\nabla} \times \boldsymbol{f} \qquad (7)$$

Neither the Dirac nabla $\mathcal{D}$ nor its conjugate $\mathcal{D}^*$ delivers quaternionic functions from quaternionic functions. They are not proper quaternionic operators.

Thus, the d'Alembert operator cannot be split into two operators that map quaternionic functions onto quaternionic functions.

In contrast the operators $\nabla^*\nabla$, ∇ and ∇^* are all three proper quaternionic operators.

6.6   Quaternionic format of Dirac equation

The initial goal of Dirac was to split the Klein Gordon equation into two first order differential equations. He tried to achieve this via the combination of matrices and spinors. This leads to a result that does not lead to an actual second order differential equation, but instead it leads to two different first order differential equations for two different spinors that can be coupled into a second order partial differential equation that looks like a Klein Gordon equation. The homogeneous version of the Klein Gordon equation is a wave equation. However, that equation misses an essential right part of the Klein-Gordon equation.

Quaternionic differential calculus supports first order differential equations that in a natural way lead to a second order partial differential equation that differs significantly from a wave equation.

The closest quaternionic equivalents of the first order Dirac equations for the electron and the positron are:

$$\nabla \psi = (\nabla_0 + \mathbf{V})(\psi_0 + \boldsymbol{\psi}) = m\varphi \tag{1}$$

$$\nabla^* \varphi = (\nabla_0 - \mathbf{V})(\varphi_0 + \boldsymbol{\varphi}) = m\psi \tag{2}$$

$$\nabla^* \nabla \psi = (\nabla_0 - \mathbf{V})(\nabla_0 + \mathbf{V})(\psi_0 + \boldsymbol{\psi}) = m^2\psi \tag{3}$$

$$\nabla^* \nabla \psi = \nabla^* \nabla \psi = (\nabla_0 \nabla_0 + \langle \mathbf{V}, \mathbf{V} \rangle)\, \psi = m^2\psi \tag{4}$$

$$\nabla \nabla^* \varphi = \nabla^* \nabla \varphi = (\nabla_0 \nabla_0 + \langle \mathbf{V}, \mathbf{V} \rangle)\, \varphi = m^2\varphi \tag{5}$$

A similar equation exists for spherical coordinates.

These second order equations are not wave equations. Their set of solutions does not include waves.

6.7 Interpretation of the Dirac equation

The original Dirac equation can be split into two equations. One of them describes the behavior of the electron. The other equation describes the behavior of the positron.

The positron is the anti-particle of the electron. These particles feature the same rest mass, but other characteristics such as their electric charge differ in sign. The positron can be interpreted as an electron that moves back in time. Sometimes the electron is interpreted as a hole in a sea of positrons. These interpretations indicate that the functions that describe these particles feature different parameter spaces that differ in the sign of the scalar part.

6.7.1 Particle fields

The fields that characterize different types of particles can be related to parameter spaces that belong to different versions of the quaternionic number system. These fields are coupled to an embedding field on which the particles and their private parameter spaces float.

The reverse bra-ket method shows how fields can on the one hand be coupled to eigenspaces and eigenvectors of operators which reside in quaternionic non-separable Hilbert spaces and on the other hand can be coupled to pairs of parameter spaces and quaternionic functions. Quaternionic functions can be split into scalar functions and vector functions. In a quaternionic Hilbert space several different natural parameter spaces can coexist. Natural parameter spaces are formed by versions of the quaternionic number system. These versions differ in the way that these number systems are ordered.

The original Dirac equations might represent this coupling between the particle field and the embedding field.

6.8   Alternatives

6.8.1   Minkowski parameter space

In quaternionic differential calculus the local quaternionic distance can represent a scalar that is independent of the direction of progression. It corresponds to the notion of coordinate time t. This means that a small coordinate time step Δt equals the sum of a small proper time step $\Delta \tau$ and a small pure space step $\Delta \boldsymbol{x}$. In quaternionic format the step $\Delta \tau$ is a real number. The space step $\Delta \boldsymbol{x}$ is an imaginary quaternionic number. The original Dirac equation does not pay attention to the difference between coordinate time and proper time, but the quaternionic presentation of these equations show that a progression independent scalar can be useful as the scalar part of the parameter space. This holds especially for solutions of the homogeneous wave equation.

In this way coordinate time is a function of proper time τ and distance in pure space $|\Delta \boldsymbol{x}|$.

$$|\Delta t|^2 = |\Delta \tau|^2 + |\Delta \boldsymbol{x}|^2$$

Together t and $\boldsymbol{x}$ deliver a spacetime model that has a Minkowski signature.

$$|\Delta \tau|^2 = |\Delta t|^2 - |\Delta \boldsymbol{x}|^2$$

6.8.2   Other natural parameter spaces

The Dirac equation in quaternionic format treats a coupling of parameter spaces that are each other's quaternionic conjugate. The β matrix implements isotropic conjugation. An adapted conjugation matrix can apply anisotropic conjugation. This concerns conjugations in which only one or two dimensions get a reverse ordering. In that case the equations handle the dynamic behavior of anisotropic particles such as quarks. Quarks correspond to solutions that have anisotropic parameter spaces. Also for these quarks exist advanced particle solutions and retarded antiparticle solutions.

7 Lorentz transformation

Differences between positions in subsequent members of the sequence of static status quos of the Hilbert Book Model can be interpreted as displacements. The displacement is a coordinate transformation. For the properties of this transformation it does not matter where the displacement starts or in which direction it is taken.

In order to simplify the description we will use the name **Hilbert Book page** or **sheet** for a static status quo of the Hilbert Book model.

The same holds for displacements that concern sequence members that are located further apart. The corresponding displacements form a group. The displacement is a function of both the position and the sequence number. The displacement $z, t \to z', t'$ can be interpreted as a coordinate transformation and can be described by a matrix. Here t is coordinate time.

$$\begin{bmatrix} t' \\ z' \end{bmatrix} = \begin{bmatrix} \gamma & \delta \\ \beta & \alpha \end{bmatrix} \begin{bmatrix} t \\ z \end{bmatrix} \tag{1}$$

The matrix elements are interrelated. When the displacement concerns a uniform movement, the interrelations of the matrix elements become a function of the speed v. Here v is the speed measured as displacement per progression interval. The group properties together with the isomorphism of space fix the interrelations.

$$\begin{bmatrix} t' \\ z' \end{bmatrix} = 1/\sqrt{1 + kv^2} \begin{bmatrix} 1 & kv \\ -v & 1 \end{bmatrix} \begin{bmatrix} t \\ z \end{bmatrix} \tag{2}$$

If k is positive, then there may be transformations with $kv^2 \gg 1$ which transform progression into a spatial coordinate and vice versa. This is considered to be unphysical. The Hilbert book model also supports that vision.

The condition $k = 0$ corresponds to a Galilean transformation

$$\begin{bmatrix} t' \\ z' \end{bmatrix} = \begin{bmatrix} 1 & 0 \\ -v & 1 \end{bmatrix} \begin{bmatrix} t \\ z \end{bmatrix} \tag{3}$$

The condition $k < 0$ corresponds to a Lorentz transformation. We can set $kc^2 = -1$, where c is an invariant speed that corresponds to the maximum of v.

$$\begin{bmatrix} t' \\ z' \end{bmatrix} = 1/\sqrt{1 - v^2/c^2} \begin{bmatrix} 1 & -v/c^2 \\ -v & 1 \end{bmatrix} \begin{bmatrix} t \\ z \end{bmatrix} \tag{4}$$

The Lorentz transformation corresponds with the situation in which a maximum speed occurs.

Since in each progression step photons step with a non-zero space step and both step sizes are fixed, the speed of the photon at quantum scale is fixed. No other particle goes faster, so in the model a maximum speed occurs. With other words when sequence members at different sequence number are compared, then the corresponding displacements can be described by Lorentz transformations.

Lorentz transformations introduce the phenomena that go together with relativity, such as *length contraction*, *time dilatation* and *relativity of simultaneity* that occur when two *inertial reference frames* are considered.

$$\Delta t_c = \left(\Delta t_p - \Delta z_p \, v/c^2\right)/\sqrt{1 - v^2/c^2} \tag{5}$$

$$(\Delta t_c)^2(1 - v^2/c^2) = \left(\Delta t_p - \Delta z_p \, v/c^2\right)^2$$

The term $\Delta z_p \, v/c^2$ introduces time dilatation. If $\Delta t_p = 0$ then depending on v and Δz_p the time difference Δt_c is non-zero.

Progression, interpreted as proper time, is a Lorentz invariant scalar. As a consequence the quaternionic first order partial differential equations are Lorentz covariant. The same holds for the quaternionic second order partial differential equations.

8 Tensor differential calculus

We restrict to 3+1 D parameter spaces.

Parameter spaces can differ in the way they are ordered and in the way the scalar part relates to the spatial part.

Fields are functions that have values, which are independent of the selected parameter space. Fields exist in scalar fields, vector fields and combined scalar and vector fields.

Combined fields exist as continuum eigenspaces of normal operators that reside in quaternionic non-separable Hilbert spaces. These combined fields can be represented by quaternionic functions of quaternionic parameter spaces. However, the same field can also be interpreted as the eigenspaces of the Hermitian and anti-Hermitian parts of the normal operator. The quaternionic parameter space can be represented by a normal quaternionic reference operator that features a flat continuum eigenspace. This reference operator can be split in a Hermitian and an anti-Hermitian part.

The eigenspace of a normal quaternionic number system corresponds to a quaternionic number system. Due to the four dimensions of quaternions, the quaternionic number systems exist in 16 versions that differ in their Cartesian ordering. If spherical ordering is pursued, then for each Cartesian start orderings two extra orderings are possible. All these choices correspond to different parameter spaces.

Further it is possible to select a scalar part of the parameter space that is a scalar function of the quaternionic scalar part and the quaternionic vector part. For example it is possible to use quaternionic distance as the scalar part of the new parameter space.

Tensor differential calculus relates components of differentials with corresponding parameter spaces.

Components of differentials are terms of the corresponding differential equation. These terms can be split in scalar functions and in vector functions. Tensor differential calculus treats scalar functions different from vector functions.

Quaternionic fields are special because the differential operators of their defining functions can be treated as multipliers.

8.1 The metric tensor

The metric tensor determines the local "distance".

$$g_{\mu\nu} = \begin{bmatrix} g_{00} & g_{01} & g_{02} & g_{03} \\ g_{10} & g_{11} & g_{12} & g_{13} \\ g_{20} & g_{21} & g_{22} & g_{23} \\ g_{30} & g_{31} & g_{32} & g_{33} \end{bmatrix} \tag{1}$$

The consequences of coordinate transformations $dx^\nu \Rightarrow dX^\nu$ define the elements $g_{\mu\nu}$ as

$$g_{\mu\nu} = \frac{dX^\mu}{dx^\nu} \tag{2}$$

8.2 Geodesic equation

The geodesic equation describes the situation of a non-accelerated object. In terms of proper time this means:

$$\tag{1}$$

$$\frac{\partial^2 x^\mu}{\partial \tau^2} = -\Gamma^\mu_{\alpha\beta} \frac{dx^\alpha}{d\tau} \frac{dx^\beta}{d\tau}$$

In terms of coordinate time this means:

$$\frac{\partial^2 x^\mu}{\partial t^2} = -\Gamma^\mu_{\alpha\beta} \frac{dx^\alpha}{dt} \frac{dx^\beta}{dt} + \Gamma^0_{\alpha\beta} \frac{dx^\alpha}{dt} \frac{dx^\beta}{dt} \frac{dx^\mu}{dt} \tag{2}$$

8.2.1 Derivation:

We start with the double differential. Let us investigate a function X that has a parameter space existing of scalar τ and a three dimensional vector $\boldsymbol{x} = \{x^1, x^2, x^3\}$. The function X represents three dimensional curved space. The geodesic conditions are:

$$\frac{\partial^2 X^\lambda}{\partial \tau^2} = 0 \; ; \; \lambda = 1,2,3 \tag{1}$$

First we derive the first order differential.

$$dX^\lambda = \sum_{\beta=1}^3 \frac{\partial X^\lambda}{\partial x^\beta} dx^\beta \tag{2}$$

We can use the summation convention for subscripts and superscripts. This avoids the requirement for summation symbols.

$$\frac{dX^\lambda}{d\tau} = \frac{\partial X^\lambda}{\partial x^\beta} \frac{dx^\beta}{d\tau} \tag{3}$$

$$d^2 X^\lambda = \sum_{\beta=1}^3 \left(\frac{\partial X^\lambda}{\partial x^\beta} d^2 x^\beta + dx^\beta \sum_{\alpha=1}^3 \frac{\partial^2 X^\lambda}{\partial x^\beta \partial x^\alpha} dx^\alpha \right) \tag{4}$$

Now we obtained the double differential equation.

$$\frac{d^2 X^\lambda}{d\tau^2} = \frac{\partial X^\lambda}{\partial x^\beta} \frac{d^2 x^\beta}{d\tau^2} + \frac{\partial^2 X^\lambda}{\partial x^\beta \partial x^\alpha} \frac{dx^\alpha}{d\tau} \frac{dx^\beta}{d\tau} = 0 \tag{5}$$

The geodesic requirement results in:

$$\frac{\partial X^\lambda}{\partial x^\beta} \frac{d^2 x^\beta}{d\tau^2} = -\frac{\partial^2 X^\lambda}{\partial x^\beta \partial x^\alpha} \frac{dx^\alpha}{d\tau} \frac{dx^\beta}{d\tau} \tag{6}$$

If we use summation signs:

$$\sum_{\beta=1}^3 \frac{\partial X^\lambda}{\partial x^\beta} d^2 x^\beta = -\sum_{\beta=1}^3 \left(dx^\beta \sum_{\alpha=1}^3 \left(\frac{\partial^2 X^\lambda}{\partial x^\beta \partial x^\alpha} dx^\alpha \right) \right) \tag{7}$$

Next we multiply both sides with $\frac{\partial X^\lambda}{\partial x^\beta}$ and sum again:

$$\sum_{\lambda=1}^3 \left(\frac{\partial x^\lambda}{\partial X^\mu} \left(\sum_{\beta=1}^3 \frac{\partial X^\lambda}{\partial x^\beta} d^2 x^\beta \right) \right) = -\sum_{\lambda=1}^3 \left(\frac{\partial x^\lambda}{\partial X^\mu} \sum_{\beta=1}^3 \left(dx^\beta \sum_{\alpha=1}^3 \left(\frac{\partial^2 X^\lambda}{\partial x^\beta \partial x^\alpha} dx^\alpha \right) \right) \right) \tag{8}$$

We apply the fact:

$$\sum_{\lambda=1}^{3} \left(\frac{\partial x^\lambda}{\partial X^\mu} \frac{\partial X^\lambda}{\partial x^\beta} \right) = \delta_\beta^\mu \tag{9}$$

This results into:

$$d^2 x^\mu = \sum_{\lambda=1}^{3} \left(\frac{\partial x^\lambda}{\partial X^\mu} \sum_{\beta=1}^{3} \left(dx^\beta \sum_{\alpha=1}^{3} \left(\frac{\partial^2 X^\lambda}{\partial x^\beta \partial x^\alpha} dx^\alpha \right) \right) \right) = \Gamma_{\alpha\beta}^\mu dx^\alpha dx^\beta \tag{10}$$

Without summation signs:

$$\Gamma_{\alpha\beta}^\mu dx^\alpha dx^\beta \overset{\text{def}}{=} \left(\frac{\partial x^\mu}{\partial X^\lambda} \frac{\partial^2 X^\lambda}{\partial x^\alpha \partial x^\beta} \right) dx^\alpha dx^\beta \tag{11}$$

$$\frac{d^2 x^\mu}{d\tau^2} = -\Gamma_{\alpha\beta}^\mu \frac{dx^\beta}{d\tau} \frac{dx^\alpha}{d\tau} \tag{12}$$

$$\frac{d^2 x^\mu}{d\tau^2} = -\left(\frac{\partial x^\mu}{\partial X^\lambda} \frac{\partial^2 X^\lambda}{\partial x^\alpha \partial x^\beta} \right) \frac{dx^\beta}{d\tau} \frac{dx^\alpha}{d\tau} \tag{13}$$

$$\frac{d^2 x^\mu}{dt^2} = -\left(\frac{\partial x^\mu}{\partial X^\lambda} \frac{\partial^2 X^\lambda}{\partial x^\alpha \partial x^\beta} \right) \frac{dx^\beta}{dt} \frac{dx^\alpha}{dt} + \left(\frac{\partial x^0}{\partial X^\lambda} \frac{\partial^2 X^\lambda}{\partial x^\alpha \partial x^\beta} \right) \frac{dx^\beta}{dt} \frac{dx^\alpha}{dt} \frac{dx^\mu}{dt} \tag{14}$$

8.3   Toolbox

Coordinate transformations:

$$S_{\nu'\rho'}^{\mu'} = \frac{\partial x^{\mu'}}{\partial x^\mu} \frac{\partial x^\nu}{\partial x^{\nu'}} \frac{\partial x^\rho}{\partial x^{\rho'}} S_{\nu\rho}^\mu \tag{1}$$

The Christoffel symbol plays an important role:

$$2 g_{\alpha\delta} \Gamma_{\beta\alpha}^\delta = \frac{\partial g_{\alpha\beta}}{\partial x^\gamma} + \frac{\partial g_{\alpha\gamma}}{\partial x^\beta} + \frac{\partial g_{\beta\gamma}}{\partial x^\alpha} \tag{2}$$

$$\Gamma_{\alpha\beta}^\mu \overset{\text{def}}{=} \frac{\partial x^\mu}{\partial X^\lambda} \frac{\partial^2 X^\lambda}{\partial x^\alpha \partial x^\beta} \tag{3}$$

$$\Gamma_{\beta\alpha}^\delta = \Gamma_{\alpha\beta}^\delta \tag{4}$$

Covariant derivative $\nabla_\mu \alpha$ and partial derivative $\partial_\mu \alpha$ of scalars

$$\partial_{\mu'} \alpha = \frac{\partial x^{\mu'}}{\partial x^\mu} \partial_\mu \alpha \tag{5}$$

Covariant derivative $\nabla_\mu V^\nu$ and partial derivative $\partial_\mu V^\nu$ of vectors

$$\nabla_\mu V^\nu = \partial_\mu V^\nu + \Gamma_{\mu\lambda}^\nu V^\lambda \tag{6}$$

$$\nabla_\mu \varphi_\nu = \partial_\mu \varphi_\nu - \Gamma_{\mu\nu}^\lambda \varphi_\lambda \tag{7}$$

$$\nabla_\mu g_{\alpha\beta} = 0 \tag{8}$$

$$\nabla_\mu g^{\alpha\beta} = 0 \tag{9}$$

$$g^{\nu\mu}g_{\nu\mu} = \delta_\nu^\mu \tag{10}$$

$$g = \det(g_{\nu\mu}) \tag{11}$$

$$g' = \left(\det\left(\frac{\partial x^{\mu'}}{\partial x^\mu}\right)\right)^{-2} g \tag{12}$$

$$\det\left(\frac{\partial x^{\mu'}}{\partial x^\mu}\right) \text{ is Jacobian} \tag{13}$$

$$d^4x \overset{\text{def}}{=} dx^0 dx^1 dx^2 dx^3 \tag{14}$$

$$d^4x' = \det\left(\frac{\partial x^{\mu'}}{\partial x^\mu}\right) d^4x \tag{15}$$